The setup and optimization of a complete global proteomics two-dimensional liquid chromatography system, using Spider Fractionation

Eris Aas Bakketeig

60 credits

Department of Chemistry

Faculty of Mathematics and Natural Sciences

UNIVERSITY OF OSLO

10/2021

The setup and optimization of a complete global proteomics two-dimensional liquid chromatography system, using Spider Fractionation

The setup and optimization of a complete global proteomics two-dimensional liquid chromatography system, using Spider Fractionation

http://www.duo.uio.no/

Trykk: Reprosentralem, Universitetet i Oslo

Abstract

In global proteomics, samples can contain hundreds of thousands of peptides or proteins. To analyze such samples, it is essential to use powerful techniques that maximize the peak capacity of the system. Two-dimensional liquid chromatography (2D LC) in combination with tandem mass spectrometry (MS/MS) is an excellent approach for peptide analysis; with maximum peak capacity achieved with reversed phase (RP) as stationary phase (SP) in both column dimensions, and changing the pH from high in the first separation to low in the second. This is especially potent for off-line systems when the output from the first analysis is collected per a fractionation scheme utilizing concatenation, i.e. pooling of fractions with very different retention into the same collection vials. Concatenation reduces the number of collection vials needed, reducing analysis time while maintaining high resolution.

A problem with off-line 2D LC is the loss of samples due to sample handling between the two dimensions. To address this, Reubsaet, *et al.* presented a loss-less 2D LC system using RP-RP with high-low pH and concatenation of fractions [1]. In this study, this system was reproduced, along with some other cutting-edge tools, with the goal of achieving a complete method for global proteomics, from sample preparation to detection. Included in the method were sample preparation by easy extraction and digestion (SPEED) for sample preparation and the Evosep One LC-platform. Central to the study was the Spider Fractionator, a tool for automatization of fraction concatenation.

The system was set up with in-house packed analytical columns, a Spider Fractionator and Evosep One. More than 5000 proteins were identified from digested HeLa standards. The Spider Fractionator was also optimized with a new design including custom 3D-printed additions, which increased robustness and repeatability. SPEED was performed for pancreatic islets from mice, however with low numbers of identifications. Much time was also spent on troubleshooting standard LC-equipment. Nonetheless, the cutting-edge techniques and instruments involved showed promising compatibility.

In summary, a combination of 2D LC with concatenation of fractions, a Spider Fractionator and Evosep One was set up and partly optimized. This system proved efficient and seemed promising for protein identification.

Preface

The work presented in this study was performed at the research station for Bioanalytical Chemistry at the Department of Chemistry, University of Oslo. I would like to thank my supervisors, Elsa Lundanes, Henriette E. Berg, Christine Olsen, Léon Reubsaet, Tuula A. Nyman, Bernd Thiede, and Steven R. H. Wilson, for their guidance, wisdom, and support. Special thanks goes to Christine, for taking on the supervisor mantle when needed.

I also owe great thanks to Inge Mikalsen, who was invaluable during troubleshooting of instrumentation, Maria E. Stensland, who guided and aided me with the Evosep One analyses, and Shadab Abadbour, who prepared pancreatic islets for me to work with.

I would also like to thank everyone in the Bioanalytical chemistry group for all our great times spent together, whether spent laughing, or sharing the feeling of "a Thursday that feels like a Monday". It has truly been an honor to work with all of you. A special thank you goes to my fellow master students Elisa, Tonje, and Harald for all our time spent working, joking, and talking together. Especially for meeting at the "online office" during lock-down. It is hard to imagine what these years would have been like without you.

And finally, thank you to my friends and family, and especially to my mother, my father, my grandmother, and to Silje, Jonas and Rikke. I could not have done this without your love and support.

Oslo, Norway, October 2021

Eris Aas Bakketeig

Abbreviations

2D	Two-dimensional
3D	Three-dimensional
ACN	Acetonitrile
AGC	Automated gain control
AVG	Average
BCA	Bicinchoninic acid
BSA	Bovine serum albumin
CF	Concatenated Fractions
Cyt C	Cytochrome C
DDA	Data-dependent acquisition
DTT	Dithiothreitol
ESI	Electrospray ionization
FA	Formic acid
FASTA	FAST-All
HF	Ultra-high-field
HFBA	Heptafluorobutyric acid
HILIC	Hydrophilic interaction liquid chromatography
IAM	Iodoacetamide
ID	Inner diameter
LC	Liquid chromatography
m/z	Mass-to-charge ratio
MeOH	Methanol
MP	Mobile phase
MS	Mass spectrometry
MS/MS	Tandem mass spectrometry
NH4Ac	Ammonium acetate
nanoLC	Nano liquid chromatography

PLOT	Porous layer open tubular
PRM	Parallel reaction monitoring
PSM	Peptide spectrum match
RP	Reversed phase
RSD	Relative standard deviation
SCX	Strong cation exchange
SD	Standard deviation
SFXX	Spider Fractionation experiment XX
SP	Stationary Phase
SPE	Solid phase extraction
SPEED	Sample preparation by easy extraction and digestion
SPP	Superflously porous particles
SRM	Single reaction monitoring
TFA	Trifluoroacetic acid
TIC	Total ion chromatogram
UV	Ultraviolet

Table of Contents

1. Introduction

1.1 Proteomics

The complete protein profile of a given cell, tissue or organism is referred to as a proteome [2]. Proteomics is the study of proteomes, a field encompassing both identification and quantification of proteins ranging in scale from a single protein to the complete proteome of an organism [3, 4] (p.53). Within the field of proteomics, there are two major approaches usually referred to as top-down and bottom-up proteomics. The top-down approach consists of separation and detection of intact proteins. In the bottom-up approach (**Figure 1**), the proteins are enzymatically digested into peptides prior to analysis. The identified peptides are then processed with powerful computational tools, enabling the identification of the original, whole proteins [3] (p.56). When attempting large-scale identification of multiple proteins, bottom-up has proved to be the preferred approach. By working with peptides, the analyst avoids some of the issues with protein solubility, stability, and stickiness [5]. Additionally, peptides are also easier to separate with LC and to sequence with MS, improving detection efficiency [5].

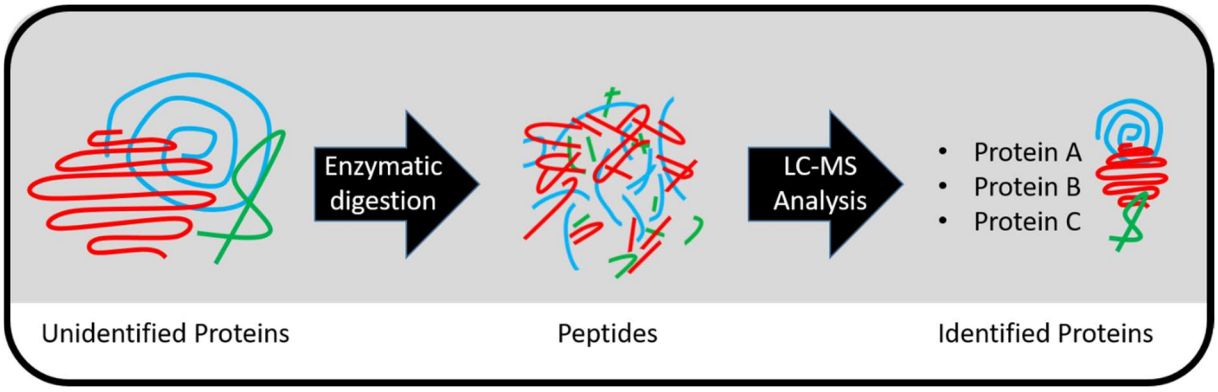

Figure 1 Illustration of the bottom-up approach. Proteins are digested into peptides prior to analysis. Analysis is performed with LC-Ms, and powerful computational tools then reassemble the proteins, providing a list of identifications.

Thanks to modern developments, thousands of proteins can be routinely identified in a single experiment. The combination of powerful tools for bottom-up analysis of large numbers of proteins from a single sample is referred to as global proteomics, known colloquially as "shotgun proteomics" [5, 6].

1.1.1 Enzymatic digestion

Key to the bottom-up approach is the enzymatic digestion of proteins into peptides. Enzymatic digestion is achieved with a protease, of which the most common is trypsin [7]. Trypsin is efficient, stable, commercially available, and cleaves the proteins by known patterns. Trypsin cleaves the protein chains at the carboxy-terminal (C-terminal) of arginine and lysine residues, unless they are followed by a proline [5, 8].

Prior to enzymatic digestion, the proteins need to be extracted. This is commonly performed through the addition of detergents, such as sodium dodecyl sulfate (SDS), and chaotropic agents, such as urea. These extraction reagents needs to be removed from the solution prior to digestion. This is commonly performed with techniques such as filtration and on-pellet precipitation [9, 10]. Alternatively, another approach to protein extraction, which does not require the removal of contaminants, is in-solution digestion. In-solution digestion uses reagents that are compatible with digestion, with the most common being the addition of urea with high concentration, which is diluted to non-interfering concentrations prior to digestion [9].

A typical in-solution digestion process is performed by first adding urea to extract the proteins. Then, reduction of disulfide bridges between cysteines is performed through the addition of dithiotreitol (DTT), and the cysteines are then alkylated through addition of e.g. iodoacetic acid (IAA). The sample solutions are then diluted to non-interfering concentrations, and trypsin is added, and the mixture is incubated overnight at 37 °C. The digestion is stopped by adding acid, thus lowering the pH and stopping the process [8].

1.1.2 Sample preparation by easy extraction and digestion

The use of urea as chaotropic agent during protein extraction is common in proteomics for a reason. It is efficient, easy, robust and highly repeatable [9]. Unfortunately, it does also lead to carbamylations, a post-translational modification occurring as a side-effect of the tryptic digestion, and complicates the MS analysis [11]. A new method that avoids the use of urea is SPEED [9], which extracts proteins through acidification and subsequent neutralization. SPEED is rapid, simple, applicable to all common sample types, and does not remove any sample during the sample preparation process, making it loss-less [9].

1.2 UV-detection

The ultraviolet (UV) detector is a commonly used detector in LC. While alternatives such as mass spectrometers, yield superior selectivity and sensitivity, the simple and robust instrumentation of the UV-detector makes it an incredibly valuable detector for any compound containing chromophores, when MS-level selectivity and sensitivity is not required [12] (p.80). UV-detectors function by measuring the absorbance of light with specific wavelengths passing through the sample and being absorbed by chromophores. Absorbance A is obtained according to Beer's Law:

$$A = \varepsilon bc,$$

where ε is molar absorptivity, b is the length of the light path, and c is the analyte concentration [12] (p.81).

1.3 Mass spectrometric detection

Mass spectrometers are powerful analytical instruments that separate and/or detect ions based on their mass-to-charge ratio (m/z). Various mass spectrometers are available, and they all complete three tasks: ionizing the analytes in an ion source, selecting out specific analyte ions with mass analyzers, and finally detecting the analyte ions with detectors [13] (p.559).

1.3.1 Electrospray ionization

To enable detection with MS, the analytes need to carry a charge. To ensure that the analytes are charged, an ion source ionizes the analyte molecules. The favored ion source in LC, especially when performing advanced proteomics, is ESI [14]. An ESI-source (**Figure 2)** operates by ejecting sample solution through a charged needle, with a nebulizing gas (usually N_2) at the outlet. The high voltage applied between the needle and a counter electrode at the MS inlet creates a highly charged jet of solvated analyte ions that form a Taylor cone. The resultant charged droplets are sent towards the MS inlet, and explode when the electrostatic repulsion between ions exceeds the surface tension of the droplets. These explosions are repeated until dry analyte ions in gas phase emerge and enter the MS [12, 15] (p.86-87). It is worth noting that the actual ionization most often occurs in the mobile phase (MP) through pH adjustment [12] (p.86). ESI is excellent for bottom-up proteomics as it is a very soft ionization technique, i.e. analytes are fragmented less during ionization [16, 17].

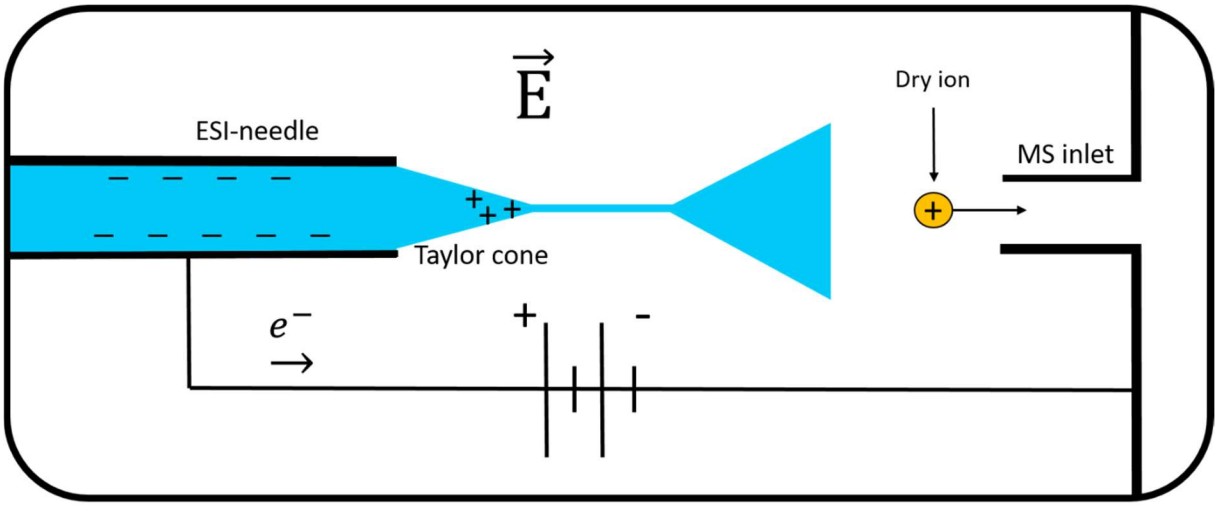

Figure 2 The principle for ESI performed in positive mode. The charged analyte ions in solution are ejected from the ESI-needle. The ESI needle carries a positive charge and there is a countercharge applied to the MS inlet. The electric field produced from these charges, and the speed with which the solution is ejected, forms the Taylor cone. The ions are gathered in the spray, and ejected as charged droplets. These droplets explode due to electrostatic repulsion several times until the dry ions in gas phase emerge and enter the MS-inlet.

When ESI is used with low flow rates, the nebulizing gas is no longer necessary. ESI with low flow rates and no nebulizing gas is referred to as nanoESI. Although this term strictly speaking only is applicable to systems with flow-rates of approx. 20 nL/min [18], there is precedence for referring to systems with sub-µm/min flow rates as nanoESI as many of the same benefits are achieved [19]. The main benefits of nanoESI include reduced solvent consumption, increased sensitivity, and improved ionization efficiency [15, 19]. The increased sensitivity and ionization efficiency stems from the formation of smaller droplets. Less solvent per droplet results in fewer droplet explosions required to acquire dry ions, which result in more dry ions reaching the MS [14, 20].

1.3.2 Mass analyzers

The most characteristic part of MS-instruments are the mass analyzers. Mass analyzers separate ions by their m/z, often by manipulating electric fields, e.g. for the quadrupole, ion-trap, and Orbitrap instruments [13] (p.572, 575-577). A quadrupole consists of four parallel metal rods pairwise charged with high voltage currents that generate an adjustable electric field. This field can be adjusted rapidly to only allow ions with certain m/z to pass through to a detector [13] (p.572). The third component of the MS is the detector, which is often a collision-induced

detector. Some powerful mass analyzers also double up as the detector. One such mass analyzer is the powerful Orbitrap.

1.3.3 Orbitrap mass spectrometer

The Orbitrap consists of a central spindle electrode, and two outer barrel-electrodes separated by an insulating piece [21], as illustrated in **Figure 3**.

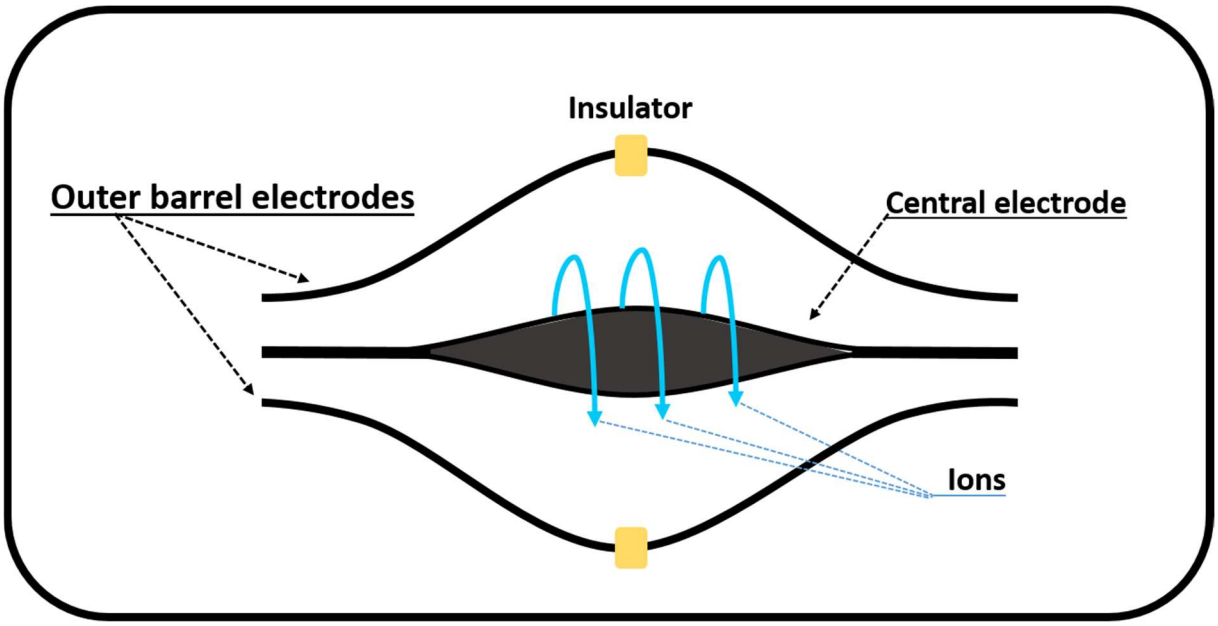

Figure 3: The Orbitrap, which consists of a central electrode and two outer barrel electrodes separated by an insulator. The insulator is usually a ceramic ring [22]. Ions orbit the central electrode and move back, while moving back and forth along the spindle electrode. This axial movement induces an image current as the ions move between the two barrel electrodes. The frequency of the axial movement is translated into *m/z*-ratios through the application of Fourier transformation [22].

Ions that enter the Orbitrap orbit the central electrode due to the generated electric field around the spindle balancing out the centripetal acceleration. The electric potentials of the outer barrel electrodes induce axial movement back and forth along the central electrode. It is the frequency of this axial movement, being dependent on m/z, which is detected as an image current [13] (p.577). An image current is the change in image charge, which again is the movement of charges within the metal of the outer electrodes induced by the movement of analyte ions. The closer an analyte cation is to a metal electrode, the closer to the metals surface the negative charges in the metal move, and vice versa. Several image currents are detected at the same time, with the

frequency of each current corresponding to a given m/z [13, 22] (p.577). The frequencies are separated from each other through the application of Fourier transformation [13] (p.577).

Orbitrap technology is still developing. One advancement was the high-field (HF) Orbitrap (Thermo Fischer Scientific, Waltham, MA, USA), which has a more compact design with higher field strengths [23]. The HF Orbitrap has the benefits of increased resolving power and data acquisition rate [23, 24]. Another advancement, albeit not recent, was the combination of multiple mass analyzers in one instrument, in a technique known as MS/MS [25].

1.3.4 Tandem mass spectrometry

MS/MS is a technique typically involving the serial coupling of two or more mass analyzers. It is most common to couple two mass analyzers, and there are several commercially available instruments of this kind. Common instruments include the triple quadrupole [26], and the combination of a quadrupole and an Orbitrap [27]. In addition to the two mass analyzers, a collision cell for fragmentation is required. In triple quadrupoles the middle quadrupole functions as the collision cell. Ions with certain m/z-ratios are allowed through the first mass analyzer. These ions are then fragmented in the collision cell, and the fragment ions subsequently enter the second mass analyzer, in which the fragment ions again are filtered by their m/z-ratios [28]. MS/MS can be run in several different modes, with a selection shown in **Figure 4**. These modes differ in how many ions are allowed through the mass analyzers. In single reaction monitoring (SRM), a single m/z ratio is selected for each of the mass analyzers [28]. In a product ion scan, one or a few ions are selected in the first mass analyzer, before everything is sent through the second [29]. A mode that is only available to powerful MS/MS-instruments, such as the quadrupole-orbitrap-combination, is parallel reaction monitoring (PRM). PRM is a technique that can be described as running multiple product ion scans at shorter time intervals, improving sensitivity, selectivity, and dynamic range [30, 31]. This is well suited for data-dependent acquisition (DDA), in which the MS selects the n most abundant ions, before subsequently performing PRM on these n ions. The DDA approach is well established as a method for use in global proteomics [32, 33].

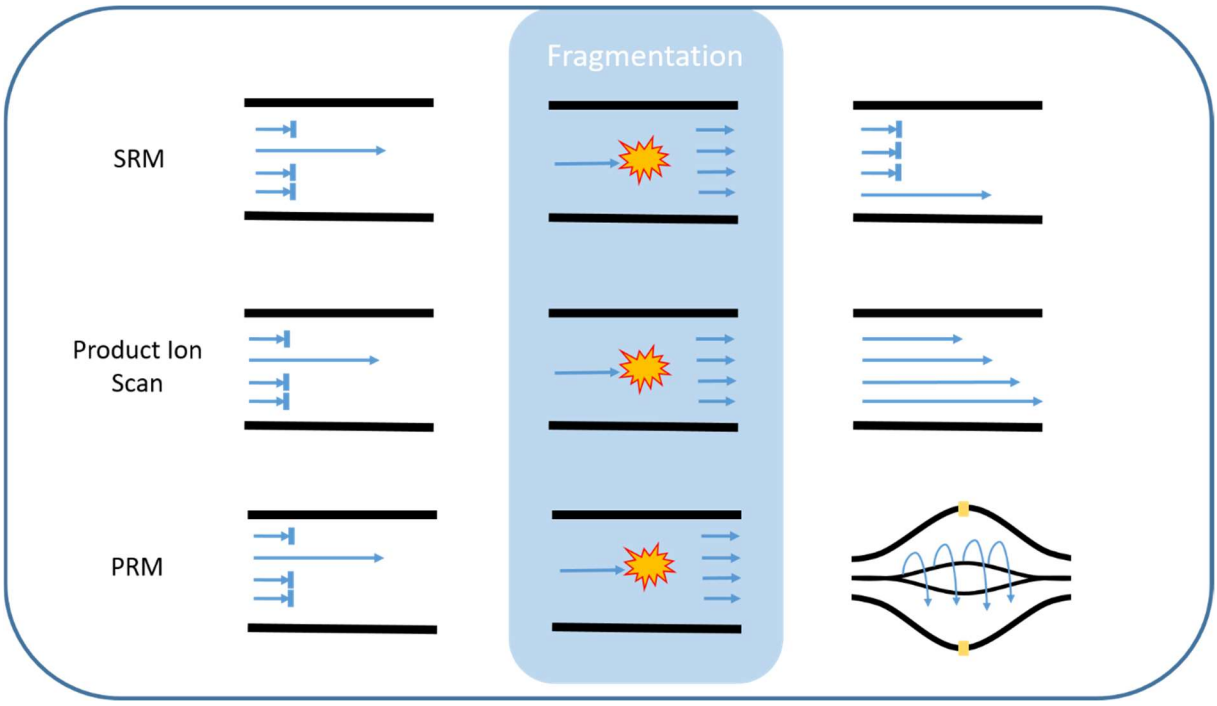

Figure 4 Illustration of a selection of MS/MS modes. In SRM, ions with one *m/z* are allowed through the first mass analyzer. The ions are then fragmented in the collision cell, and only ions with one *m/z* are allowed to pass through to the detector. In product ion scan, only ions of one *m/z* are allowed through the first mass analyzer. These ions are fragmented, and all product ions are allowed through the second mass analyzer for detection. In PRM, several product ion scans are performed in short time intervals. PRM is only possible with powerful mass spectrometers, such as Orbitraps. Adapted from [30].

1.3.5 Dynamic range

Protein identification can quickly become challenging, due to the large number of analytes, the miniscule presence of many proteins, and the limitations of dynamic range. The dynamic range describes the ability of a detector to simultaneously detect analytes of very different concentrations, where the highly concentrated analytes obscure the signals from low-concentration analytes [5, 34]. With large proteomes, the difference in protein concentration is usually spanning several orders of magnitude, with some proteins being in the high mg/mL range, and others being in the sub-pg/mL range [35]. To combat this, powerful instrumentation and techniques are required. Performing MS/MS in PRM mode with DDA is a powerful way to increase dynamic range [31]. As the problem with dynamic range is worse for more complex samples, reducing this complexity is beneficial. Chromatographic separation is a powerful way to reduce the complexity of a sample prior to MS analysis [36].

1.4 Liquid chromatography

As both ESI-MS and UV detection are dependent on the concentration of sample, it is beneficial to separate and concentrate the various analytes in the sample prior to detection. When handling protein-containing samples, LC is often the preferred tool, as these samples rarely are volatile enough for separation by gas chromatography.

Various chromatographic principles and column formats are available, and define the capabilities of a chromatographic system (**Section 1.4.1**). For limited sample amounts nanoLC methodology and instrumentation is often necessary (**Section 1.4.2**), and 2D LC is a powerful tool when separating very complex samples (**Section 1.4.3**), especially in global proteomics. A powerful technique used for 2D LC in global proteomics is the compiling of fractions known as concatenation (**Section 1.4.4**).

1.4.1 Chromatographic principles and columns

The retention in the chromatographic columns is based on the retention of the analytes on the SP, based on several physical and chemical properties. This includes hydrophobicity for RP; charge difference for strong cation exchange (SCX); and hydrophilicity for hydrophilic interaction liquid chromatography (HILIC) [12] (p.67-68, 73).

Reversed phase chromatography

The most widely used chromatographic principle in LC is RP [12] (p.69). With RP, the analytes are retained mainly based on their hydrophobicity. The SP is often comprised of carbon chains attached to porous silica particles, with octadecyl (C18) being the most common [13] (p.672). The MP is usually a mixture of an organic solvent, such as methanol (MeOH) or acetonitrile (ACN), and water, with the retention of analytes decreasing with increased ratio of organic solvent. A buffer or acid for pH-control is also usually added to the mixture. Controlling the pH is important for several reasons, as silica-based particles and columns degrade under basic conditions; the charge states of analytes, which can vary with pH, can affect the retention of compounds; and the use of ESI depends on ionization in the MPs (as mentioned in **1.3.1**) [1, 12] (p.71, 86.)

Analytical columns and particles

The most common column format is the packed column. There are also alternative column formats, such as monolithic and open tubular columns. For packed columns, the SP is most often attached to spherical porous silica-particles [37]. The size of the particles and the pore sizes are very important properties, which affect the chromatographic capabilities of the system. Particle size affects the efficiency, as smaller particles reduce the time needed to reach solute equilibration [13] (p.640). Smaller particles have the unfortunate side effect of increasing the pressure needed to move MP through the column [12] (p.59). No matter the size, uniformity is desired as this reduces band broadening due to eddy dispersion, thus increasing efficiency [13] (p.674). The size of the pores in the particles is also very important, as these should be sufficiently large as to accommodate the analytes. Most of the surface area of the particles are inside the pores. For the analytes to be retained properly, it is important that the analytes can reach the SP [13] (p.671). To improve the uniformity of the particles, and thus the efficiency of the column, superficially porous particles (SPPs), often referred to as core-shell particles, were developed. SPPs have a solid non-porous core, surrounded with a thin porous outer layer. With SPPs, it is possible to reach much higher resolution without drastically increasing the back-pressure [13] (p.674). The column itself is also very important. Smaller columns boosts sensitivity, allowing for analysis of lower sample amounts [38]. While conventional LC columns have inner diameters (ID) around 4.6 mm, chromatographers are pushing the IDs into low μm-range. When IDs become 100 μm or narrower, it is referred to as nano liquid chromatography (nanoLC) [12] (p.54).

1.4.2 Nano liquid chromatography

NanoLC has become an important tool in proteomics, allowing for analysis with high sensitivity, small sample amounts and low solvent consumption. When reducing the ID of the column, radial dilution of the analytes is reduced, increasing analyte concentration [37] (**Figure 5**). When using a concentration-sensitive detector, such as ESI-MS, the sensitivity is enhanced in accordance with the downscaling factor *f*, shown in **Equation 1:**

Equation 1:
$$f = \frac{d_{conv}^2}{d_{nano}^2},$$

where d_{conv} and d_{nano} are the IDs of a conventional-sized column and a nano-scale column, respectively. The downscale factor states that the radial dilution of chromatographic bands is proportional to the column radius, and decreases with smaller column IDs [14, 37, 39].

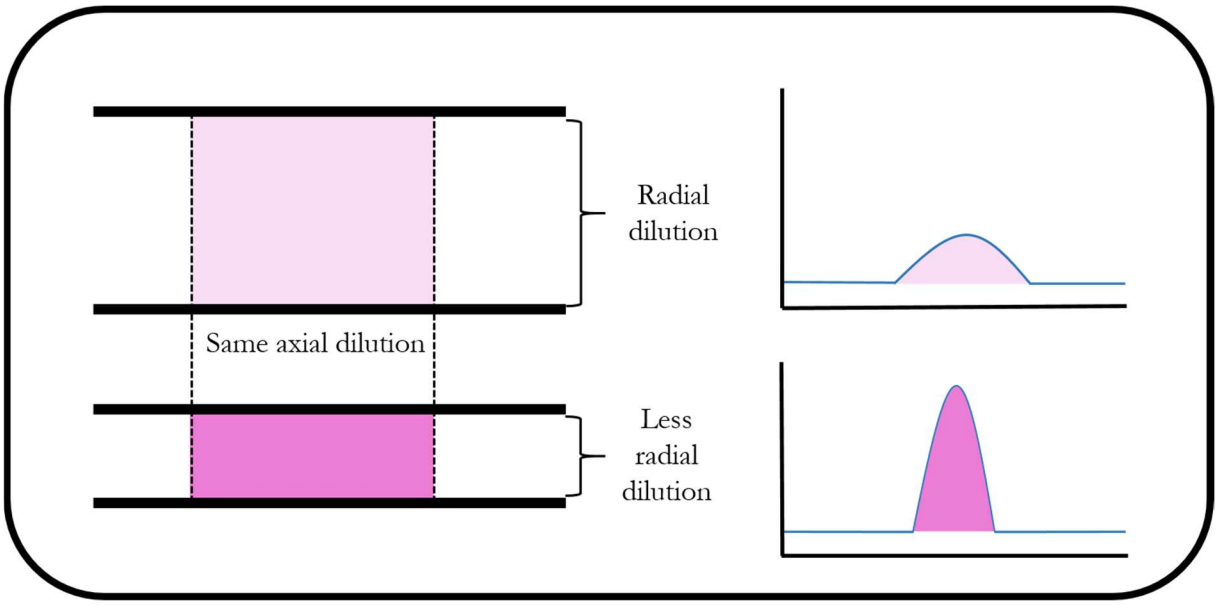

Figure 5 Illustration of the increased sensitivity gained with smaller ID columns. When column ID decreases the radial dilution is reduced, while the axial dilution stays the same. This focuses the analytes more, increasing sensitivity per the downscale factor. Adapted from [14].

The negatives when using nanoLC-columns include a loss in system robustness and an increase in demand on the operator [40]. It is, however, noteworthy that the low flow rates do not increase analysis time, as the linear velocities achieved with smaller columns stay proportional to those observed for larger sized columns [14].

1.4.3 Two-dimensional liquid chromatography

Another way to improve efficiency for global proteomics is through the application of 2D LC, which can drastically increase the peak capacity of a system [36, 41]. The peak capacity represents the theoretical maximum number of peaks that can be separated in a system [14]. 2D LC is performed by subjecting a sample to separation on two different columns with different separation mechanisms. These separation mechanisms can be different chromatographic principles, such as HILIC-RP, which has separation on a HILIC column in the first dimension, and an RP column in the second [42]. The hyphenation of SCX-RP has been the go-to combination for 2D peptide analysis [36]. However, several studies show that the most powerful combination for 2D LC separation of peptides is RP-RP with different pH between the two dimensions [1, 36, 43-47]. To understand how the two dimensions interact and affect the peak capacity of the system, an important concept must be explained: the degree of orthogonality between the dimensions.

Orthogonality in two-dimensional liquid chromatography

The selectivity of a chromatographic column is dependent on several factors. The selectivity is dependent on the chosen chromatographic principle (i.e. RP, HILIC, SCX, etc.), but there are several other factors at play. These factors include temperature, pH, type of SP, the MP composition, the particle pore size, etc. [36]. Because of this, when discussing combinations of 2D LC columns, it is more appropriate to talk of *separation mechanisms,* rather than just principles. When combining two different analytical columns, the overlap of their retention mechanisms is explained through their degree of orthogonality [47]. In mathematics, orthogonality describes the relation between perpendicular vectors. For 2D LC, orthogonality describes the overlap of retention for similar analytes in different columns (with different retention mechanisms) [48]. For instance, if peptides were separated in an RP-RP system with identical SPs and conditions, the degree of orthogonality would be 0%, as they are theoretically identical. With two completely different retention mechanisms, the degree of orthogonality would be 100%, which would maximize efficiency (**Figure 6**). Efficiency would be maximized because the peak capacity of a completely orthogonal 2D LC system equals the product of the peak capacities of each dimension [48]. In practice, however, it is unfeasible to achieve 100% orthogonality.

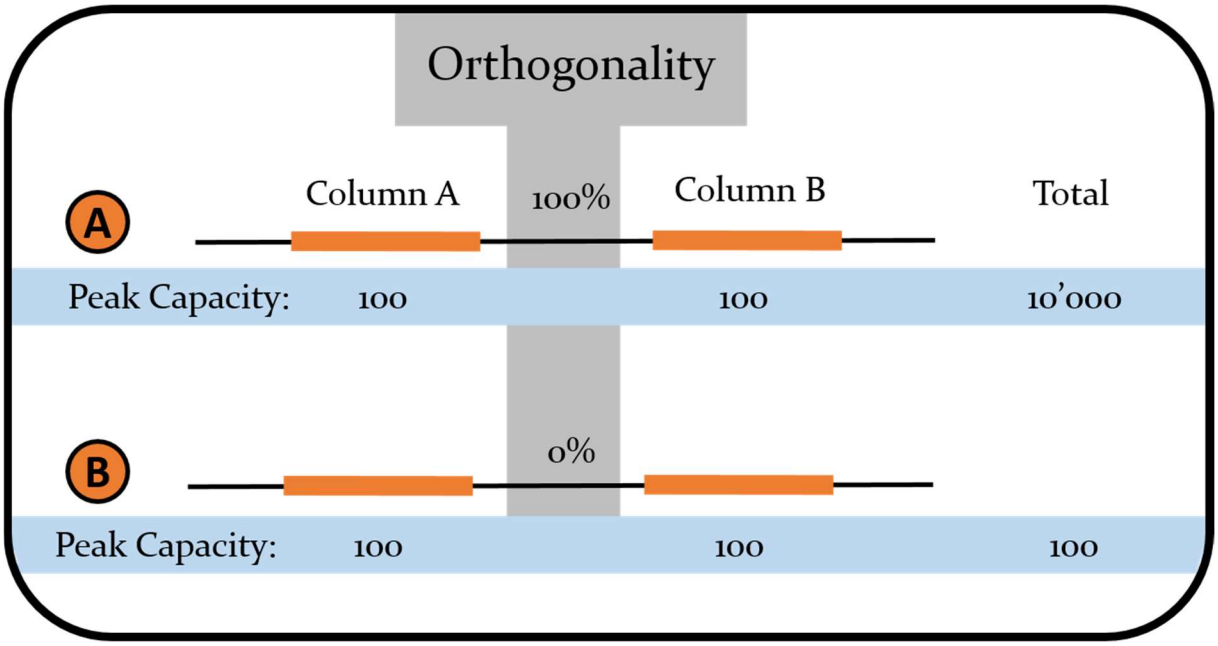

Figure 6 Illustration of how orthogonality affects peak capacity. In (A) Column A and B are completely orthogonal (100%), so the total peak capacity is the product of the peak capacities of the columns. In (B) Column A and B have 0% orthogonality, meaning they have identical retention mechanisms. This means no increase in total peak capacity is gained, as it remains at 100.

It is also important to remember that the orthogonality only enhances the efficiency that is already there. Using a combination of more efficient analytical columns can yield higher peak capacities even with less orthogonality. This is the case for RP-RP with differing pH-values [36]. Peptides, being zwitterions, have different retention under basic and acidic conditions, due to changes in charge distribution [49]. Although RP-RP systems have a lower degree of orthogonality, RPs superior efficiency compared to other principles yields superior peak capacities [36].

It is noteworthy, that the hyphenation of 2D LC-MS is a particularly powerful combination, as the MS introduces a separate separation mechanism, providing a third dimension (with its own orthogonality), and boosting the peak capacity of the system [48].

Approaches in two-dimensional liquid chromatography

When performing global proteomics, *comprehensive* 2D LC is usually performed. With comprehensive 2D LC, the entire eluted sample is transferred from the first column to the second [48]. The comprehensive approach can be performed in two ways; on-line and off-line (**Figure 7**).

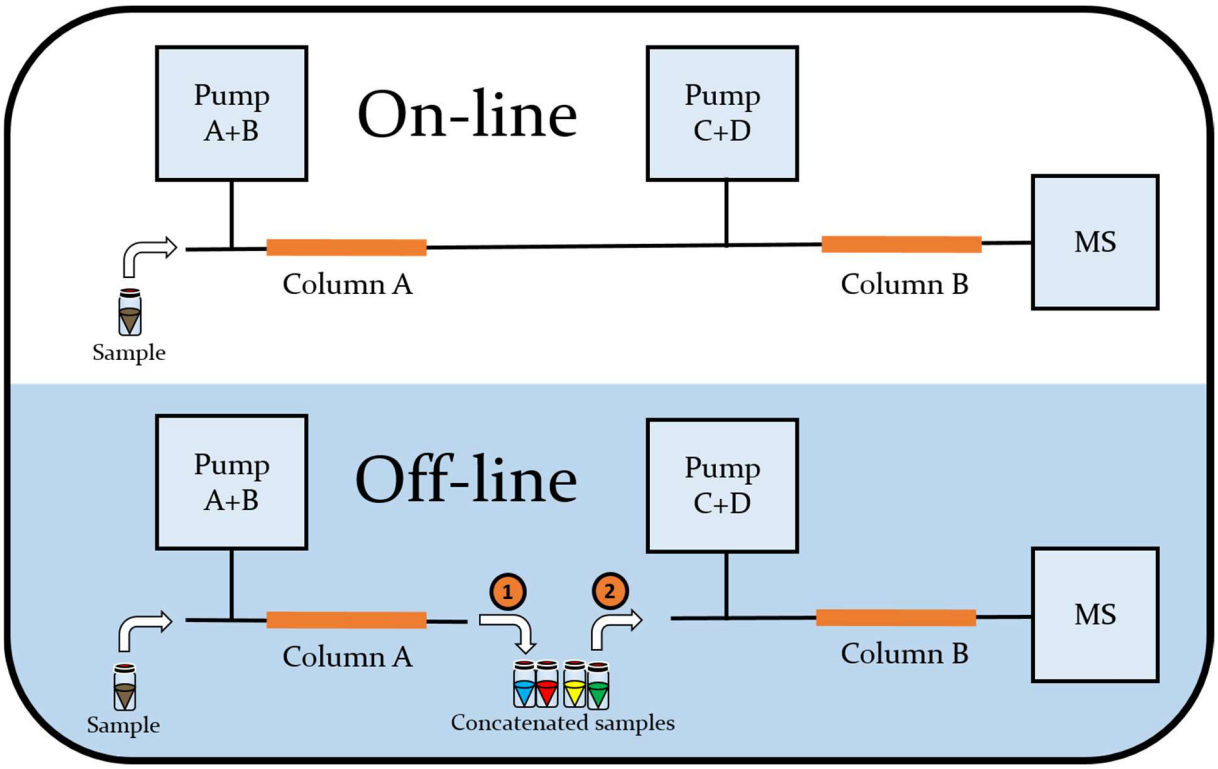

Figure 7 Illustration of on-line vs off-line 2D LC. In an on-line system (top) the sample is injected onto the system which has both analytical columns A and B coupled in series. Two sets of Pumps (A+B and C+D) are necessary to deliver two different MPs to the system during a single run. In an off-line system (below) the two separations occur on separate systems, with the sample separated on column A, then (1) the fractions are collected (here also concatenated), treated, and (2) injected onto the second system, which is a normal LC-MS system.

In off-line systems, the two analytical columns are separate, and the eluted analytes are collected, prepared for injection, and applied to the second column. In on-line systems, the two columns are coupled in a series, with the entire 2D LC separation happening in the same operation. A major advantage of the on-line systems vs off-line is minimal sample loss from transfer and treatment of the eluted sample between dimensions [48]. The downsides with on-line systems are mainly their complexity, requiring additional pumps, trapping columns and other complex instrumentation to operate [36]. Newer approaches have achieved approximate loss-less transfer for comprehensive off-line 2D LC analysis [1], proving the off-line approach to be very promising for global proteomics.

1.4.4 Concatenation: a fraction collection strategy

With comprehensive off-line 2D LC, the eluted sample is collected and applied to a second column. If this eluted sample was collected in a single vial, the effect of the first separation would essentially have been nullified. To take advantage of the first separation, the eluted sample is collected as fractions. This concept is referred to as *fractionation* [48].

When collecting fractions, it is beneficial to have as many fractions as possible to maximize the gain from the first separation. Each fraction is injected to the second dimension column, one at a time, and as such, the duration of the experiment is extended with each added fraction [36]. As it quickly becomes demanding to have too many fractions in separate vials, it is beneficial to collect the fractions in a small number of vials. This concept is referred to as *concatenation* [1, 49] (**Figure 8**). With an 8-vial concatenation scheme, a large number of fractions, e.g. 64, can be collected in only 8 vials. As long as the compounds in the fractions in the same vial have sufficiently different retention, concatenation improves the peak capacity of the system without increasing experiment duration [44, 49, 50].

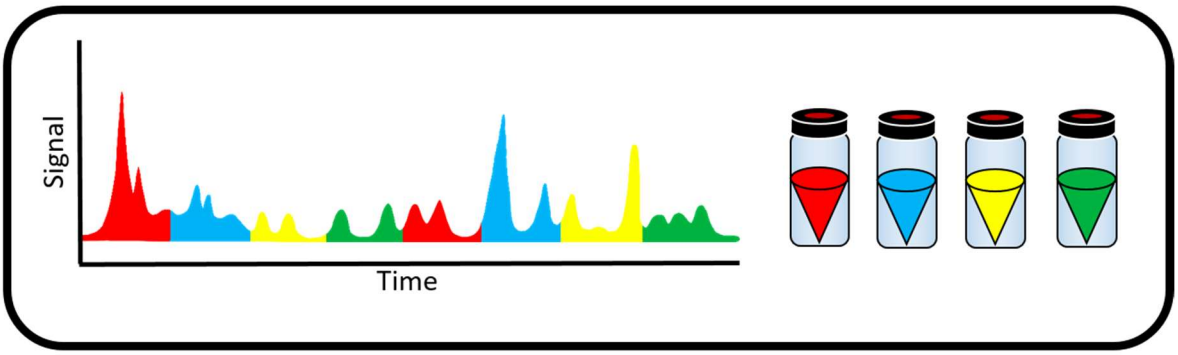

Figure 8 Illustration of the concatenation of fractions in a 4-vial scheme. Injected analytes are separated, as is illustrated in the chromatogram seen to the left, with each colored part representing a fraction. There are eight fractions in total. Without concatenation, it would be necessary to have eight vials to collect all of them. With concatenation, however, it is possible to pool fractions with analytes that have sufficiently different retention in the same vial. This is illustrated as the 1st and 5th fraction are collected in the red vial, the 2nd and 6th are collected in the blue vial, the 3rd and 7th are collected in the yellow, and the 4th and 8th are collected in the green. It could also be possible to shorten the fraction time and increase the number of fractions, without increasing the number of collection vials needed, as long as the retention is sufficiently efficient.

1.5 Cutting-edge tools for global proteomics

As described, comprehensive off-line 2D LC-MS/MS for global proteomics has seen many advancements in knowledge, technique and instrumentation. Some cutting-edge tools have shown promise for proteomics, the combination of which could provide extraordinary efficiency. This includes the Spider Fractionator [44] (**1.5.1**), which is a tool for automatization of concatenation of fractions for off-line 2D LC. Another is the Evosep One (**1.5.2**), which is a powerful LC-platform, specialized for routine proteomics analysis. A third interesting tool is the 3D-printer (**1.5.3**). The introduction of the 3D-printer to analytical chemistry laboratories has introduced a new world of exciting opportunities.

1.5.1 The Spider Fractionator, a tool for automatizing fractionation

When collecting fractions during concatenation, automatization should be considered. Small volumes per fraction (in the nL range [1]) are collected, presenting possible loss of sample from moving the column end between collection vials. In addition, elution times are usually long for proteomics. The fractionation can therefore quickly end up demanding complex systems or methods.

Robustness and precision is achieved with an automated rotor-valve-based system, such as the Spider Fractionator (**Figure 9**) presented by Kulak, *et al.* [44]. The Spider Fractionator consists of a rotor valve that directs the column flow to one of several exit ports. From each exit port, tubing leads to a collection vial, for concatenation of fractions. As the analytes are separated on the first dimension column, the flow is directed to the different vials, switching at set time intervals dependent on the concatenation scheme. The switching of flow to different exit ports can be controlled by software and fully automatized. The Spider Fractionator has its name from the spider-like design of the original design: with the 8 pieces of output-tubing resembling the legs of a spider. At time of writing, there are no commercially available Spider Fractionators, but there is one currently under development by PreOmics GmbH (Martinsried, Germany) [44].

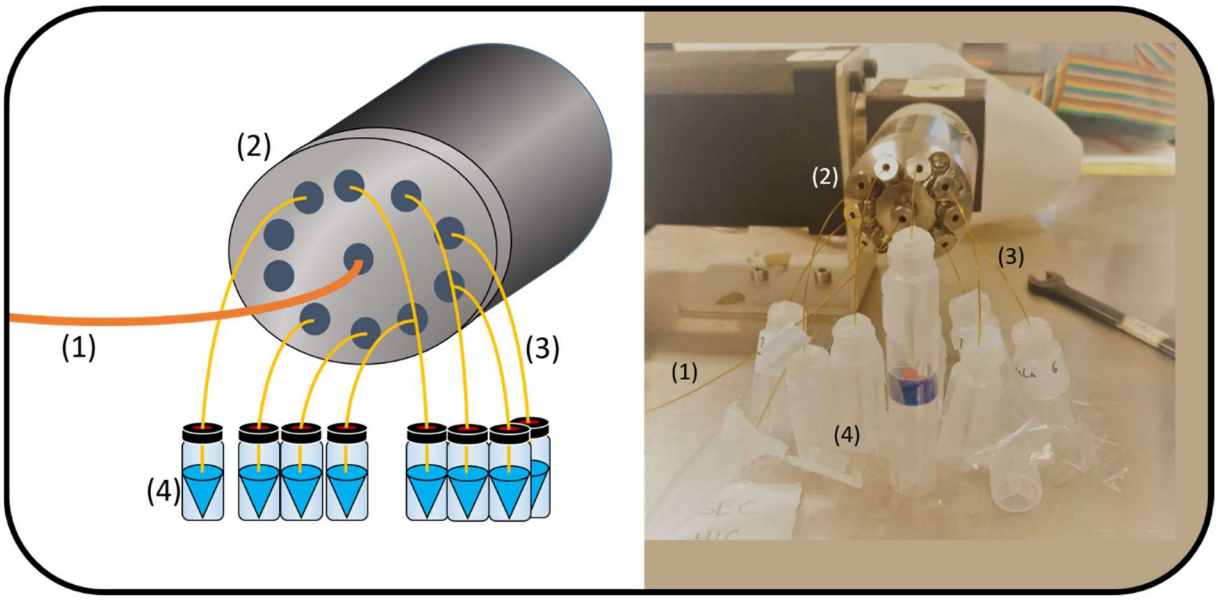

Figure 9: Illustratin (left) and photograph (right) of the Spider Fractionator. The flow from the analytical column (1) is directed into a rotor valve device (2). The flow is redirected through one of (here eight) output tubes (3) and enter the collection vials (4). The flow is switched to different output tubes when the rotor-valve receives a signal from software, according to a concatenation scheme [44].

An additional benefit with the Spider Fractionator is that it is very compatible with the loss-less off-line proteomics workflow presented by Reubsaet, *et al.* [1]. More specifically, that by submerging the ends of the capillaries directing the column flow into the vials containing sufficient volumes of 0.2% formic acid (FA), the concatenated fractions (CFs) leaving the Spider Fractionator are pH-adjusted and the organic solvent component is diluted automatically. The CFs are then ready for injection on the second dimension system immediately, without need for treatment, which could lead to loss of peptides [1].

1.5.2 Evosep One, a liquid chromatography platform

Among the many innovations in the field of proteomics, is an alternative sample loading and injection approach called speLC [51]. For speLC, the sample is applied to a C18 solid phase extraction (SPE) microcolumn. SPE columns are commonly used during sample preparation, washing the sample of contaminants before eluting the analytes into a container before injection. For speLC, instead of eluting the retained analytes from the SPE column into a container, the SPE column is connected on-line to the analytical column, functioning as a trap column [51]. The speLC approach achieves high throughput and no sample-to-sample carry-over, as each SPE column is discarded after use [37, 51].

Building on the speLC approach is the commercially available LC-system, Evosep One (Evosep Biosystems, Odense, Denmark) [52]. Evosep One **(Figure 10**) utilizes speLC for loading the sample while simultaneously producing and storing a chromatographic gradient in a long storage loop (i.e. 3-4 meters, ≤100 µm ID). The analytes are suspended in this pre-formed gradient in the storage loop. They are then focused through the application of a second gradient (referred to as an offset gradient [52]), before they are injected onto the nanoLC column by a high-pressure pump. The detection is then performed with MS [52]. The offset gradient increases the peak capacity of the system through phase-focusing of the analyte peptides.

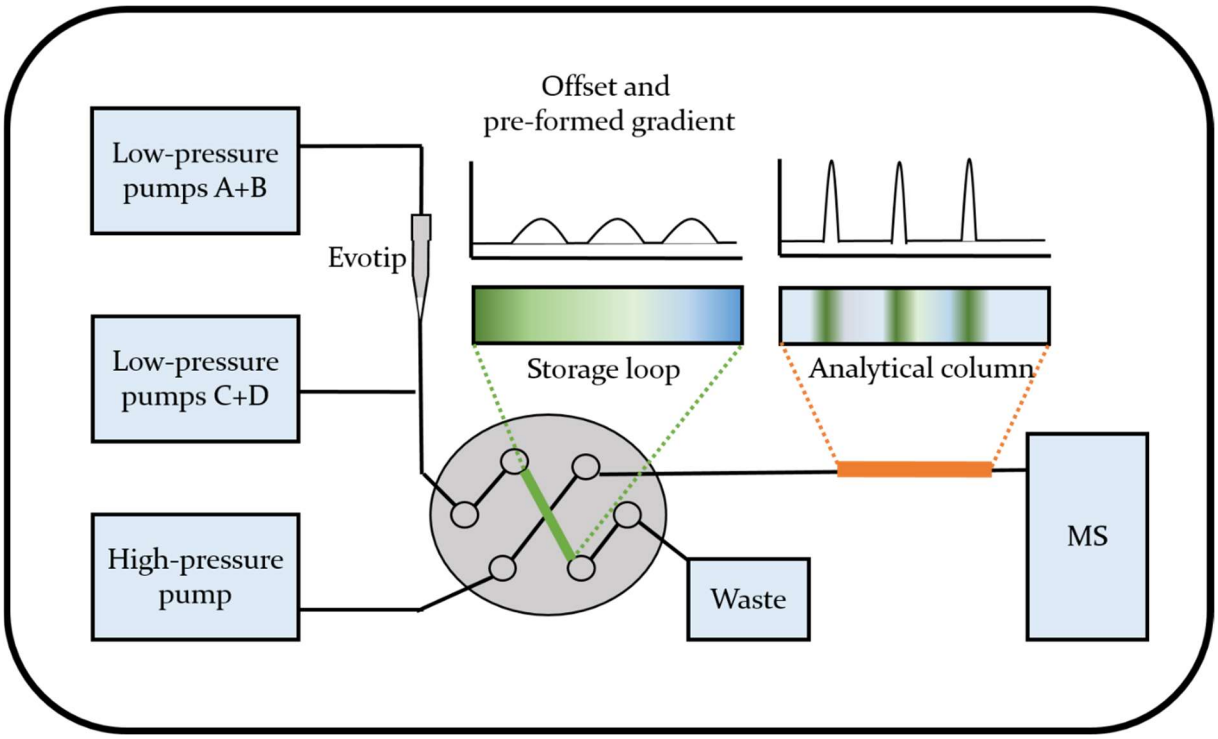

Figure 10 Illustration of the Evosep One. Low-pressure pumps A and B loads the sample from the Evotip, and Low-pressure pumps C and D are used to form and offset the pre-formed gradient in the long Storage loop. The single high-pressure pump is then used to inject the analytes suspended in the preformed gradient onto the analytical column, where the analytes are further separated and sent to an MS for detection. Adapted from [53].

Evosep One is an instrument designed for routine analysis with high throughput. To achieve this, several of the processes of the Evosep One are performed in parallel. For instance, analytical column equilibration is performed while the analytes and the preformed gradient are loaded into the storage loop [52]. Evosep One also utilizes Evotips™ (Evosep Biosystems), which are SPE columns specially made for the Evosep One [52]. Recently, a new set of powerful methods

applicable to the Evosep One were introduced. One of these is the Extended Method, which utilizes a longer gradient for maximum proteome coverage with limited starting material [54].

1.5.3 3D-Printing as a tool in bioanalytical chemistry

3D-printers have long been powerful manufacturing tools in industry and medicine, and have in recent years found their way into bioanalytical laboratories, being cheaper and more precise than ever [55]. With a 3D-printer, it is possible to create and fine-tune custom-designed objects from a wide range of materials with astounding precision [55, 56]. In analytical laboratories, these 3D-printed objects range from common laboratory equipment such as holders, racks, and mixers, to LC-pumps, LC-columns and even complete systems in the form of microfluidic systems in the chip format [55]. 3D-printers also allow for in-house fabrication of prototypes, creating new possibilities for creative manufacture in the laboratory, as well as printing finished designs on demand [56]. There are, of course, limitations to the technology. For instance, the 3D-printer becomes increasingly difficult to operate in proportion to the complexity of the printed product, and there are limitations on resolution, which is needed to print fine details [56]. There are also challenges with the materials used, as the various solvents and chemicals used in laboratories can react with the materials [55, 57]. There is, however, little doubt that many innovations will be made in analytical chemistry thanks to the increasing availability of 3D-printing technology.

1.6 Aim of study

When performing bottom-up protein analysis, high sensitivity and efficiency is essential for maximizing identifications. The aim of this study was to set up a method for protein identification method, incorporating several cutting-edge tools and techniques, to maximize the number of protein identifications, minimize sample loss, and maintain robustness.

The method was a global proteomics method utilizing comprehensive off-line 2D LC with RP-RP with high-low pH and a loss-less concatenation strategy adapted from Reubsaet, *et al.* [1]. Central to the method was the Spider Fractionator, which would increase robustness, repeatability, and ease the fractionation process. The Evosep One was included as the LC-system of choice for the analysis of the concatenated fractions, due to the increase in efficiency gained from the speLC technique, combined with the robustness, high throughput and user friendly interface of a commercialized system. SPEED was chosen as the sample preparation method, due to the technique boasting miniscule sample-loss during the extraction and digestion of proteins [9]. This had great synergy with the loss-less 2D LC method that was the basis of the complete method. HeLa cell digests were used as standards for the tests, with pancreatic islets from mice being the sample of choice for the ultimate tests of the complete system.

As such, the aim of this study can be summed up in five milestones, shown in **Figure 11**.

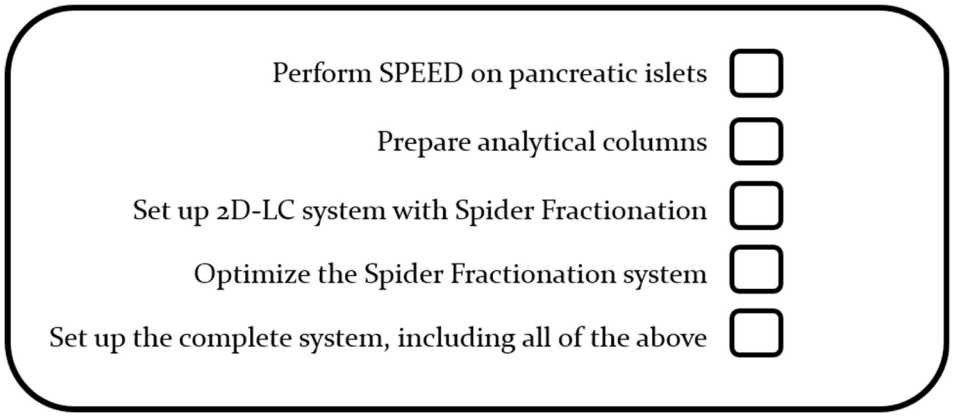

Figure 11 The five goals of this study.

2. Experimental

2.1 Chemicals, equipment and solutions

2.1.1 Solvents and reagents

ACN, MeOH, and water, all LC-MS grade, were purchased from VWR (Radnor, PA, USA), and were used unless otherwise specified. In addition, for use in some experiments, type 1 water was prepared with a Milli-Q® Integral Water Purification System from Merck Millipore (Billerica, MA, USA). FA (≥99%) and ammonia (25%) were also from VWR. Ammonium acetate (NH_4Ac), Bovine Serum Albumin (BSA), Trizma® base (tris) were purchased from Sigma-Aldrich, a subsidiary of Merck KGaA (Darmstadt, Germany). Trifluoroacetic acid (TFA) was purchased from Uvasol® Solvents, another subsidiary of Merck KGaA. Heptafluorobutyric acid (HFBA) (99%), was from Acros Organic, a part of Thermo Fischer Scientific. 10 mg/mL trypsin digest (Thermo Fischer Scientific) solved in water was provided PhD Candidate Henriette E. Berg, as were solutions of 1M DTT and IAM, both from Sigma Aldrich.

2.1.2 Standard solutions

HeLa Digest Standard (Thermo Fischer Scientific) was solved in basic mobile phase (MPA, see **Table 1)** to concentrations of 0.1 μg/μL, 0.2 μg/μL and 0.05 μg/μL. Thiourea (May & Baker Ltd, Dagenham, England, UK) was solved in MPA to concentrations of 0.05 μg/μL. Thiourea was also solved in water to concentrations from 0.001-1 μg/μL. Uracil and caffeine (Fluka and KEBO Lab AB, respectively, both subsidiaries of Merck) were solved in water to concentrations from 0.1-1 μg/μL. In addition, 1.8 pmol/μL Dionex™ Cytochrome C (Cyt C) Digest standard (Thermo Fischer Scientific) was used, as was a 0.2 μg/μL Cyt C digest, provided by master student Inga Mork Aune. A Cyt C digest solution with a concentration of 1 μg/μL was prepared following the Cyt C digest protocol in **Appendix 6.1.5**.

2.1.3 Cell samples

The samples were cells from two cell pellets; one containing human SW480 cells and one containing pancreatic islets from mice. The SW480 cell pellet (Thermo Fischer Scientific) was prepared by PhD Candidate Henriette E. Berg, and contained 10^8 cells. The pancreatic islets

were harvested from mice by. Dr. Shadab Abadpour at the Centre of Excellence – Hybrid Technology Hub. Approx. 60 islets were harvested from 8 mice, with each islet usually containing 1500-2000 cells. During transportation of the islets, approx. half were lost, due to insufficient packaging (a petri dish). The islets were floating in cell medium, and were washed with Gibco™ Dulbecco's Phosphate Buffered Saline (DPBS) from Thermo Fisher Scientific and rinsed and centrifuged four times, before storing the pellet at -80 °C.

2.1.4 General equipment

All measurements of the mass of solids for preparation of solutions were measured on a METTLER AT200 analytical scale from Mettler Toledo (Columbus, OH, USA). Solutions in small-volume containers were homogenized with a Hula Dancer digital from IKA (Staufen, Germany). Graphite/vespel ferrules and stainless steel nuts and unions were provided by Valco Instruments Co. Inc. (VICI®) (Houston, TX, USA). The ovens used were either a GC-17A from Shimadzu (Kyoto, Japan) or a GC800 series oven from Fisons (Manchester, England, UK). The centrifuges used were a Centrifuge 5424 R and a Concentrator plus from Eppendorf AG (Hamburg, Germany). Safe-lock tubes (1.5 mL) and protein lo-bind tubes (1.5 or 2.0 mL) were purchased from Eppendorf AG. Autosampler vials (0.3 mL) were from VWR.

2.1.5 Preparation of mobile phases

Two pairs of MPs were prepared as described by Reubsaet *et al* [1]. The first pair had a pH of approx. 10 and are referred to as MPA and MPB respectively. A second pair of MPs were made prepared with a pH of 2, denoted as MPA_2 and MPB_2. The composition of the MPs are shown in **Table 1**.

Table 1: MP compositions of the basic (undenoted) and acidic (denoted 2) MPs.

Mobile Phase	Composition	pH
MPA	2% ACN in 20 mM NH_4AC	10
MPB	80% ACN in 20 mM NH_4AC	10
MPA_2	2% ACN in 0.2% FA	2
MPB_2	80% ACN in 0.2% FA	2

The basic MPs were pH-adjusted to approx. 10 with ammonia-solution, and controlled with pH-strips (Fischer Scientific UK Ltd, Loughborough, UK). MPA_2 and MPB_2 were adjusted to pH 2 with FA, and controlled with pH-strips. Prior to use, all MPs were degassed with helium (99.999%) (Nippon Gases Norge AS, Oslo, Norway) for at least 15 min, unless the pump in use was outfitted with a degasser.

2.2 Sample preparation

Sample preparation was performed with SPEED on cells from cell pellets described in **Section 2.1.3**, according to the SPEED protocol in **Appendix 6.1.1**. The SPEED protocol includes a protein concentration measurement step, which was performed with Bicinchoninic Acid (BCA™) Protein Assay Kit [58] – Reducing Agent Compatible, and a Nano Drop 2000, both from Thermo Fischer Scientific. After SPEED was performed, the samples were rinsed of salts and other contaminants with 100 µL C18 Ziptips (Agilent Technologies, Santa Clara, CA, USA), according to the Ziptip protocol in **Appendix 6.1.3**.

2.2.1 Sample preparation experiments

SW480 cells were prepared with SPEED in 4 replicates. 0.6 µL trypsin (10 µg/µL) was added to each replicate for digestion. The samples were then subjected to rinsing with Ziptip, and analysis with Evosep, as described in **Appendix 6.1.3** and **Section 2.4.3,** respectively**.**

Two solutions of pancreatic islets and one solution of SW480 were prepared with SPEED. The solutions were each aliquoted into two sample solutions, marked as 1 and 2. The solutions of SW480, the blank, and the first pancreatic islets (Mus A1 and A2) were each added 2 µL of trypsin (0.5 µg/µL, diluted from 10 µg/µL trypsin with water). The second set of pancreatic islet aliquots (Mus B1 and B2) were added 5 µL 0.05 µg/µL trypsin (0.05 µg/µL, diluted from 0.5 µg/µL trypsin with water). The pancreatic islet samples were named Mus (from the latin word for mouse). All samples (4 Mus, 2 SW480, and 1 blank) were then rinsed with Ziptip and analyzed with the Evosep One platform, as described in **Section 2.4.3.**

2.3 Preparation of analytical columns

The analytical columns used for all of the experiments were prepared in-house with particles extracted from an Accucore™ 150 C18 LC Column (Thermo Fischer Scientific) with a particle size of 2.6 μm and a pore size of 150 Å. The extraction process was performed by PhD Candidate Henriette E. Berg, by removing the filter in one end of the column and flushing out the particles with MeOH, using an LC-pump. The MeOH was then allowed to evaporate overnight.

The columns themselves were prepared by fritting fused silica capillaries (Molex, Lisle, IL, USA) with IDs of 50 μm and 100 μm with a FritKit from Next Advance (Troy, NY, USA). The FritKit contained the solutions Kasil® 1624 (potassium silicate) and formamide, which were mixed at a 3+1 ratio. The capillaries were flushed with MeOH or ACN, by using the pressure bomb system (**Figure 12**) designed by Engineer Inge Mikalsen. The capillaries were then held into the mixture of Kasil 1624 and formamide for 3-5 seconds, allowing capillary forces to pull the mixture into the capillaries. The capillaries were then placed in an oven at 100°C overnight (at least 8 hours). The frits were cut down to 4-5 mm length, which was monitored with a light microscope (Motic, Xiamen, China). The fritted capillaries were packed with a slurry consisting of approx. 30 mg Accucore particles solved in 1 mL MeOH or ACN. The slurry was mixed in an ultrasound bath at 45 °C for 15 min prior to the packing. The particle slurry was then forced through the fritted capillaries with nitrogen gas (99.99% (Nippon Gases), using the pressure bomb system (**Figure 12**). The packing was performed on a magnetic stirrer, with a 3x3 mm ball magnet (VWR) added to the slurry vials.

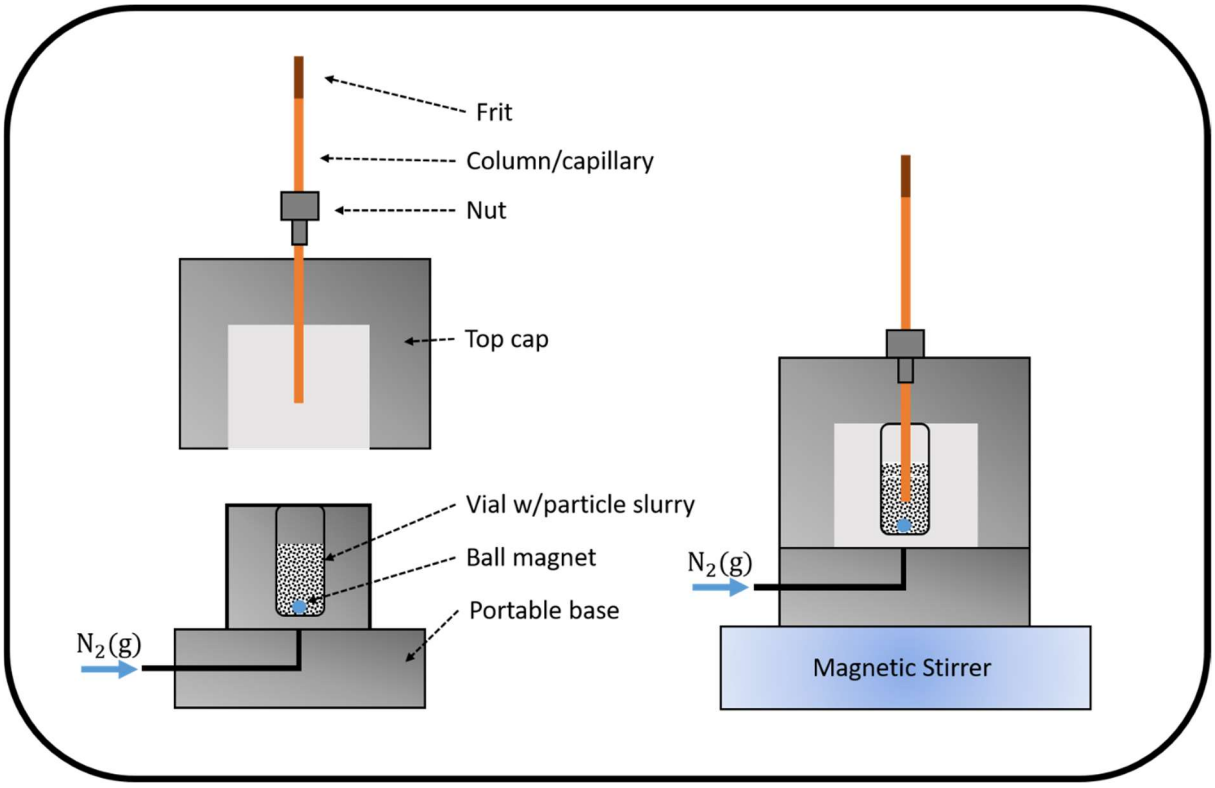

Figure 12: Schematic of the pressure bomb system. Adapted from [59, 60]. The fritted capillary to be packed with particles was fastened within the top cap with the frit pointing upwards. The capillary was then inserted into the vial filled with particle slurry and the top cap was fastened to the portable base. Nitrogen gas was applied through the base, forcing particle slurry through the capillary. The portable base was quickly moved onto a magnetic stirrer, and the ball magnet in the solution ensured stirring during the packing process.

2.4 Instrumentation

2.4.1 Liquid chromatography with UV detection

Four LC-pumps were used for different experiments. The LC-pumps were a Proxeon EASY nLC 1000 (Thermo Fischer Scientific), a nanoAcquity UPLC (Waters, Milford, MA, USA), an Agilent 1200 (Agilent Technologies), and an Easy nLC 1200 (Thermo Fischer Scientific). The LC-UV system is shown in **Figure 13**.

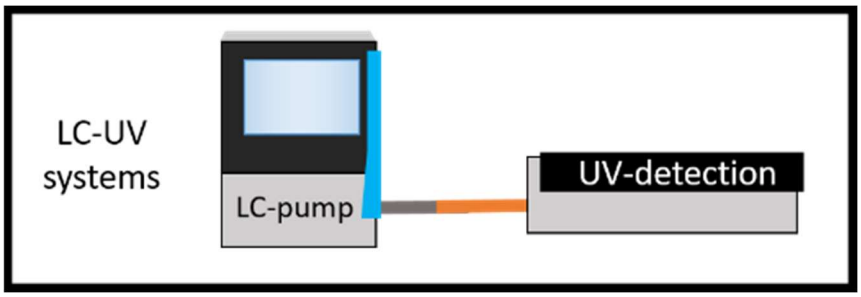

Figure 13: Illustration of the LC-UV system.

All LC-UV systems used in-house packed Accucore C18 columns (**2.3)** with IDs of 100 µm and lengths between 15-22 cm. All pumps except for the Agilent 1200 pump had autosamplers. The Agilent pump required a manual 4-port injector and a 10 µL syringe for sample injection. Detectors used were a Knauer UV-detector TCnav software (PerkinElmer, Waltham, MA, USA), and a Dionex UV-detector with Chromeleon software. Restrictors were added to the ends of the capillaries leading out from the UV-detectors. The restrictors were 2-4 cm long silica capillaries with IDs of 30 µm. The LC-pumps and detectors used are shown in **Table 2**. Basic MPs were used, and the MP composition gradients used were Gradient A (**Figure 14**), which was adapted directly from Reubsaet, *et al.* [1], and isocratic runs at 50% MPB. The wavelengths measured for various standards are shown in **Table 3**.

Table 2: The pumps and detectors used for the LC-UV experiments.

System #	Pump	Detector
1	Proxeon Easy nanoLC 1000	Knauer UV-Detector
2	nanoAcquity UPLC	Knauer UV-Detector
3	Agilent 1200	Knauer UV-Detector
4	Easy nanoLC 1200	Knauer UV-Detector
5	Easy nanoLC 1200	Dionex UV-Detector

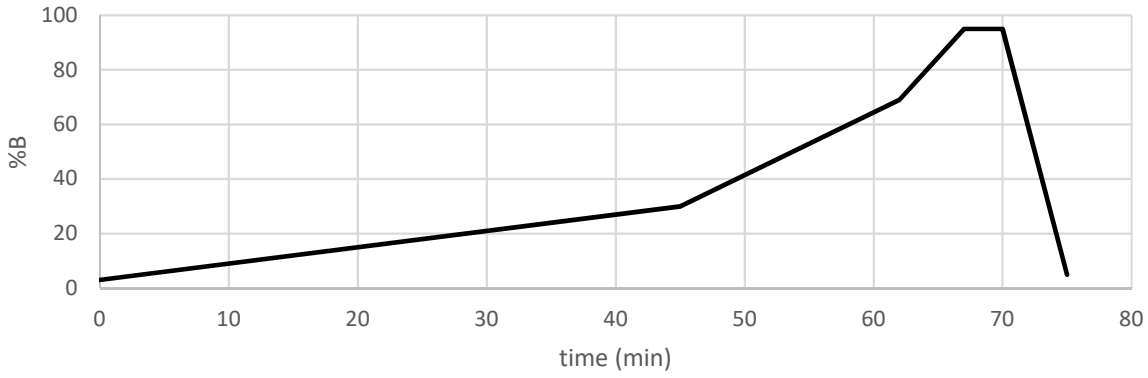

Figure 14: Profile of Gradient A. The gradient used for fractionation experiments. Adapted from Reubsaet, et al. [1]. The flow rate was 200 nL/min.

Table 3 The wavelengths used for UV-detection of various standards.

Solution	λ (nm)
Uracil	256
Thiourea	210
Caffeine	272
Peptides*	210

***Peptides include all peptides from digested samples of HeLa and Cyt C.**

2.4.2 Liquid chromatography-mass spectrometry system in-house

An LC-MS system was set up, consisting of an Easy nanoLC 1000 pump and a Q-Exactive Orbitrap MS with an ESI source and Xcalibur™ software (version 4.2 SP1), all from Thermo Fischer Scientific. The system is illustrated in **Figure 15**. The tubing used was nanoViper™ Fingertight Fittings (Thermo Fischer Scientific) with IDs of 20 µm. Analytical column equilibration was performed prior to all analyses for at least 5 column volumes. The MS parameters used with the Q-Exactive Orbitrap are given in **Table 4**. Blanks of MPA were injected with Gradient B (**Figure 16**), and Gradient A (**Figure 14**) and Gradient C (**Figure 17**) were used for analyses with basic and acidic MPs.

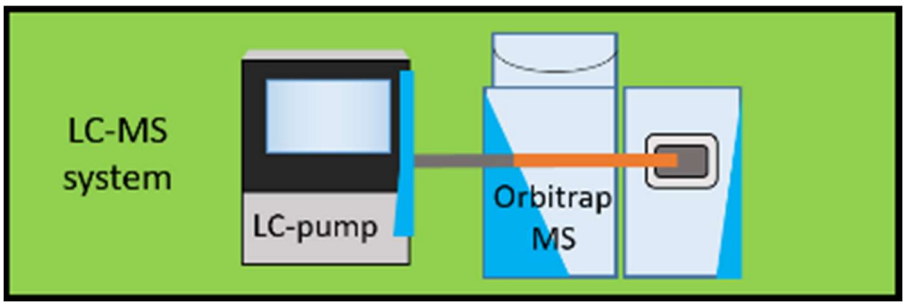

Figure 15: Illustration of the LC-MS system.

Table 4 The MS parameters used with the Q-Exactive Orbitrap.

Runtime	0 to 140 min
Polarity	Positive
MS	
Resolution	70,000
AGC target	5.00E+05
Maximum injection time	50 ms
Scan range	350 to 1500 *m/z*
MS/MS	
Resolution	17,500
AGC target	1.00E+05
Maximum injection time	35 ms
Loop count	3
Isolation window	1.6 *m/z*
Minimum AGC target	8.00E+03
Charge exclusion	-
Dynamic exclusion	60.0 s

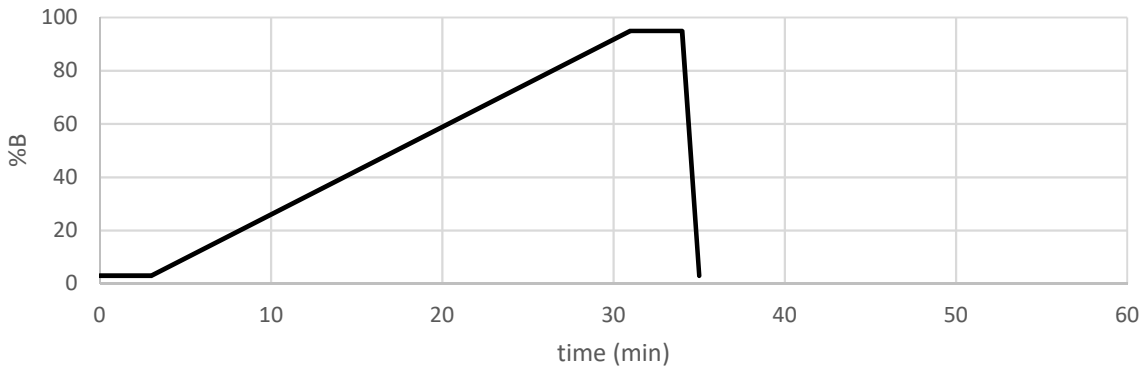

Figure 16. Profile of Gradient B. The gradient used for blanks, which were performed between each injection at low pH. The flow rate was 200 nL/min.

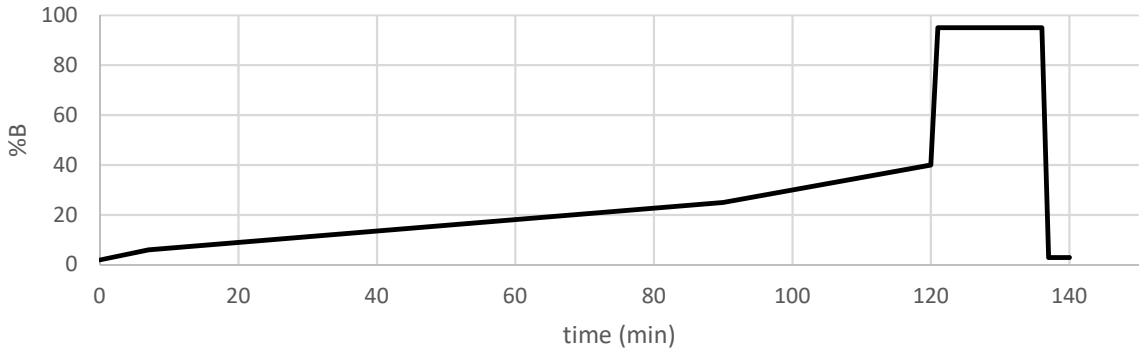

Figure 17. Profile of Gradient C. Used for analysis of concatenated samples, and other samples separated under acidic conditions. Adapted from Reubsaet, *et al.* The flow rate was 200 nL/min.

2.4.3 The Evosep One platform

The Evosep One platform was used with a Q-Exactive HF Orbitrap as the detector. Samples were applied to Evotips, per the Evotip protocol in **Appendix 6.1.4**, and the Evotips loaded with samples were analyzed with the standardized Extended Method. The analytical column was an EV-1106 analytical column, which is a column with C18 AQ beads (1.9 µm), 150 µm ID, and a length of 15 cm. The MS parameters used are shown in **Table 5.** Evosep One experiments were performed in laboratories at Oslo University Hospital under the guidance of Dr. Maria Ekman Stensland. All data was processed with Proteome Discoverer 2.3.0.523, with the workflows shown in **Appendix Figures A 1-2.**

Table 5 The MS parameters used for Q-Exactive HF orbitrap with Evosep One, using Evosep's Extended method. AGC is short for automatic gain control.

Runtime	**0 to 88 min**		
Polarity	Positive		
MS		**MS/MS**	
Resolution	60,000	**Resolution**	60,000
AGC target	3.00E+06	**AGC target**	1.00E+05
Maximum injection time	15 ms	**Maximum injection time**	50 ms
Scan range	375 to 1500 *m/z*	**Loop count**	12
		Isolation window	1.2 *m/z*
		Minimum AGC target	1.00E+03
		Charge exclusion	1, 6
		Dynamic exclusion	30.0 s

2.4.4 The Spider Fractionation platform

Fractionation experiments were performed with the Easy nanoLC 1200 pump, with a 100 µm ID x 20.9 cm Accucore C18 column, and a Spider Fractionator. For the second dimension, two different systems were used. The first was that of an Easy nanoLC 1000 pump, a 50 µm ID x 21 cm Accucore C18 column, a Q-Exactive Orbitrap, used with Gradient C (**Figure 17**) and the MS parameters shown in **Table 4**. The other system used for the second dimension was the Evosep One platform, described in **2.4.3**. All tubing consisted of nanoVipers (Thermo Fischer Scientific) with an ID of 20 µm. The Spider Fractionation system is illustrated in **Figure 18.** Analytical column equilibration was performed prior to all analyses for at least 5 column volumes.

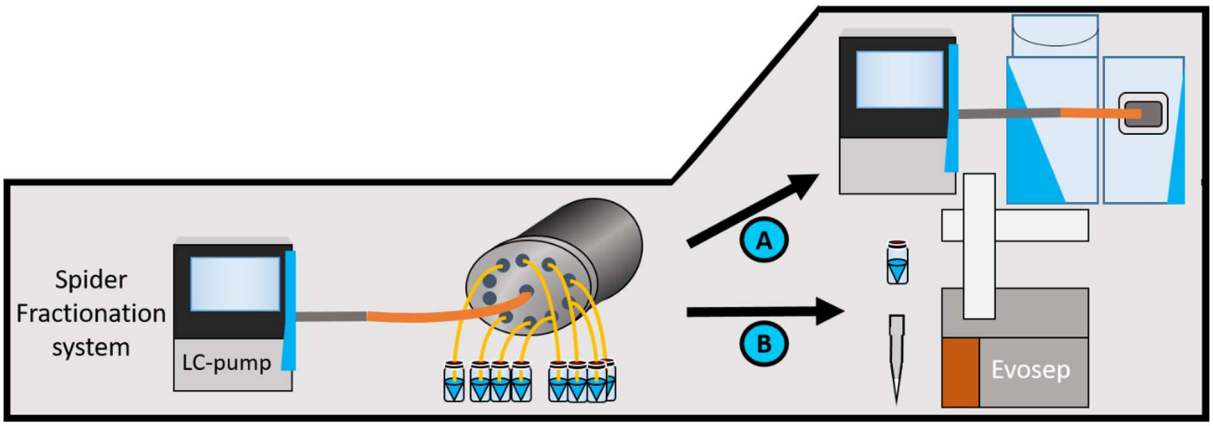

Figure 18: The Spider Fractionation system. Consisted of an LC-pump and the Spider Fractionator for concatenation of fractions. Second dimension analysis was performed with (A) the in-house LC-MS system and (B) the Evosep One platform.

The Spider Fractionator

The Spider Fractionator (**Figure 9**), consisted of a 10-port Multiposition Microelectric Valve Actuator (model EMTMA-CE, VICI®) that could redirect the flow from an input port to one of ten output ports. The flow was directed to different output ports, one at a time, in a semi-automated process performed with a remote control. As can be seen in **Figure 9**, the eight out-directing capillaries send the column flow into the autosampler vials. These capillaries, henceforth referred to as *spider-legs*, were silica capillaries with an ID of 30 µm, and lengths varying from 5.7 to 8.3 cm (volumes of 40-59 nL), depending on the length necessary to ensure submersion in the 0.2% FA solutions in the vials.

Fractionation Conditions

For fractionation, the column output was collected in 8 separate autosampler vials according to the following concatenation scheme: The 1st, 9th, 17th, 25th, 33rd, and 41st fractions were collected in the first vial; the 2nd, 10th, 18th, 26th, 34th, and 42nd in the second, etc. Each fraction was collected for 90 seconds, which translates to 300 nL per fraction with the flow rate of 200 nL/min. In total, 48 fractions were collected in the 8 vials, with 6 fractions totaling 1.8 µL in each vial. The vials were pre-filled with 8.2 µL 0.2% FA (pH 2), yielding an end volume of 10 µL per fraction.

2.4.1 The optimized Spider Fractionation system

The optimized Spider Fractionation system ended up consisting of an Agilent 1200 LC-pump used with ChemStation softare (Rev.B.04.03) (Agilent Technologies). The tubing was silica capillaries with 20 µm ID, and a 4-port injector valve with a loop volume of 50 nL was used for injection. The detection was performed with a Dionex UV detector. The Spider Fractionator was optimized with a new design, referred to as the *Vertical Spider Fractionator*. The system is showed in **Figure 19**.

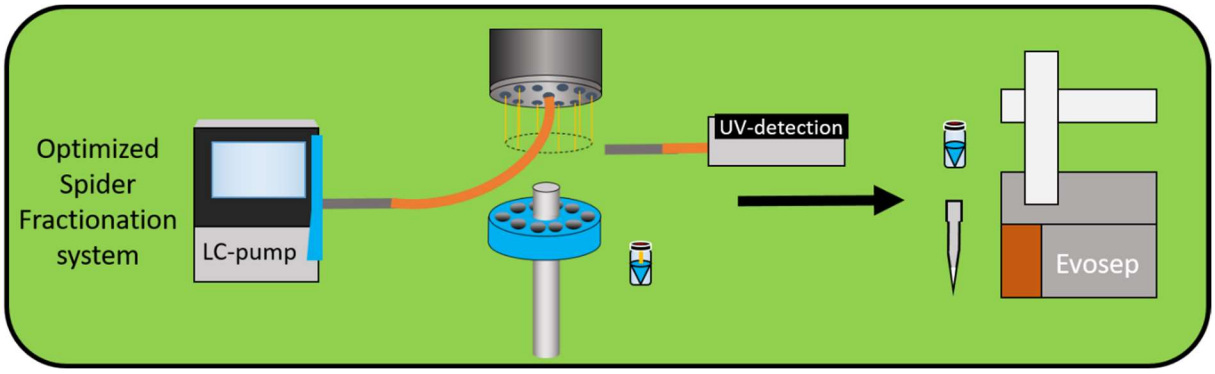

Figure 19 The optimized Spider Fractionation system.

The runs were performed either isocratic at 50% MPB, or with Gradient D (**Figure 20**). The analytical columns used were two in-house packed Accucore C18 columns with IDs of 100 µm, and lengths of 24.0 cm and 18.5 cm, respectively. In addition, a commercial ACE 3 C18 column (Advanced Chromatography Technologies Ltd (ACE®), Aberdeen, UK) with 100 µm ID and a length of 15 cm was used.

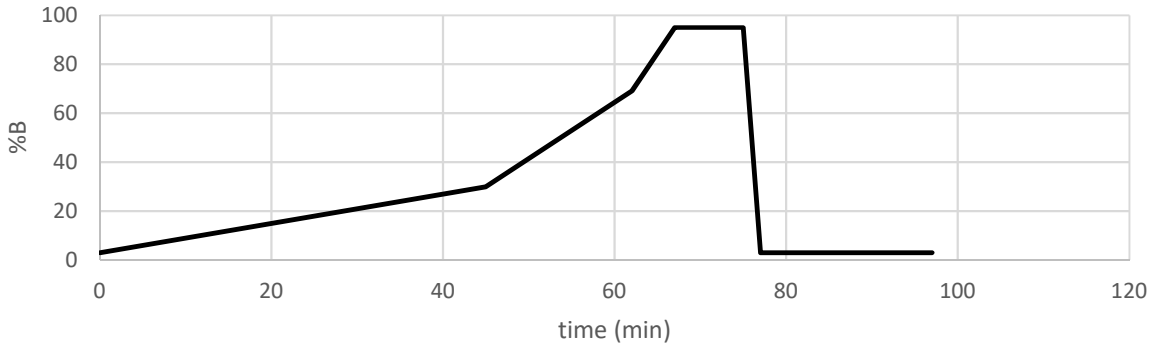

Figure 20: Profile of Gradient D. The gradient used for fractionation with the optimized fractionation system. The flow was increased from 200 nL/min to 450 nL/min after reaching the 95% organic component (from 75 min).

The Vertical Spider Fractionator

The Vertical Spider Fractionator was the optimized spider fractionator made with the help of Engineer Inge Mikalsen. The 10-port-selector was rotated so the exit ports all pointed downwards, with all spider-legs being 8 cm x 10 µm. An adjustable sample vial rack was 3D-printed by Engineer Inge Mikalsen and added to the system, as was a spider-leg collector, which collected the spider-legs and directed them vertically into the vials, as illustrated in **Figure 21**. The 3D-printer used was a Form 3B (Formlabs, Somerville, MA, USA).

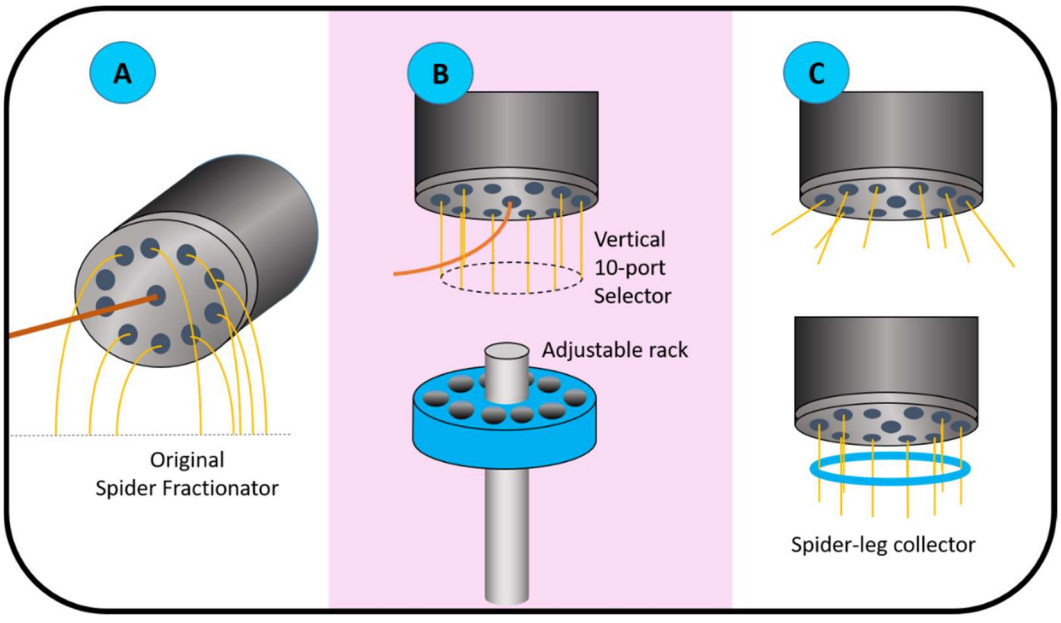

Figure 21: Illustrations of the improvements and additions to the Vertical Spider Fractionator. To the left (A) is the original, vertical Spider fractionator. In the middle (B), it is shown how the 10-port selector is rotated to point vertically downwards, as is the addition of the 3D-printed sample vial rack that can be moved up and down. To the right (C) is the 3D-printed spider-leg collector, which directs the spider-legs vertically into the sample vials.

3. Results and discussion

The goal of the present study was the establishment of a complete proteomics method with the combination of sample preparation with SPEED, in-house packed analytical columns, fractionation with the Spider Fractionator, and second dimension separation and detection with the Evosep One platform. The SPEED method was evaluated in **Section 3.1**, and the packing of analytical columns is presented in **Section 3.2**. The chromatographic capabilities of these columns were evaluated with LC-UV and LC-MS, as presented in **Section 3.3.** The Spider Fractionation system was set up and used for fractionation experiments, as detailed in **Section 3.4**, and attempted optimized in the optimized Spider Fractionation system, as discussed in **Section 3.5** The systems used for the experiments are illustrated in **Figure 22**. Even though the sample preparation with SPEED was carried out after the setup of the Spider Fractionation system, it is presented first due to sample preparation being performed prior to further separation and analysis.

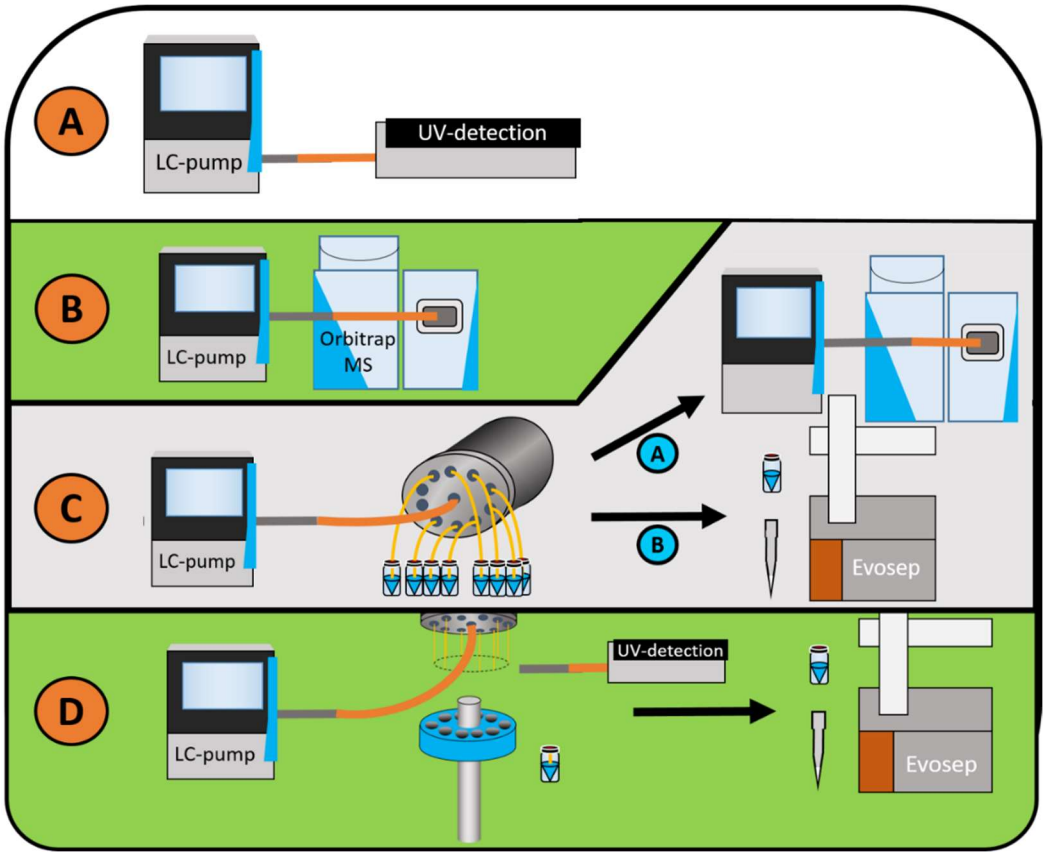

Figure 22 The systems used for the chromatography-based experiments. (A) The LC-UV system used for initial tests and attempts at evaluation of the chromatography. (B) the LC-MS system used for evaluation of the chromatography. (C) the Spider Fractionation platform used for fractionation experiments. (D) the optimized Spider Fractionation platform.

3.1 Sample preparation with SPEED

As the goal of this study was achieving a complete system for protein analysis, the sample preparation step was important. SPEED was chosen, due to it being a simple, inexpensive and universal method for tryptic digestion of proteins into peptides. SPEED is performed in-solution with a single extraction step, requiring little transfer of sample [9]. This is in accordance with one of the goals of the method: minimizing sample loss when possible. Efficiency is also desired, and SPEED is stated to yield improved efficiency compared to the commonly used detergent-based methods, with as much as a 40% increase in peptide and protein identifications [9]. SPEED has also been used for global proteomics with fractionation (in the form of StageTips [61]) to promising effect [9]. The Evosep One platform (**Section 2.4.3**) was used to analyze samples of SW480 cells and of pancreatic islets.

3.1.1 Challenges with protein concentration determination

The SPEED protocol (**Appendix 6.1.1**) was followed for preparation of SW480 cells, but there were issues with the concentration determination step following the protein extraction. This step used the BCA kit to determine concentrations of proteins in each protein-containing solution, which was important to ensure correct dilution and addition of trypsin for the later digestion step. A calibration curve of solutions containing varying amounts of BSA solved in water was prepared and used to determine protein concentrations with BCA, as per the BCA protocol (**Appendix 6.1.2**). Several attempts at BCA were performed. In every attempt, one or more solutions did not react properly, and it turned out impossible to estimate the concentrations. This could be due to problems with the BCA kit, with the reagents contained in it possibly being contaminated or otherwise expired. It is also possible that the pipettes used struggled with delivering the appropriate miniscule volumes in the low μL range. The BSA solutions were considered as the possible cause of the issues, as there were problems with getting reactions in the calibration standards at times. However, several stock solutions of BSA were prepared and used, so this was not likely to be the source of error.

Following the lack of protein concentration estimates, the addition of trypsin, being dependent on the protein concentration, had to be estimated and chanced at. This led to a too high ratio of protein to trypsin, which most probably adversely affected the digestion.

In summary, there were troubles with BCA, leading to too much trypsin being added to the samples in the sample preparation with SPEED.

3.1.2 Identification of proteins in SW480 cells

The cell samples prepared with SPEED and analyzed with the Evosep One Platform yielded the protein and peptide identifications shown in **Table 6.** A total ion chromatogram (TIC) for sample SW480-03 is shown in **Figure 23** as an example chromatogram. The numbers of protein identifications were low for approx. 1 million of these cells. The repeatability was also poor, as was seen by the high relative standard deviations (RSDs). Both of these observations could probably be credited to the excessive volumes of trypsin added (approx. 10x the correct volume, see **Appendix 6.2.2**). By adding too much trypsin, the trypsin would have cleaved other trypsin proteins, producing large amounts of peptides from the trypsin [3] (p.63). The presence of these highly concentrated enzyme-derived peptides would adversely affect the signals due to the limited dynamic range of the MS.

Table 6: The numbers of protein groups and peptides in SW480 cells determined with Proteome Discoverer after preparation with SPEED and analysis using the Evosep One platform. Included in the table are the relative standard deviations.

Sample	Master Proteins	Peptides
SW480-01	388	1080
SW480-02	209	589
SW480-03	649	1877
SW480-04	1096	3945
SW480-05*	N/A**	N/A**
SW480-06*	1104	3473
RSD	59%	67%

***Sample 05 and 06 were analyzed in a different experiment, having been prepared with SPEED together with the pancreatic islets discussed in 0. **No proteins or peptides were identified in this sample due to the MS stopping mid-run.**

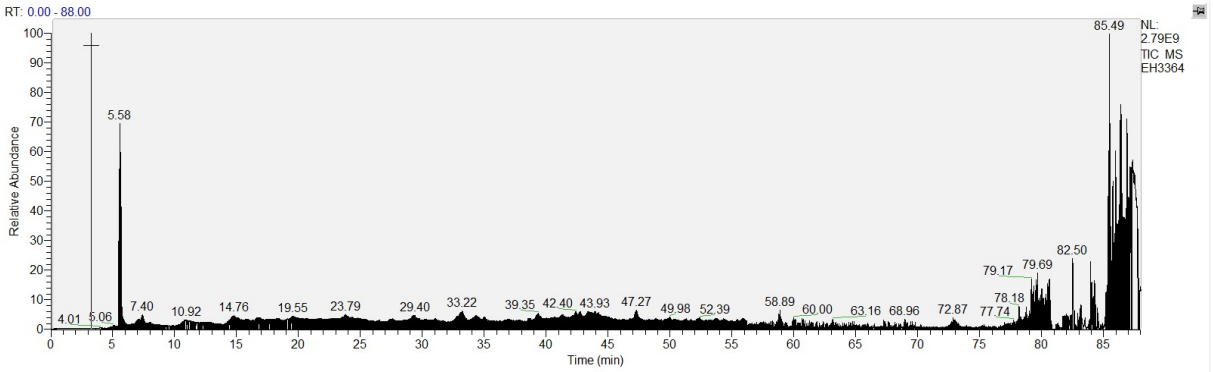

Figure 23 TIC for SW480-03. Pancreatic islets prepared with SPEED and analyzed with the Evosep One platform

In summary, SW480 cell samples were prepared with SPEED and analyzed with Evosep. The resulting identification numbers proved lower than expected, and with a high standard deviation. This was possibly due to the addition of excessive volumes of trypsin.

3.1.3 Identification of proteins in pancreatic islets

Samples of pancreatic islets from mice were also prepared. It should be noted, however, that more than half of the cells were lost during transportation, lowering the amount available for analysis. In addition, when attempting to lower the volume of trypsin added to the samples, the added trypsin volume still turned out too high due to a miscalculation. As the protein concentrations were unknown, the mouse samples were added different volumes of trypsin. Mus A1, A2, and the blank were added 1.0 µg trypsin, and Mus B1 and B2 were added 0.25 µg trypsin. The trypsin added was 77x and 19x the correct volume for these protein amounts, respectively (see **Appendix 6.2.2**). The identified peptides and proteins analyzed with the Evosep One platform are shown in **Table 7.** A TIC for Mus A1 is shown in **Figure 24**.

Table 7: Number of identified proteins and peptides in the pancreatic islet samples. The samples were prepared with SPEED and analyzed with the Evosep One platform. The SW480-samples, the Blank, and the Mus A1 and A2 were all added 1 µg trypsin, while Mus B1 and B2 were added 250 ng trypsin.

Sample	Unique Proteins	Unique Peptides
Mus A1	600	1480
Mus A2	N/A*	70
Mus B2	N/A*	122
Mus B1	N/A*	104
Blank	N/A*	89

***No proteins were identified in these runs due to the number of identified peptides being too low (<200) for the Proteome Discoverer software to identify them.**

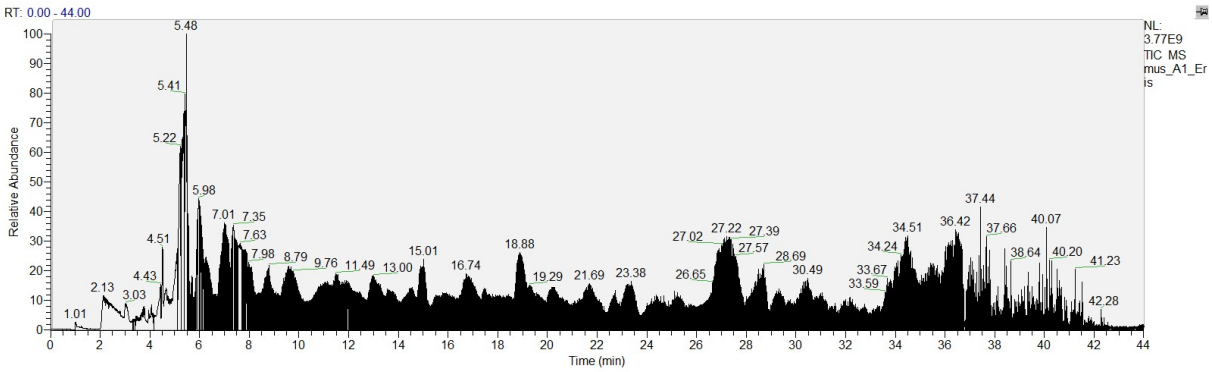

Figure 24 TIC for Mus A1. Pancreatic islets prepared with SPEED and analyzed with the Evosep One platform.

It was observed that the numbers protein identifications in most of the pancreatic islet samples were too low to yield a proper number from Proteome Discoverer. The exception was Mus A1, where some proteins were identified. Considering the challenges involved with loss of sample during initial transportation, and the large volumes of trypsin added for digestion, lower numbers of identifications were expected. The successful identifications in Mus A1 (which had the larger volume of trypsin added) indicated that the trypsin addition might not be the sole cause of the poor numbers of identifications. Regarding the repeatability issue observed for the SW480 cell sample replicates, not much could be deduced, as there were too few replicates of the pancreatic islet samples available, as 3 out of 4 samples yielded insufficient numbers of identifications to be measureable with the software.

As these were pancreatic islets, the presence of characteristic master proteins were investigated for Mus A1. Insulin, somatostatin, and glucagon were all confirmed, proving that the method at least was finding proteins expected for cells from pancreatic islets [62].

In summary, pancreatic islet cell samples from mice were prepared with SPEED and analyzed with the Evosep One platform. The resulting identifications were low for one of four samples, with the rest failing due to too few identifications. This was expected due to excessive addition of trypsin and loss of sample during transportation. The presence of master proteins characteristic of pancreatic islet activity indicate that the method at least is identifying the expected proteins.

3.1.4 Final thoughts on the use of SPEED

The lack of identifications for pancreatic islets and the high standard deviations for the SW480 cell identifications indicates that the SPEED method was somewhat difficult to apply. The problems with the BCA, the transport of samples, and the large volume of trypsin added, were challenges that probably all affected the numbers of identifications, as well as the lack of repeatability. SPEED is probably still a candidate for sample preparation strategy of choice; however, more time and testing would be needed for proper application.

3.2 Packing of analytical columns

The nanoLC columns were packed in-house due to cost efficiency, as emptying a single conventional LC-column can provide particles for packing a large batch of nanoLC columns. The cost efficiency is especially relevant when high pH separations are performed, as the capillary walls and particles (both silica) degrade at high pH levels [1, 63]. In-house packing of columns with Accucore particles has also been proven to be fast and reproducible [59]. The Accucore C18 150 particles were chosen for their good performance for peptide analysis with high peak capacities [64]. The increased performance is due to their larger pore sizes (150Å), and the efficiency gain from being SPPs.

Several analytical columns were packed and used for this study, with lengths varying from 15 to 25 cm, and IDs of 100 and 50 μm. As several columns were used for preliminary studies, the exact lengths and IDs of the most important columns are noted for the relevant experiments. The preparation of guard columns with the same particles to protect the analytical columns was considered [12] (p.57). However, due to the short expected lifetime of the silica columns and particles under basic conditions, the use of guard columns was discarded, as it would complicate the system and potentially add extra-column band broadening from the need for additional fittings.

3.2.1 Challenges with column packing

When packing columns, two challenges had to be addressed. The first concerned the solutions in the Frit Kit expiring. The Frit Kit consisted of formamide, and the fritting solution Kasil 1624. Kasil 1624 seemed to have expired, with visible gelation having occurred, which made it difficult to achieve proper frit formation. After acquiring a new FritKit, no issues arose with further fritting. It is noteworthy that the Kasil 1 solution, included in the frit kit to improve frit formation when added, had a significantly shorter lifespan compared to the other solutions. Kasil 1 seemed to gelate after about a month after first time opening.

The second challenge was with the packing process itself, and concerned the sedimentation rate of particles in organic solvent. The particles were suspended in the slurry, and stable suspension was necessary for achieving efficient packing with proper particle distribution in the columns [65]. As the particles eventually would settle as sediment in organic solvents, the packing process was temperature-dependent. Due to significantly fluctuating temperatures in the laboratory, it was at times more difficult to pack columns to the wanted length of 25 cm during late-fall and

winter. The effect of temperature in column packing is documented in the literature, with the packing efficiency being doubled at 70 °C compared to room temperature [65]. It is also known that packing efficiency is more difficult for columns longer than 15 cm, due difficulties with avoiding sedimentation when longer packing times are required [65]. It therefore seems valuable to look into the use of an oven or a similar way to increase temperature for future column packing of longer columns.

An important note is that neat ACN, rather than MeOH, was used as solvent in the packing slurry for packing most of the columns, due to an early misconception. While trying to figure out why there were problems with packing long columns, the switch to ACN was performed due to its lower viscosity compared to the initially used MeOH [59]. There is precedence for using neat ACN for packing [65]. However, as increasing viscosity has been shown to correlate with faster sedimentation rates [59], the change in solvent to one with increased viscosity may have resulted in poorer particle distribution in the columns, possibly hampering the efficiencies of the columns [65].

In summary, packing of nano-volume analytical columns is a simple, cost-efficient way of preparing many columns, which was essential due to the degrading of Silica-based columns in basic MPs. The columns prepared had IDs of 50 and 100 μm, and lengths from 10-25 cm. The challenges faced were with sedimentation of particles in slurry during packing, and with the FritKit expiring. In addition, ACN was used as solvent in the packing slurry, which increased the sedimentation rate, possibly hampering the packing process.

3.3 Evaluation of the chromatography

To ensure the repeatability and quality of the chromatographic capabilities of the columns and systems in use, evaluation of the chromatography for peptides was performed with UV- and MS detection. UV detection was initially chosen due to availability and its simplicity.

3.3.1 Bacterial growth in basic mobile phases

Before starting the evaluation, a challenge with the MPs should be addressed. After 2-3 weeks visible clumps of bacteria were observed in the MPA reservoir (2% ACN in 20 mM NH_4Ac). This was most likely due the buffer used, NH_4Ac. This buffer, especially with high pH, has very good conditions for bacterial growth, and has been used as a buffer to purposefully grow bacteria [66]. Having clumps of bacteria entering the pump or the rest of the system could clog the tubing, or possibly harm the pump. To combat this bacterial infection of the MPs, new MPs were prepared every week.

3.3.2 Evaluating the chromatography with UV detection

As described in **Section 2.4.1**, five LC-UV systems were set up for this purpose. The first pump had a massive internal leak; the second was unable to deliver stable flow when running gradient programs for MP composition; and the third was unable to deliver stable flow at the wanted low flow rates (200 nL/min). Moreover, after acquiring a functioning pump, it became apparent that the UV-detector used was malfunctioning. The detector only produced a line in the chromatograms, not even responding to the removal of the flow cell during a run. It was then replaced with a different UV detector, ending up with a system consisting of an Easy nLC 1200 pump and a Dionex UV detector.

The peptide bond CO-NH has absorption between 185-220 nm [67]. It did not appear to be a strong chromophore, which made it necessary to have high concentrations of peptides in standards and samples. The solutions of Cyt C and HeLa used did not have sufficient concentrations for detection using the UV detector. As such, the UV detector was replaced with a Q-Exactive Orbitrap MS.

In summary, LC-UV was used in an attempt to evaluate the chromatography. After struggling with several instruments, and ultimately having too low concentrations of HeLa and Cyt C to detect them with the UV detector, the system was replaced with an LC-MS system.

3.3.3 Evaluating the chromatography with mass spectrometry

To evaluate the chromatography, some standards were analyzed in-house with the Q-Exactive Orbitrap system. 1.8 pmol/μL Dionex™ Cytochrome C (Cyt C) Digest (Thermo Fischer Scientific), and 0.02 μg/μL HeLa digest were analyzed with basic MPs and an in-house packed Accucore C18 column of 100 μm ID x 20.9 cm, using Gradient A. In addition, 20 ng/μL HeLa was injected with HeLa was injected on an in-house packed Accucore C18 column of 50 μm ID x 21.0 cm, with Gradient C (**Figure 17**) and acidic MP_2s. For the all experiments, the volumes injected were 8 μL, with loading volumes of 10 μL. The flow rate was set to 200 nL/min. The MS parameters used are shown in **Table 4.** Blanks were run between each injection of HeLa, with the same MS parameters, apart from the shorter Gradient B (**Figure 16**), which had the shorter gradient time of 35 min.

The switch to LC-MS led to some challenges with basic MPs on an MS run in positive mode. The challenges might also have been attributed to the use of a column that was past its prime. Selected TICs for tests with basic MPs for both a Cyt C and a HeLa test are shown in **Appendix 6.3.1.** Most of the peptides were eluted immediately, or they ended up in the blanks. The quality of the separation was poor, and attempts to identify peptides and proteins with Proteome Discoverer resulted in failed processing due to too few peptide identifications (<200). To take a step back and see if the system performed better with more normal conditions, acidic MP_2s were used, as was a new column with 50 μm ID, as was used by Reubsaet, *et al* for the second dimension analysis [1].

A low number of proteins was identified under acidic conditions. The repeatability of the number of identifications, however, seemed decent, with RSDs of <15% for both peptide- and protein identifications. The poor numbers of identifications might be due to the MS parameters used, which were taken directly from Reubsaet, *et al.* [1]. The parameters were used for an ion trap-Orbitrap instrument, not a quadrupole-Orbitrap one, as was used in these experiments. This was not investigated further due to time constraints. Even so, as can be seen from the TICs, the peptides were separated over the entire gradient, with many eluting at the end. There was also an improvement over the previous attempts with basic MPs, in which no data was attainable from Proteome Discoverer due to too few identifications. The increase in number of identifications could be due to the superior degree of ionization with the combination of acidic MPs and positive mode ESI, over that with basic MPs. It could also be because of the downscaling of the chromatographic columns, from 100 μm ID to 50 μm ID, which would increase the sensitivity.

As the LC-Q-Exactive Orbitrap system was not intended to be used in the final method, but rather the Evosep One platform with a Q-Exactive HF Orbitrap, further evaluation and optimization of this system was deemed less important, and were not performed due to time constraints. The TICs and accompanying numbers of identifications from the injections of HeLa samples are shown in **Figure 25** and **Table 8**.

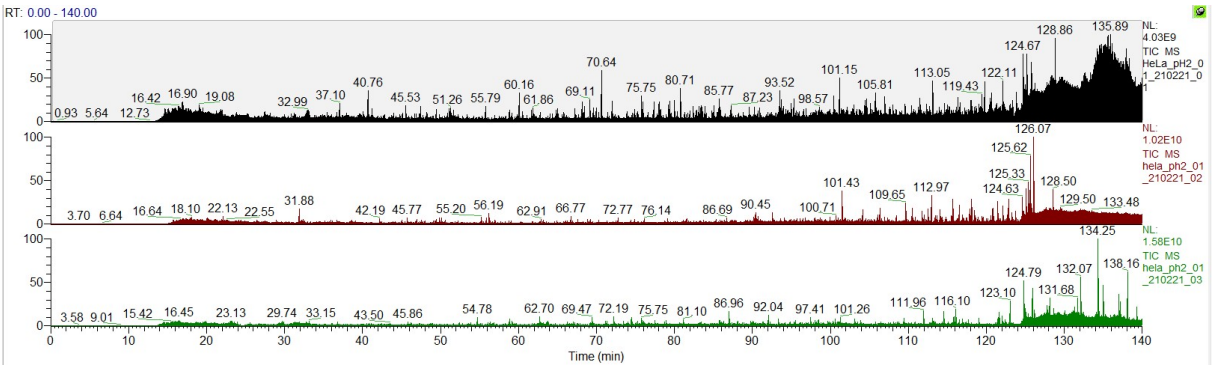

Figure 25 TICs for three replicates of 8 µL of 20 ng/µL HeLa separated with acidic MPs and analyzed with a Q-Exactive Orbitrap. The signal intensity of the 1st TIC is one order of magnitude lower than the following two.

Table 8: The number of proteins and peptides identified from the separations of 8 µL of 20 ng/µL HeLa, performed under acidic conditions. Included are the RSDs.

Sample	Unique Proteins	Unique Peptides
1	316	592
2	380	787
3	387	710
RSD	11%	14%

In summary, the LC-MS system with acidic MPs was superior to the system with basic MPs. This was most likely due to an improved column or due to the mode of ionization. Even so, the acidic experiments yielded numbers of identifications lower than expected, possibly due to the MS parameters used. Due to time constraints and prioritizing, further evaluation and optimization experiments were not performed.

3.4 The Spider Fractionator

After proving the ability of separation of the in-house packed columns with acidic MPs, the Spider Fractionator was set up and used for four Spider Fractionation experiment (SF01-04). These experiments were performed with basic MPs, under the assumption that the problems with the basic MP evaluation experiments yielded few identifications due to MS-based challenges. In these experiments 18 μL HeLa digest (0.1 μg/μL) was injected and separated. The Spider Fractionator was reassembled between each run, with new spider-legs each time. The column used was a 100 μm ID x 20.9 cm Accucore C18 column, and Gradient A was applied with basic MPs, and a loading volume of 20 μL. SF01 was analyzed in the second dimension with the Orbitrap, and SF03-04 were analyzed with the Evosep One platform. The dwell volume was not considered for the Spider Fractionation experiments, which resulted in the first fractions of each collection not containing peptides. This also led to losing the most hydrophobic peptides due to stopping the fractionation too early. The identifications were all performed with high confidence (by Proteome Discoverer), and at least 200 peptide identifications are needed for the software to process data properly. The number of proteins were also reported as master proteins, that is to say, all proteins with identical peptide compositions were compounded.

The focus for the fractionation was to obtain the maximum number of identified peptides, rather than proteins. The purpose of fractionation was the enhancement of peptide separation, which again would lead to increased protein identification. As such, the number of proteins identified in each fraction was of little interest, as the method was looked at in its entirety. After all, the peptides were separated by their hydrophobicity, and the peptides originating from the same protein may have ended up in more than one fraction.

3.4.1 Results from fractionation experiments

For 3 out of 4 experiments, the fractionation was a success. SF02 had to be discarded during fractionation due to missing a single timestamp at which the semi-automated system was to be switched. This proved the improved robustness full automatization would bring, by eliminating human error. However, full automatization was not compatible with the instrumentation used in this study. CFs of SF01 were analyzed in-house with the Q-Exactive Orbitrap MS, similar to the experiment in **3.3.3**; and CFs of SF03-04 were analyzed with the Evosep One platform. The numbers of identified peptides in each of the CFs, as well as the totals in each experiment, are presented in **Table 9**. The numbers of identified proteins are shown in **Figure 26**. Blanks were

run between every fraction for all experiments (**Appendix 6.3.3**). No peptides were identified in any of them (meaning <100 peptides found in total), indicating that there were no issues with carry-over in the 2nd dimension for any of the experiments.

Table 9: The number of unique peptides found in each individual fraction, and the total number of peptides between all the solutions fractionated with the Spider Fractionator. SF01 was analyzed using the Q-Exactive Orbitrap, while SF03-04 were analyzed with Evosep and the Q-Exactive HF Orbitrap. All data is processed with Proteome Discoverer 2.3.0.523.

Peptides			
CF #	SF01	SF03 (Evosep)	SF04 (Evosep)
1	<200*	2100*	6003
2	<200*	5481	9625
3	<200*	214	6000
4	2267	343	6311
5	319	11391	8141
6	172	7845	5716
7	335	6045	7736
8	1175	2439	5305
Total	3851	23690	35901

***The entries noted as <200 are done as such as Proteome Discoverer gives no result file when the number of high confidence identifications are less than 200.**

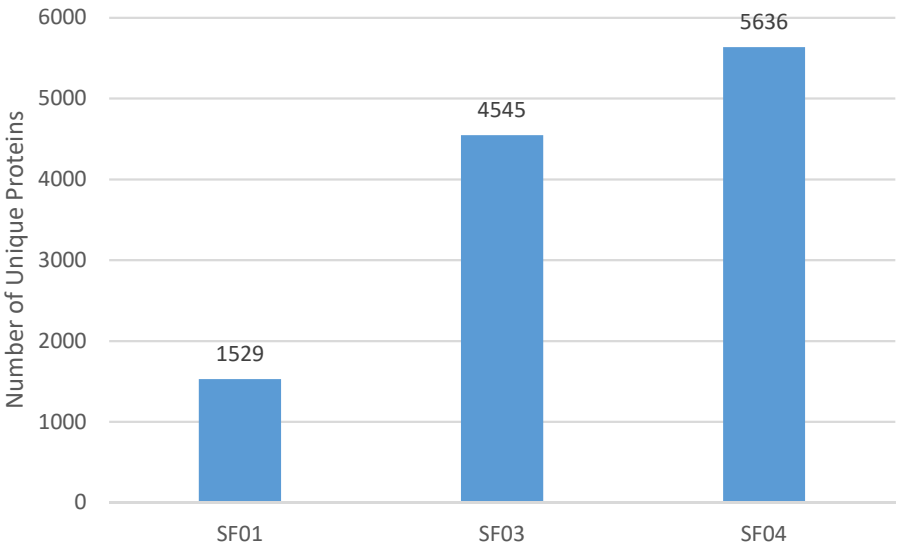

Figure 26: The total number of unique proteins identified in each of the Spider Fractionation experiments. All concatenated samples were processed together with the same consensus workflow in Proteome Discoverer 2.3.0.523.

Spider Fractionation experiment 01

Table 9 and **Figure 26** show that the numbers of identified peptides and proteins in the CFs in SF01 were significantly lower compared to those observed for the CFs in SF03-04. The first three CFs were unable to return a proper result file, due to too low numbers of identifications. It is worth noting that the flow seemingly had stopped through ports 2, 3 and 4 after SF01 fractionation was complete, i.e. no drop was formed at the end of these spider-leg when flushing them after analysis. The spider-legs were probably not fastened into the 10-port selector properly, and they must have come loose during fractionation. The ports were not clogged, as could be deduced from the pressure not increasing when switching to these ports. As the CFs were concatenated by pooling six fractions over the gradient run, it is unlikely that one CF contains so few peptides only due to poor separation. The use of a less sensitive MS compared to the one used for SF03-04, and the instrumental difficulties with properly fastening the spider-legs, are probably the reasons for the poor numbers of peptide and protein identifications in SF01.

It is noteworthy that SF01 was performed with the same MS parameters (**Table 4)** and column as the acidic evaluation experiments (**Section 3.3.3**). By comparing the amounts of identifications with those presented in **Table 8**, the repeatability seems poorer, with some CFs yielding higher and some having lower amounts of peptide identifications. The poor repeatability and low amounts of identifications for SF01 probably stem from the same sources of error affecting the evaluation experiments, most prevalently the MS parameters used.

Spider Fractionation experiments 03-04

The observed numbers of identified peptides and proteins in SF03-04 were more promising. Some of the CFs in SF03 had poor numbers of identifications, similar to those seen in SF01, but overall, the number of identifications in SF03 was much higher than that in SF01. SF04 especially, which appeared to have had none of these issues, had a large number of peptides in each CF. Apart from the repeatability issue, the identified peptide amounts in different CFs were quite similar between SF03 and SF04. That there were issues with repeatability for SF03 but not for SF04 indicates that the problems most likely stemmed from the fractionation. As there were so few samples analyzed, however, it is impossible to be certain whether SF03 or SF04 was the outlier. The advantages over SF01, however, could be due to a number of factors. A powerful Q-Exactive HF was used; the column was commercial and optimized for the system and the standardized (and optimized) method used; as well as the advantages gained with the Evosep One platform, described in **Section 1.5.2**. As there are so many benefits with the Evosep One

platform compared to the simpler LC-MS system, it is impossible to ascertain which factor among those discussed that adds in the most benefits.

Validating the fractionation

In order to validate the fractionation performance, the distribution of peptides between the CFs was also evaluated. For the distribution evaluation, the CFs containing adjacent fractions were focused on, as these in theory should contain the most overlap of the same peptides. Two of these overlaps for SF04 are seen in **Figure 27**. SF04 was chosen for these comparisons, as this was the most repeatable experiment of the three. The two overlap charts show the one with the largest overlap between adjacent ones, and the one with the smallest overlap.

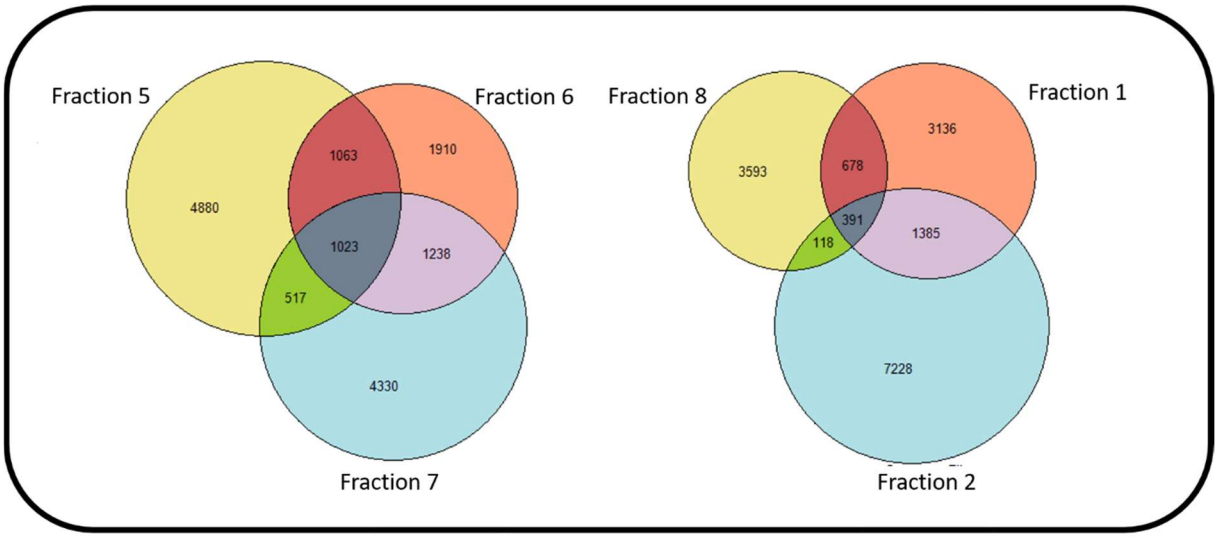

Figure 27: The peptide overlap between two sets of adjacent CFs fractions observed for SF04. The chosen sets of CFs were the set with most overlap between fractions (left), and the set with least overlap (right). The Created with Proteome Discoverer 2.3.0.523.

Figure 27 shows that, while there certainly was decent overlap between the adjacent samples, the peptides unique to each of them comprised large numbers. This was true even for the CF called Fraction 6 in **Figure 27**, which had no overlap with adjacent samples for approx. one third of its peptides. This was especially noteworthy, as this was the CF with the most overlap with its adjacent ones. For Fraction 1, with the least overlap with its neighbors, more than half of the peptides were unique to the CF from the adjacent ones. The overlaps between all adjacent CFs

for SF04 are shown in **Appendix Figure A 3**. This high percentage of peptides unique to the CFs was also reflected in the ratio between total number of unique peptides found in all the fractions together, and the sum of the unique peptides in each CF: The total:sum ratio, which is shown in **Table 10**.

Table 10: The total number of unique peptides in each collection as the sum of each fraction (SUM), and when processing all the fractions together (Total). The relation between the two is shown as percentage Total/SUM. All data is processed with Proteome Discoverer 2.3.0.523.

Unique Peptides			
	SF01	SF03 (Evosep)	SF04 (Evosep)
SUM	4268	33758	54837
Total	3851	23690	35901
Total:SUM	90%	70%	65%

The ratio between the total amount of unique peptides and the sum of all CFs correlated that most of the peptides were distributed between the CFs. The ratio was observed to be decreasing when more peptides were observed, which did make sense, as an increasing number of peptides would increase the chance of the same peptide showing up in several fractions. The ratio was still 65% for SF04, which had the lowest ratio. This meant, in this limited study, the number of unique peptides that showed up in more than one concatenated sample was at most one third of the total. This again indicated that the peptides were decently distributed between fractions.

Final thoughts on the spider fractionation experiments

The fractionation experiments performed with samples SF03-04, which were analyzed with the Evosep One platform, proved that the fractionation technique was functioning, but required powerful, precise instrumentation and methods to yield high numbers of identifications. As there were problems with repeatability for both SF01 and SF03, which were analyzed on different systems in the second dimension, the problems with repeatability most likely stem at least partially from the fractionation. As such, optimization of the fractionation system was warranted, and was explored in **3.5**.

3.5 The optimized Spider Fractionation system

As the results from SF03-04 proved the spider fractionation promising, a new system was set up to be used with an improved spider fractionator design (**Section 3.5.1**). The pump was changed to an Agilent 1200 pump, due to limitations on instrument availability at the time. The pump did have software compatible with the Spider Fractionator 10-port selector valve, possibly allowing for full automatization (**Section 3.5.2**). UV-detection was also introduced to the method, with the Dionex UV detector, in an attempt to ensure decent quality of the chromatography prior to and after each fractionation experiment (**Appendix 6.4.1**). In addition, the actual flow rate delivered by the system had to be measured (**Appendix 6.4.2).** The Evosep One platform proved to work well in earlier fractionation experiments, and was intended to be used for 2nd dimension analysis in this system as well. The optimized Spider Fractionation system did, however, encounter several challenges and intensive troubleshooting was necessary (described in detail in **Appendix 6.4.3**).

3.5.1 The Vertical Spider Fractionator

The Vertical Spider Fractionator (**Figure 21**) is an optimized version of the Spider Fractionator. It was designed, modified and had specially made 3D-printed parts made with the help of Inge Mikalsen. The final design of the Vertical Spider Fractionator is shown in **Figure 28**.

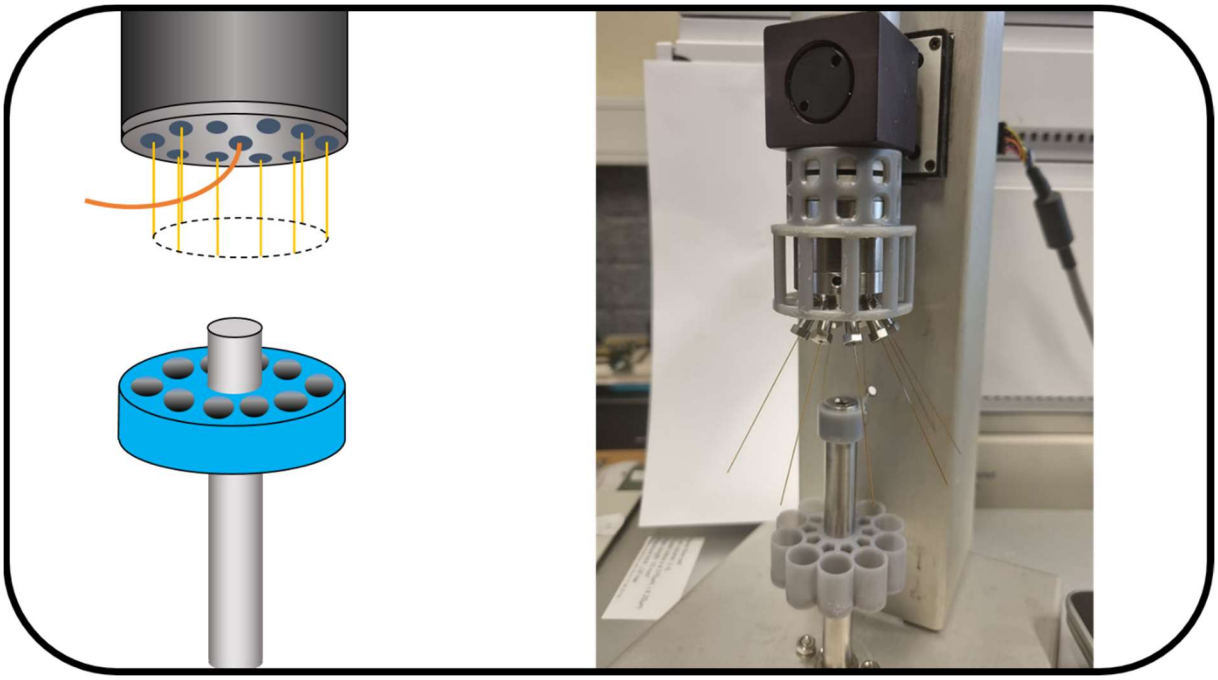

Figure 28: The Vertical Spider Fractionator with a sketch and a photography of the actual instrumentation.

Due to the low flow rate (resulting in low eluting volume in the 90 s intervals of each fraction), it was important to have the spider-legs submerged in the 0.1% FA solutions in the collection vials to ensure all column output ended up in the CFs instead of vaporizing. With the original Spider Fractionator design, the spider-legs had to be maneuvered into the vials, with varying capillary lengths, and bent at odd angles. The original Spider Fractionator is seen in **Figure 9**. For consistency, spider-legs that point straight into the vials with equal lengths were preferred. To achieve these parallel legs, three changes to the spider were made. The 10-port selector was rotated 90 degrees downwards, and the adjustable collection vial rack and the spider-leg collector was added (as illustrated in **Figure 21).** The now equal volumes of the legs would ease calculations concerning the times needed for equilibration and washing. The new legs also had reduced IDs (from 30 µm ID), with new dimensions of 8 cm x 10 µm ID, yielding volumes of 6.3 nL. This low volume is much lower than the eluting volume of 300 nL per fraction during

fractionation (with a system flow of 200 nL/min), leading to minimal amounts of peptide left in the legs after fractionation. An additional benefit was easier handling of the spider-legs and the collection vials, reducing the possibility of pulling out or loosening the legs from the ports in the 10-port selector.

In summary, the Vertical Spider Fractionator, an optimized Spider Fractionator, was designed and set up with specially-made 3D-printed components. The Spider-legs were downscaled from 30 to 10 μm ID, and had short lengths, thanks to the 3D-printed vial rack, the spider-leg collector, and the rotation of the rotor-valve, now pointing downwards. The new sider-legs had reduced, repeatable volumes, and increased robustness.

3.5.2 Attempted automatization

With different LC-software (ChemStation Rev. B.04.033) full automatization of the fractionation process was attempted, as this would ease the fractionation process dramatically, in addition to removing the possible repeatability issues stemming from the operator. This software was capable of sending the signal to the selector valve directly, and a method matching the concatenation scheme was set up in the software. Unfortunately, the software allowed no more than the maximum number of 64 signals sent during any given analysis. As the system required two signals to be sent from the software to change the ports on the Spider Fractionator one time (the software demanded a reset signal before each switch), at least 96 signals were necessary to perform the fractionation as wanted. As such, the use of the actuator remote from **Method B** had to continued, keeping the system semi-automated. With software allowing more signals (or with a different fractionation scheme with fewer signals needed) full automatization could be achieved.

In summary, the optimized spider fractionator was designed and set up, with parallel spider–legs with improved IDs and standardized lengths. Automatization was attempted, but this was not possible with the software available.

3.5.3 Testing and troubleshooting the system

When testing the optimized Spider Fractionation system, major challenges with repeatability presented themselves with the LC-UV system. To address these challenges, the column, MPs, tubing, standard solutions, the injector, and all couplings were replaced, as shown in Table 11. A detailed walkthrough of the troubleshooting performed is given in **Appendix Section 6.4**.

Table 11 The troubleshooting steps performed for this the optimized spider fractionation system.

Suspected component	Measures taken	Outcome	Figure
Autosampler	Swapped out for a manual injector.	No significant effect.	A 16
Analytical column	Swapped out for a commercial column	Sharper peaks, with many peaks indicating pressure drop in UV detector flow cell.	A 17 (A-B)
Restrictor	Swapped out for a new restrictor.	Less noise, but not repeatable intensity for the same sample.	A 17 (C-G)
Manual injector	Swapped out for autosampler, which was washed thoroughly with MeOH. (Also swapped column for an in-house packed Accucore C18).	Maintained low amount of noise, but still not repeatable signal intensities.	A 18-A 19
Tubing (30 µm ID Silica capillaries)	Replaced all tubing with 20 µm ID silica capillaries.	No significant effect.	A 20
Autosampler	Swapped out for a new manual injector.	System was clogged and stopped due to exceeding set pressure limits.	
Manual injector	Connected the pump directly to the column.	System delivered stable flow without rise in pressure.	
Manual injector	Dismantled the injector, drilled open clogged ports, and washed the injector properly with MeOH.	System still delivered stable flow without rise in pressure. Produced nice peak for 120 ng thiourea.	A 21
Cyt C concentration	Prepared 1 µg/µL Cyt C for injection.	Indistingushiable peaks and poor repeatabilty.	A 23
Cyt C digest solutions	1 µg/µL thiourea was prepared and injected for comparison.	Low repeatability in peak shapes and signal intensity.	A 24

To summarize the troubleshooting, the repeatability issues seemed to reappear after some time after fixing, with analytes seemingly ending up stuck somewhere in the system, even when swapping out close to all system components.

3.5.4 Final thoughts on the "optimized" fractionation system

Due to time constraints, further attempts at troubleshooting and optimizing the system were rendered impossible. It was later speculated that, as the injector kept presenting challenges, what kept clogging the injector possibly could be C18-particles from the column being flushed backwards into the injector. The in-house packed columns were only fritted in the flow-direction-end, and were completely open in the back-end. The columns were also cut down to only have a few centimeters of open silica capillary at the back-end. Although there was no recorded evidence of these pressure drops, a drop in pressure was observed when injecting with the manual injector. The use of a filter in the back-end of the columns should be considered for any future attempts at using a similar system.

As repeatable and stable chromatography never was achieved, or at least not proved, with the optimized Spider Fractionation system, the system was never used for any fractionation experiments. The changes to the spider fractionator and the rest of the system should theoretically improve repeatability, robustness, and efficiency, however there is no experimental data backing this up at the time of concluding this study.

4. Conclusion

In this study, the groundwork was set for a complete 2D LC method for global proteomics, from sample preparation to detection and protein identification, utilizing cutting-edge instruments and techniques. The loss-less off-line 2D LC technique was set up with analytical C18 columns packed in-house, and a Spider Fractionator in the first dimension. The Evosep One platform was used with a Q-Exactive HF Orbitrap in the second dimension. With this system >5000 proteins were identified in one HeLa sample. Unfortunately, too few samples were fractionated with the system to come to any conclusions about the actual efficiency, robustness and repeatability of the system. There were, however, some issues with repeatability that probably stemmed from a lack of robustness of the Spider Fractionator. The system was therefore optimized with 3D-printed custom components for the optimized fractionator, the Vertical Spider Fractionator, in addition to different LC-instrumentation and some changes to the methods used. This new system required large amounts of troubleshooting of the common LC equipment, which unfortunately halted the progress of the study to a standstill. Hence, no samples were fractionated with the optimized system. In addition, SPEED was performed for SW480 cells and pancreatic islets, with poor repeatability. About 600 proteins were identified in one of the pancreatic islet samples, proving the potential of the enzymatic digestion if performed properly.

Time constraints from the need for troubleshooting resulted in the complete system never being set up and tested. Nonetheless, the various techniques and instruments appeared to be compatible, albeit in need of optimization. The groundwork is set, and most of the milestones of the study were reached (**Figure 29)**. While the method needs further work and optimization, it has proved that there is potential for high peak capacities.

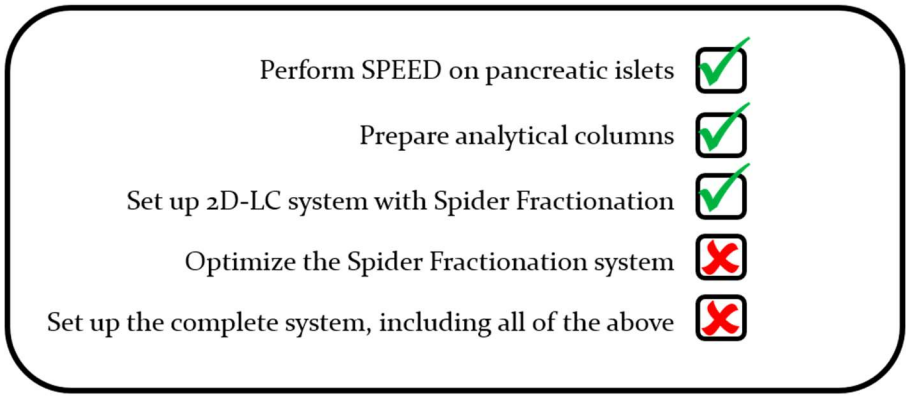

Figure 29 Overview of which of the aims of this study were met.

5. References

1. Reubsaet, L., M.J. Sweredoski, A. Moradian, B. Lomenick, R. Eggleston-Rangel, and S.D. Garbis, *Nano volume fractionation strategy for dilute-and-shoot injections in off-line loss-less proteomic workflows for extensive protein identifications of ultra-low sample amounts.* Journal of Chromatography A, 1609 (**2020**) 460507.
2. Dupree, E.J., M. Jayathirtha, H. Yorkey, M. Mihasan, B.A. Petre, and C.C. Darie, *A critical review of bottom-up proteomics: the good, the bad, and the future of this field.* Proteomes, 8 (**2020**) 14.
3. Greaves, J. and J. Roboz, *Mass spectrometry for the novice*. (**2014**): CRC Press Boca Raton, FL. p.53, 56, 63.
4. Vailati-Riboni, M., V. Palombo, and J.J. Loor, *What are Omics Sciences?*, in *Periparturient Diseases of Dairy Cows*. (**2017**), Springer. 1-7.
5. Steen, H. and M. Mann, *The ABC's (and XYZ's) of peptide sequencing.* Nature Reviews Molecular Cell Biology, 5 (**2004**) 699.
6. Nesvizhskii, A.I., F.F. Roos, J. Grossmann, M. Vogelzang, J.S. Eddes, W. Gruissem, S. Baginsky, and R. Aebersold, *Dynamic Spectrum Quality Assessment and Iterative Computational Analysis of Shotgun Proteomic Data.* Molecular & Cellular Proteomics, 5 (**2006**) 652-670.
7. Giansanti, P., L. Tsiatsiani, T.Y. Low, and A.J. Heck, *Six alternative proteases for mass spectrometry–based proteomics beyond trypsin.* Nature Protocols, 11 (**2016**) 993-1006.
8. Vandermarliere, E., M. Mueller, and L. Martens, *Getting intimate with trypsin, the leading protease in proteomics.* Mass Spectrometry Reviews, 32 (**2013**) 453-465.
9. Doellinger, J., A. Schneider, M. Hoeller, and P. Lasch, *Sample Preparation by Easy Extraction and Digestion (SPEED) - A Universal, Rapid, and Detergent-free Protocol for Proteomics Based on Acid Extraction*.* Molecular & Cellular Proteomics, 19 (**2020**) 209-222.
10. Duan, X., R. Young, R.M. Straubinger, B. Page, J. Cao, H. Wang, H. Yu, J.M. Canty, and J. Qu, *A Straightforward and Highly Efficient Precipitation/On-Pellet Digestion Procedure Coupled with a Long Gradient Nano-LC Separation and Orbitrap Mass Spectrometry for Label-Free Expression Profiling of the Swine Heart Mitochondrial Proteome.* Journal of Proteome Research, 8 (**2009**) 2838-2850.
11. Kollipara, L. and R.P. Zahedi, *Protein carbamylation: in vivo modification or in vitro artefact?* Proteomics, 13 (**2013**) 941-944.
12. Lundanes, E., L. Reubsaet, and T. Greibrokk, *Chromatography: basic principles, sample preparations and related methods*. (**2013**): John Wiley & Sons. p.54, 57, 59, 67, 69, 71, 80, 86-87.
13. Harris, D.C. and C.A. Lucy, *Quantitative chemical analysis*. (**2016**), New York, NY: Freeman Custom Publishing. p.575-577, 559, 640, 671-652, 674.
14. Wilson, S.R., T. Vehus, H.S. Berg, and E. Lundanes, *Nano-LC in proteomics: recent advances and approaches.* Bioanalysis, 7 (**2015**) 1799-1815.
15. Konermann, L., E. Ahadi, A.D. Rodriguez, and S. Vahidi, *Unraveling the Mechanism of Electrospray Ionization.* Analytical Chemistry, 85 (**2013**) 2-9.
16. Vargas Medina, D.A., E.V.S. Maciel, A.L. de Toffoli, and F.M. Lanças, *Miniaturization of liquid chromatography coupled to mass spectrometry.: 2. Achievements on modern instrumentation for miniaturized liquid chromatography*

coupled to mass spectrometry. TrAC Trends in Analytical Chemistry, 128 (**2020**) 115910.
17. Pitt, J.J., *Principles and applications of liquid chromatography-mass spectrometry in clinical biochemistry.* The Clinical biochemist. Reviews, 30 (**2009**) 19-34.
18. Wilm, M. and M. Mann, *Analytical properties of the nanoelectrospray ion source.* Analytical chemistry, 68 (**1996**) 1-8.
19. Gibson, G.T.T., S.M. Mugo, and R.D. Oleschuk, *Nanoelectrospray emitters: Trends and perspective.* Mass Spectrometry Reviews, 28 (**2009**) 918-936.
20. Schmidt, A., M. Karas, and T. Dülcks, *Effect of different solution flow rates on analyte ion signals in nano-ESI MS, or: when does ESI turn into nano-ESI?* Journal of the American Society for Mass Spectrometry, 14 (**2003**) 492-500.
21. Hu, Q., R.J. Noll, H. Li, A. Makarov, M. Hardman, and R. Graham Cooks, *The Orbitrap: a new mass spectrometer.* Journal of Mass Spectrometry, 40 (**2005**) 430-443.
22. Scigelova, M. and A. Makarov, *Orbitrap Mass Analyzer – Overview and Applications in Proteomics.* Proteomics, 6 (**2006**) 16-21.
23. Eliuk, S. and A. Makarov, *Evolution of Orbitrap Mass Spectrometry Instrumentation.* Annual Review of Analytical Chemistry, 8 (**2015**) 61-80.
24. Scheltema, R.A., J.-P. Hauschild, O. Lange, D. Hornburg, E. Denisov, E. Damoc, A. Kuehn, A. Makarov, and M. Mann, *The Q Exactive HF, a Benchtop Mass Spectrometer with a Pre-filter, High-performance Quadrupole and an Ultra-high-field Orbitrap Analyzer*.* Molecular & Cellular Proteomics, 13 (**2014**) 3698-3708.
25. De Hoffmann, E., *Tandem mass spectrometry: a primer.* Journal of Mass Spectrometry, 31 (**1996**) 129-137.
26. Strathmann, F.G. and A.N. Hoofnagle, *Current and Future Applications of Mass Spectrometry to the Clinical Laboratory.* American Journal of Clinical Pathology, 136 (**2011**) 609-616.
27. Michalski, A., E. Damoc, J.-P. Hauschild, O. Lange, A. Wieghaus, A. Makarov, N. Nagaraj, J. Cox, M. Mann, and S. Horning, *Mass Spectrometry-based Proteomics Using Q Exactive, a High-performance Benchtop Quadrupole Orbitrap Mass Spectrometer*.* Molecular & Cellular Proteomics, 10 (**2011**) M111.011015.
28. Gross, J.H., *Tandem mass spectrometry*, in *Mass spectrometry*. (**2017**), Springer. 539-612.
29. Elias, J.E. and S.P. Gygi, *Target-Decoy Search Strategy for Mass Spectrometry-Based Proteomics*, in *Proteome Bioinformatics*, S.J. Hubbard and A.R. Jones, Editors. (**2010**), Humana Press: Totowa, NJ. 55-71.
30. Peterson, A.C., J.D. Russell, D.J. Bailey, M.S. Westphall, and J.J. Coon, *Parallel Reaction Monitoring for High Resolution and High Mass Accuracy Quantitative, Targeted Proteomics*.* Molecular & Cellular Proteomics, 11 (**2012**) 1475-1488.
31. Borràs, E. and E. Sabidó, *What is targeted proteomics? A concise revision of targeted acquisition and targeted data analysis in mass spectrometry.* Proteomics, 17 (**2017**) 1700180.
32. Neilson, K.A., N.A. Ali, S. Muralidharan, M. Mirzaei, M. Mariani, G. Assadourian, A. Lee, S.C. Van Sluyter, and P.A. Haynes, *Less label, more free: approaches in label-free quantitative mass spectrometry.* Proteomics, 11 (**2011**) 535-553.
33. Bateman, N.W., S.P. Goulding, N.J. Shulman, A.K. Gadok, K.K. Szumlinski, M.J. MacCoss, and C.C. Wu, *Maximizing Peptide Identification Events in Proteomic Workflows Using Data-Dependent Acquisition (DDA)*.* Molecular & Cellular Proteomics, 13 (**2014**) 329-338.

34. Nielsen, M.L., M.M. Savitski, and R.A. Zubarev, *Extent of Modifications in Human Proteome Samples and Their Effect on Dynamic Range of Analysis in Shotgun Proteomics* S.* Molecular & Cellular Proteomics, 5 (**2006**) 2384-2391.
35. Anderson, N.L., M. Polanski, R. Pieper, T. Gatlin, R.S. Tirumalai, T.P. Conrads, T.D. Veenstra, J.N. Adkins, J.G. Pounds, R. Fagan, and A. Lobley, *The Human Plasma Proteome: A Nonredundant List Developed by Combination of Four Separate Sources*.* Molecular & Cellular Proteomics, 3 (**2004**) 311-326.
36. Gilar, M., P. Olivova, A.E. Daly, and J.C. Gebler, *Two-dimensional separation of peptides using RP-RP-HPLC system with different pH in first and second separation dimensions.* Journal of Separation Science, 28 (**2005**) 1694-1703.
37. Wilson, S., C. Olsen, and E. Lundanes, *Nano liquid chromatography columns.* Analyst, (**2019**).
38. Roth, M.J., D.A. Plymire, A.N. Chang, J. Kim, E.M. Maresh, S.E. Larson, and S.M. Patrie, *Sensitive and Reproducible Intact Mass Analysis of Complex Protein Mixtures with Superficially Porous Capillary Reversed-Phase Liquid Chromatography Mass Spectrometry.* Analytical Chemistry, 83 (**2011**) 9586-9592.
39. Chervet, J., M. Ursem, and J. Salzmann, *Instrumental requirements for nanoscale liquid chromatography.* Analytical Chemistry, 68 (**1996**) 1507-1512.
40. Noga, M., F. Sucharski, P. Suder, and J. Silberring, *A practical guide to nano-LC troubleshooting.* Journal of Separation Science, 30 (**2007**) 2179-2189.
41. Gilar, M., P. Olivova, A.E. Daly, and J.C. Gebler, *Orthogonality of separation in two-dimensional liquid chromatography.* Analytical Chemistry, 77 (**2005**) 6426-6434.
42. Chapel, S., F. Rouvière, and S. Heinisch, *Pushing the limits of resolving power and analysis time in on-line comprehensive hydrophilic interaction x reversed phase liquid chromatography for the analysis of complex peptide samples.* Journal of Chromatography A, 1615 (**2020**) 460753.
43. Dowell, J.A., D.C. Frost, J. Zhang, and L. Li, *Comparison of Two-Dimensional Fractionation Techniques for Shotgun Proteomics.* Analytical Chemistry, 80 (**2008**) 6715-6723.
44. Kulak, N.A., P.E. Geyer, and M. Mann, *Loss-less nano-fractionator for high sensitivity, high coverage proteomics.* Molecular & Cellular Proteomics, 16 (**2017**) 694-705.
45. Law, H.C.H., R.P.W. Kong, M. Li, S.S.W. Szeto, and I.K. Chu, *Implementation of a multiple-fraction concatenation strategy in an online two-dimensional high-/low-pH reversed-phase/reversed-phase liquid chromatography platform for qualitative and quantitative shotgun proteomic analyses.* Journal of Mass Spectrometry, 56 (**2021**) e4591.
46. Song, C., M. Ye, G. Han, X. Jiang, F. Wang, Z. Yu, R. Chen, and H. Zou, *Reversed-phase-reversed-phase liquid chromatography approach with high orthogonality for multidimensional separation of phosphopeptides.* Analytical Chemistry, 82 (**2010**) 53-56.
47. Yang, F., Y. Shen, D.G. Camp, and R.D. Smith, *High-pH reversed-phase chromatography with fraction concatenation for 2D proteomic analysis.* Expert Review of Proteomics, 9 (**2012**) 129-134.
48. Malerod, H., E. Lundanes, and T. Greibrokk, *Recent advances in on-line multidimensional liquid chromatography.* Analytical Methods, 2 (**2010**) 110-122.
49. Dwivedi, R.C., V. Spicer, M. Harder, M. Antonovici, W. Ens, K.G. Standing, J.A. Wilkins, and O.V. Krokhin, *Practical implementation of 2D HPLC scheme with accurate peptide retention prediction in both dimensions for high-throughput bottom-up proteomics.* Analytical chemistry, 80 (**2008**) 7036-7042.

50. Wang, Y., F. Yang, M.A. Gritsenko, Y. Wang, T. Clauss, T. Liu, Y. Shen, M.E. Monroe, D. Lopez-Ferrer, T. Reno, R.J. Moore, R.L. Klemke, D.G. Camp II, and R.D. Smith, *Reversed-phase chromatography with multiple fraction concatenation strategy for proteome profiling of human MCF10A cells.* Proteomics, 11 (**2011**) 2019-2026.
51. Falkenby, L.G., G. Such-Sanmartín, M.R. Larsen, O. Vorm, N. Bache, and O.N. Jensen, *Integrated Solid-Phase Extraction–Capillary Liquid Chromatography (speLC) Interfaced to ESI–MS/MS for Fast Characterization and Quantification of Protein and Proteomes.* Journal of Proteome Research, 13 (**2014**) 6169-6175.
52. Bache, N., P.E. Geyer, D.B. Bekker-Jensen, O. Hoerning, L. Falkenby, P.V. Treit, S. Doll, I. Paron, J.B. Müller, F. Meier, J.V. Olsen, O. Vorm, and M. Mann, *A Novel LC System Embeds Analytes in Pre-formed Gradients for Rapid, Ultra-robust Proteomics*.* Molecular & Cellular Proteomics, 17 (**2018**) 2284-2296.
53. Bache, N., P.E. Geyer, D.B. Bekker-Jensen, O. Hoerning, L. Falkenby, P.V. Treit, S. Doll, I. Paron, J.B. Müller, and F. Meier, *A novel LC system embeds analytes in pre-formed gradients for rapid, ultra-robust proteomics.* Molecular & Cellular Proteomics, 17 (**2018**) 2284-2296.
54. *EVOSEP+ Application Note: More proteome coverage in a single experiment with the **Extended method**.* (**n.d.**). DOI: evosep.com/wp-content/uploads/2020/06/Extended-Method-AppNote-Exploris.pdf
55. Ambrosi, A. and A. Bonanni, *How 3D printing can boost advances in analytical and bioanalytical chemistry.* Microchimica Acta, 188 (**2021**) 265.
56. Wang, L. and M. Pumera, *Recent advances of 3D printing in analytical chemistry: Focus on microfluidic, separation, and extraction devices.* TrAC Trends in Analytical Chemistry, 135 (**2021**) 116151.
57. Su, C.-K., *Review of 3D-Printed functionalized devices for chemical and biochemical analysis.* Analytica Chimica Acta, 1158 (**2021**) 338348.
58. He, F., *BCA (Bicinchoninic Acid) Protein Assay.* Bio-protocol, 1 (**2011**) e44.
59. Berg, H.S., K.E. Seterdal, T. Smetop, R. Rozenvalds, O.K. Brandtzaeg, T. Vehus, E. Lundanes, and S.R. Wilson, *Self-packed core shell nano liquid chromatography columns and silica-based monolithic trap columns for targeted proteomics.* Journal of Chromatography A, 1498 (**2017**) 111-119.
60. Rogeberg, M., T. Vehus, L. Grutle, T. Greibrokk, S.R. Wilson, and E. Lundanes, *Separation optimization of long porous-layer open-tubular columns for nano-LC–MS of limited proteomic samples.* Journal of Separation Science, 36 (**2013**) 2838-2847.
61. Rappsilber, J., M. Mann, and Y. Ishihama, *Protocol for micro-purification, enrichment, pre-fractionation and storage of peptides for proteomics using StageTips.* Nature Protocols, 2 (**2007**) 1896-1906.
62. Donohue, M.J., R.T. Filla, D.J. Steyer, W.J. Eaton, and M.G. Roper, *Rapid liquid chromatography-mass spectrometry quantitation of glucose-regulating hormones from human islets of Langerhans.* Journal of Chromatography A, 1637 (**2021**) 461805.
63. Kirkland, J.J., J.W. Henderson, J.J. DeStefano, M.A. van Straten, and H.A. Claessens, *Stability of silica-based, endcapped columns with pH 7 and 11 mobile phases for reversed-phase high-performance liquid chromatography.* Journal of Chromatography A, 762 (**1997**) 97-112.
64. Vehus, T., K.E. Seterdal, S. Krauss, E. Lundanes, and S.R. Wilson, *Comparison of commercial nanoliquid chromatography columns for fast, targeted mass spectrometry-based proteomics.* Future Science OA, 2 (**2016**) null.
65. Capriotti, F., I. Leonardis, A. Cappiello, G. Famiglini, and P. Palma, *A Fast and Effective Method for Packing Nano-LC Columns with Solid-Core Nano Particles*

Based on the Synergic Effect of Temperature, Slurry Composition, Sonication and Pressure. Chromatographia, 76 (**2013**) 1079-1086.
66. Kornberg, H., *The metabolism of C2 compounds in micro-organisms. 1. The incorporation of [2-14C] acetate by Pseudomonas fluorescens, and by a Corynebacterium, grown on ammonium acetate.* Biochemical Journal, 68 (**1958**) 535.
67. Issaq, H.J., *The role of separation science in proteomics research.* Electrophoresis, 22 (**2001**) 3629-3638.
68. Evosep. *Evotips*. (**n.n.**) 09.10.21; Available from: https://www.evosep.com/evotip/.

6. Appendix

6.1 Protocols

6.1.1 SPEED protocol

The protocol followed for enzymatic digestion of protein standards and cell pellets with SPEED.

1. Thaw cell pellet, DTT and IAM on ice in the dark. DTT should lie on top of the ice, as it thaws slowly, and IAM is light sensitive.
2. Prepare the following solutions:
    a) 1 mL 2 mg/mL BSA
    b) 10 mL water
    c) 300 μL TFA
    d) 3 mL 2M tris (ensure pH = 12 with pH strips)
3. Take 10 μL cells from cell pellet/protein standard.
4. Add 40 μL TFA to each sample. (cells:TFA 1:4, v/v)
5. After 2-3 min, add 400 μL 2M tris to each sample (10x volume of TFA)
6. Perform BCA, according to the BCA protocol (Section 6.1.2).
7. Add 4.5 μL 1M DTT to each sample, and shake at 700 rpm for 25 min at 56 °C.
8. Add 9 μL IAM to each sample, and shake at 700 rpm for 20 min at room temperature in the dark.
9. Add 2.1 μL 1M DTT to each sample, and shake at 700 rpm for 15 min at room temperature in the dark.
10. Take out sample solution and add TFA+2M tris (1+10) to get 100 μL of 1 μg/mL protein. Repeat for each sample. (Concentration was found with BCA in step 6).

11. Add 500 μL water to each sample (sample:water 1:5 (v/v)).
12. Add trypsin in a ratio (w/w) of 1:100 (for protein concentrations of 1 μg/mL).
13. Incubate overnight in shaker at 37 °C.
14. Add 12 μL TFA to end digestion. Ensure pH = 2 with pH strips.
15. Evaporate solvent by centrifugation, and perform Ziptip (**Section 6.1.3**) for rinsing of samples.

6.1.2 BCA protocol

The protocol followed to determine protein concentrations of samples during SPEED, with BCA.

1. Prepare standards for calibration.
    a. Prepare μL 2 mg/mL BSA solved in water. (2000 μg/mL).
    b. Dilute to 1000 μg/mL, then 500 μg/mL, 250 μg/μL, 125 μg/μL, and 25 μg/μL.
    c. The final standard is a blank of only water.
2. Mix working reagents A and B at 50:1 ratio to required volume (200 μL per sample+100 μL).
3. Dilute samples 10x to avoid interference from reagents.
4. Transfer 25 μL of each sample solution and standard to microwells.
5. Add 200 μL working reagent mix to each well, and shake for 30 sek.
6. Cover and incubate at 37 °C for 30 min.
7. Cool down to room temperature and measure UV absorption with Nanodrop at 562 nm.

6.1.3 Ziptip protocol

The protocol followed for rinsing of samples with Ziptips after sample preparation with SPEED.

1. Prepare the following solutions:

   a) 1% HFBA — 990 µL water + 10 µL HFBA

   b) 0.1% HFBA — 450 µL water + 50 µL HFBA

   c) 50% ACN — 500 µL water + 500 µL ACN

   d) 1.1% FA in 50% ACN — 500 µL water + 500 µL ACN + 1 µL FA

2. Solve each sample in 100 µL 0.1% HFBA.
3. Wet the Ziptip with 50% ACN
4. Equilibrate the Ziptip with 1% HFBA.
5. Pull sample through the Ziptip and back out 10 times.
6. Wash the Ziptip with 0.1% HFBA
7. Elute sample with 0.1% FA in 50% ACN.
8. Repeat steps 3-7 for each sample.
9. Evaporate solvent with centrifuge and resolve samples, which are then ready for analysis.

NB! The pipette should not be completely emptied (pushed all the way down) before step 7.

6.1.4 Evotip protocol

The Evotip Protocol describes how samples were applied to Evotips, as recommended by Evosep [68].

1. Wet the Evotips in isopropanol.
2. Wash the tips with 20 μL MeCN. Then centrifuge for 60 s at 700 g.
3. Soak the Evotips in isopropanol until they turn white. Then equilibrate with 20 μL 0.1% FA, and centrifuge for 60 s at 700 g.
4. Load 20 μL sample on the Evotip, and centrifuge for 60 s at 700 g.
5. Wash the Evotips with 20 μL 0.1% FA, and centrifuge for 60 s at 700 g.
6. Finally, transfer 100 μL 0.1% FA to the Evotips, then centrifuged for 10 s at 700 g. This last step ensures that the tips are kept wet until analysis.

6.1.5 Trypsination of Cytochrome C Protocol

Protocol followed for enzymatic digestion with trypsin of 1 μg/μL Cyt C.

1. 4 μg/μL Cyt C is prepared by dissolving 2 mg Cyt C in 0.5 mL 50 mM Tris-HCl.
2. The solution is diluted to 1 mg/mL in 5 protein lo-bind safe-lock tubes.
3. 10 μL 1 mg/mL trypsin is transferred to each sample.
4. Incubate overnight on shaker at 37 °C.
5. Add 5 μL 1% FA. Check that the pH is 2, or add more 1% FA. Samples are ready to be diluted and analyzed.

6.2 Additional experimental information

6.2.1 Workflows for Proteome Discoverer

The workflows used for processing of MS-data with Proteome Discoverer is shown in **Figure A 1**. The consensus workflow used for ensuring high confidence of identifications for the processed data is shown in **Figure A 2**.

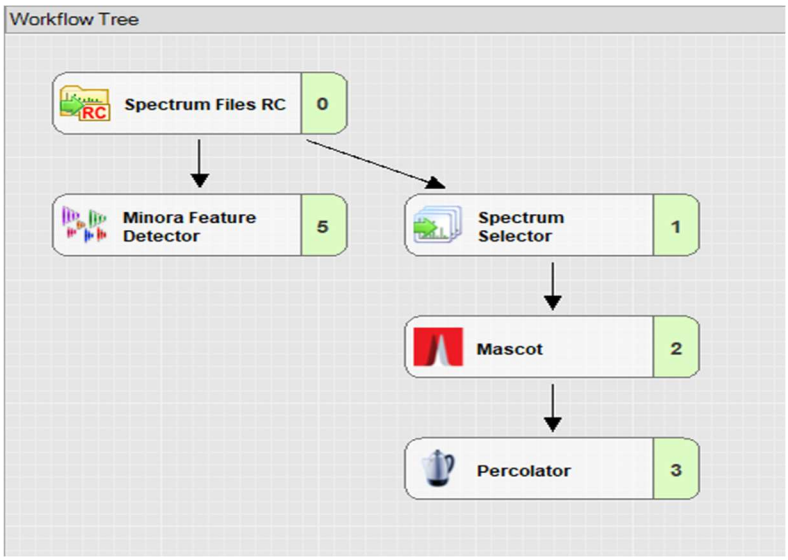

Figure A 1 Processing Workflow used for processing of proteomics data with Proteome Discoverer 2.3.0.523.

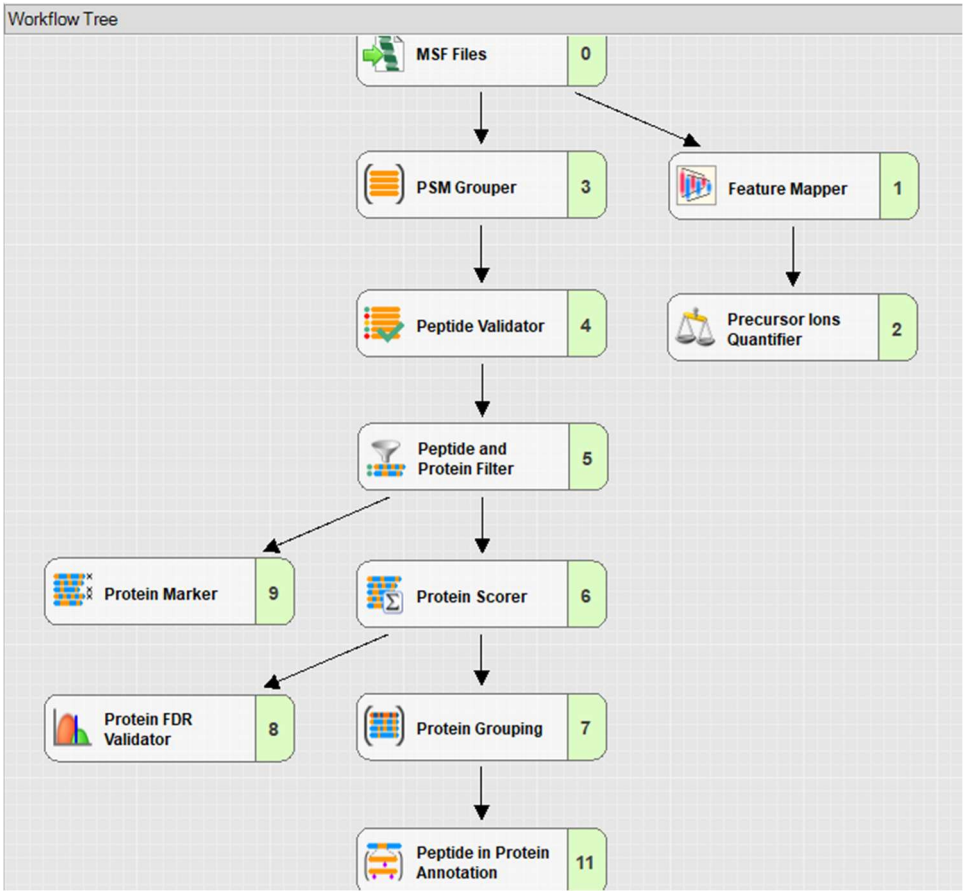

Figure A 2: Consensus Workflow used for processing of proteomics data with Proteome Discoverer 2.3.0.523.

6.2.2 Approximation of protein concentration for SPEED

Due to the problems with performing BCA to determine protein concentration during SPEED, the protein concentrations had to be approximated from estimated protein concentrations in the cells, and takin into account the dilutions performed prior to the addition of trypsin. Due to a miscalculation and a misunderstanding, wrongful concentrations of samples were used in the estimation of trypsin needed, and too large amounts of trypsin were added.

SW480 cells

For the SW480 cells, which contained 10^8 cells, were known to contain 600 µg protein, when 10 µL were extracted (approx. 10^6 cells). Prior to the addition of trypsin, the samples (10 µL cells) were added TFA, tris, DTT and IAM to a total volume of 460.6 µL. The 600 µg proteins were diluted $\frac{460.6}{10} \approx 46$ times. This meant the protein concentration was approx. $\frac{600\ \mu g}{460.6\ \mu L} \approx 1.3\ \mu g/\mu L$ prior to dilution with TFA+tris and addition of trypsin.

The concentration estimated in the lab was 2.0 µg/µl, and the samples were therefore diluted 1:1 with TFA+tris, prior to addition of trypsin. This step diluted the experimental protein concentration to $\frac{1.3\frac{\mu g}{\mu L}}{2} = 0.65\ \mu g/\mu L$. The amount of protein in these 100 µL samples was $0.65\frac{\mu g}{\mu L} * 100\ \mu L = 65\ \mu g$. From this, the amount of trypsin that should be added (trypsin:protein 1:100 (w/w)) was 0.65 µg. Instead, 6 µg of trypsin was added. In other words, approx. 10 times too much trypsin was added to these samples.

Pancreatic islets

For the pancreatic islets, each islet usually contained approx. 3000 cells. There were about 50-60 islets in the batch received, however about half the islets were lost during transportation. As an estimate, 20 islets, divided into two samples of 10 µL, each contained approx. $3000\ cells * \frac{20}{2} = 6 * 10^4\ cells$. As this is one hundredth of the cells for the SW480 cell pellets, the protein amounts are expected to be 100 times lower. This yields a final concentration of $\frac{1.3\frac{\mu g}{\mu L}}{100} = 13\frac{ng}{\mu L}$ protein, prior to dilution with TFA+Tris 1+10.The concentration was believed to be 1 µg/µL, so these samples were not diluted with TFA+Tris 1+10. The amount of protein in these 100 µL samples was $\frac{13ng}{\mu L} * 100\ \mu L = 1.3\ \mu g$. From this the amount of trypsin that should be added was $\frac{1.3\ \mu g}{100} = 13\ ng$. Instead, as described in AA, 1 µg trypsin was added to the samples Mus A1 and Mus A2, and 250 ng trypsin was added to the samples Mus B1 and B2. In other words, 77x and 19x the correct amount of trypsin was added to Mus A and Mus B samples, respectively. All this, of course, assuming the assumptions made about the samples are valid.

6.3 Additional results

6.3.1 Adjacent peptide overlaps for concatenated fractions

Overlap of peptides in all adjacent fractions in Experiment SF04 is shown in **Figure A 3**.

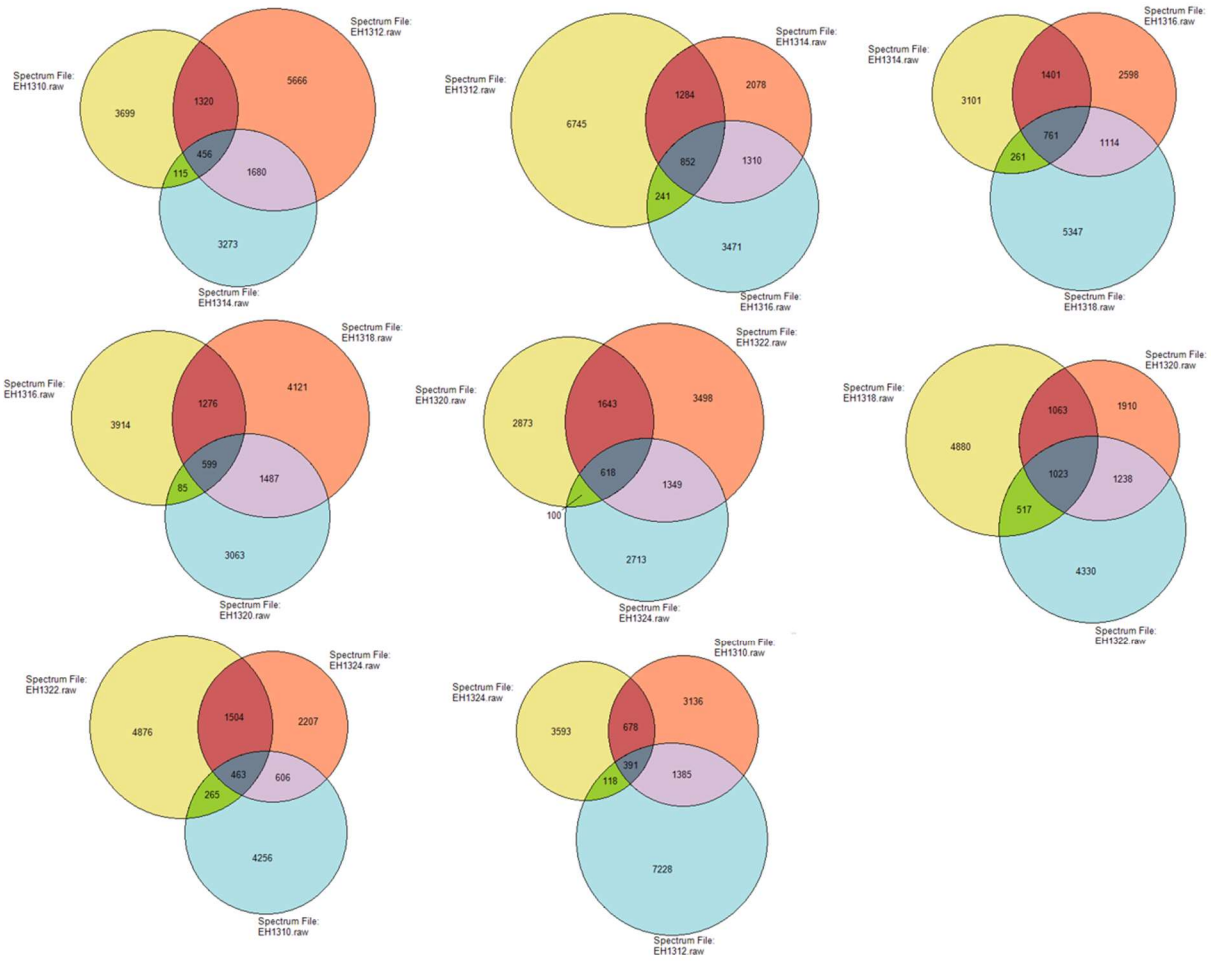

Figure A 3 The peptide overlap between adjacent fractions observed for SF04. Created with Proteome Discoverer.

6.3.2 Chromatograms from the evaluation of chromatography

TICs for three replicates of 8 µL 1.8 pmol/µL Cyt C Digest separated at pH 10 are shown in **Figure A 4**, with blanks performed prior, between each, and after the replicates, shown in **Figure A 5**. TICs for four replicates of 8 µL 20 ng/µL HeLa digest separated at pH 10 are shown in **Figure A 6**, with blanks performed between each, and after the replicates, shown in **Figure A 7**. The blanks accompanying the injections of 8 µL 20 µg/µL HeLa digest with pH 2

(shown in **Figure 25**) are shown in **Figure A 8**. All chromatograms are recorded with a Q-Exactive Orbitrap and Excalibur software.

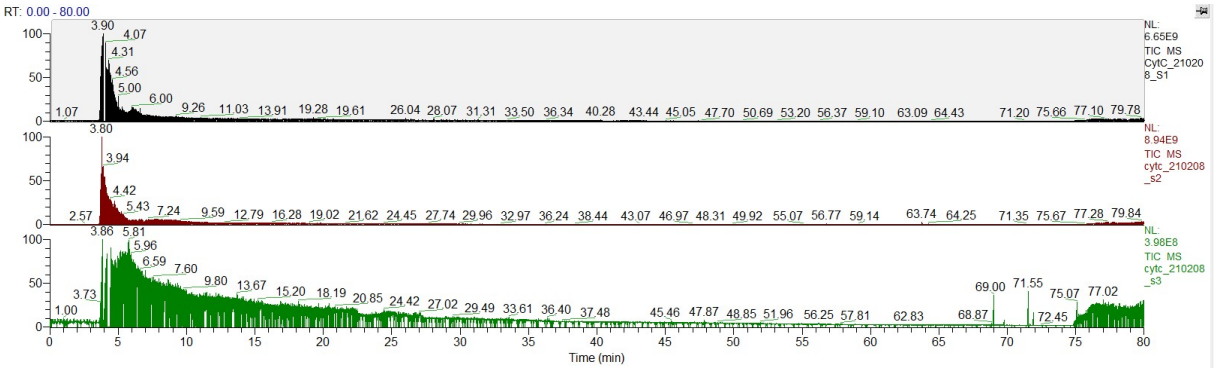

Figure A 4: TICs for 8 µL 1.8 pmol/µL Cyt C digest, performed at pH 10.

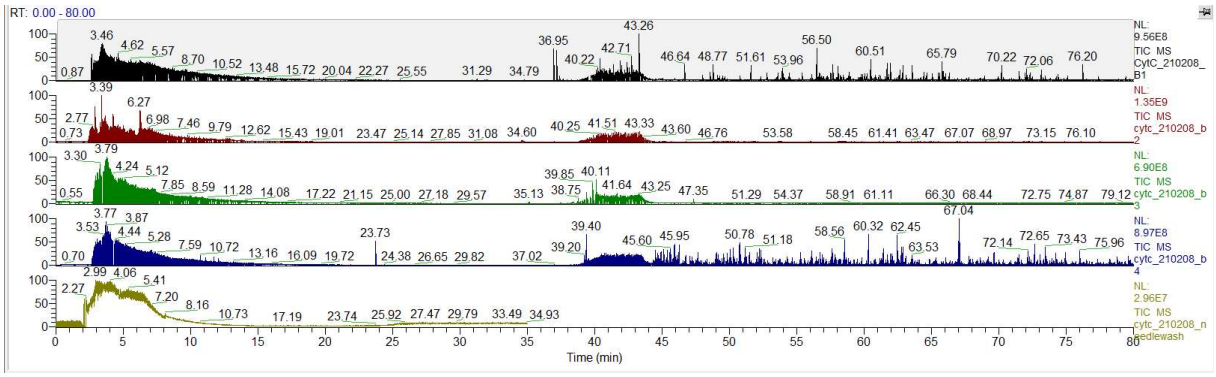

Figure A 5: TICs for blanks accompanying the Cyt C digest experiments. Performed at pH 10.

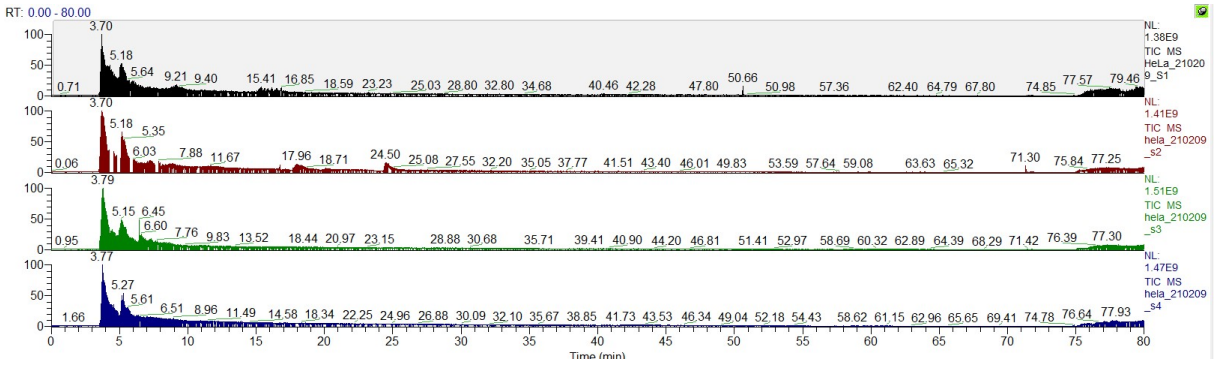

Figure A 6: TICs for 8 µL 20 ng/µL HeLa digest, performed at pH 10.

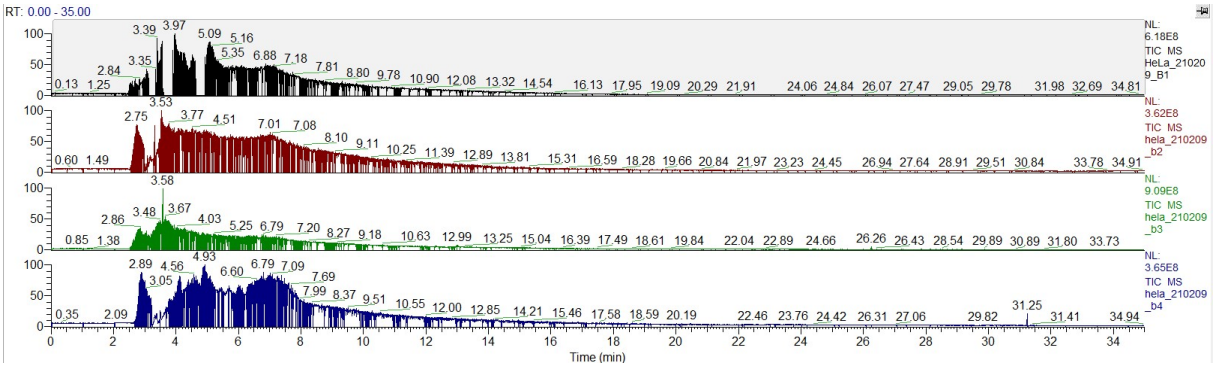

Figure A 7: TICs for blanks accompanying the HeLa experiments at pH 10. Performed at pH 10.

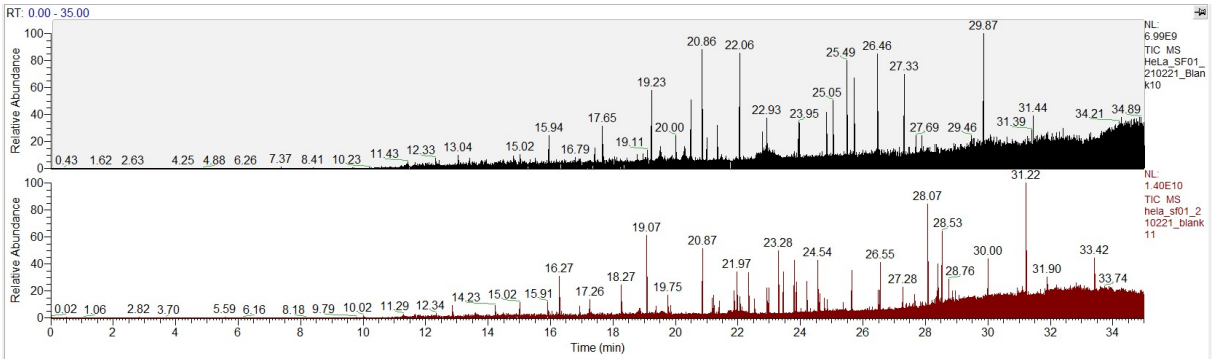

Figure A 8: TICs for blanks accompanying the HeLa experiments at pH 2. Performed at pH 2.

6.3.3 Chromatograms for the fractionated samples

TICs for SF01, SF03, and SF04 are shown in Figure A 9Figure A 10Figure A 11, respectively. Similarly. TICs for the blanks run between them are shown in Figure A 12, Figure A 13, Figure A 14, respectively.

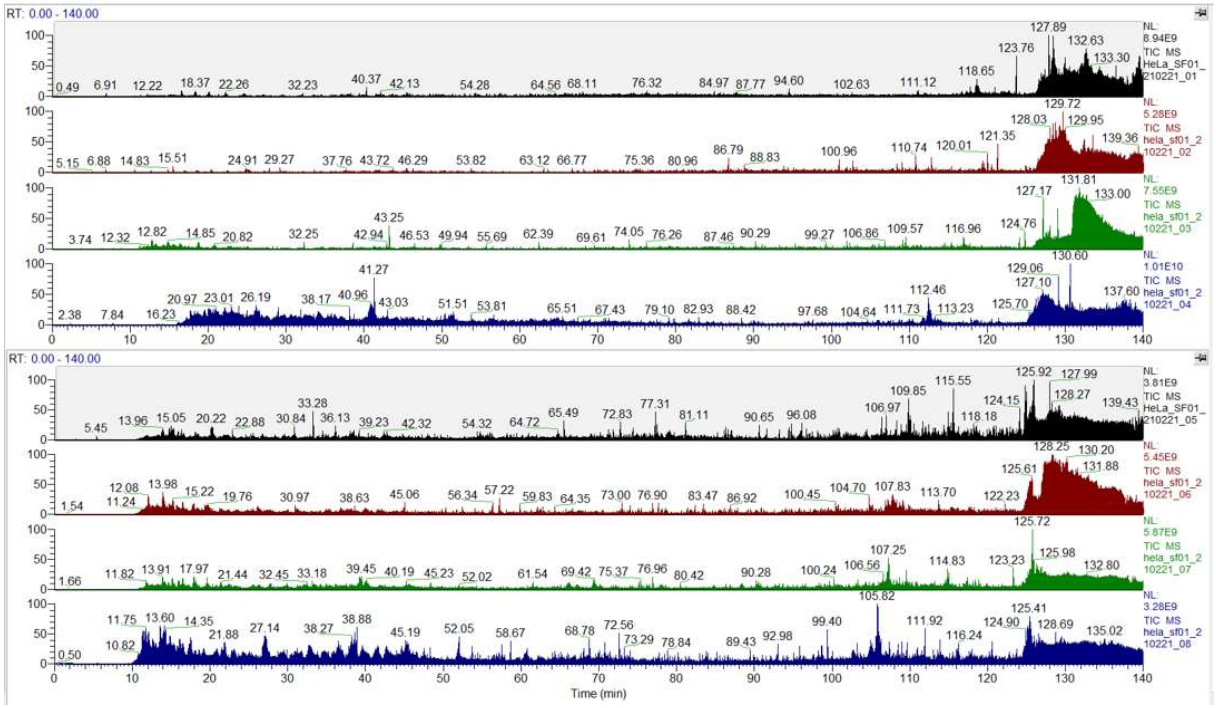

Figure A 9 TICs for each fraction of 18 µL 0.1 µg/µL HeLa fractionated with Spider Fractionation in Experiment SF01. The detection was performed with a Q-Exactive Orbitrap.

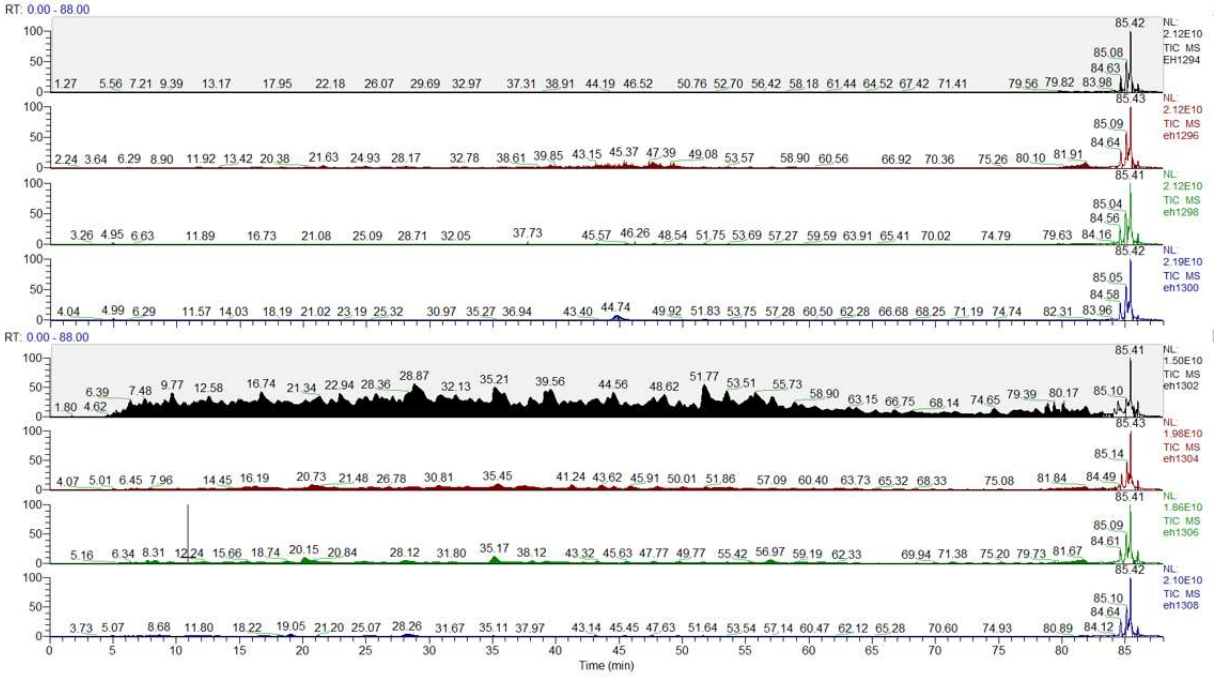

Figure A 10 TICs for each fraction of 18 µL 0.1 µg/µL HeLa fractionated with Spider Fractionation in Experiment SF03. The detection is performed with a Q-Exactive HF Orbitrap, using Evosep One with the Extended method.

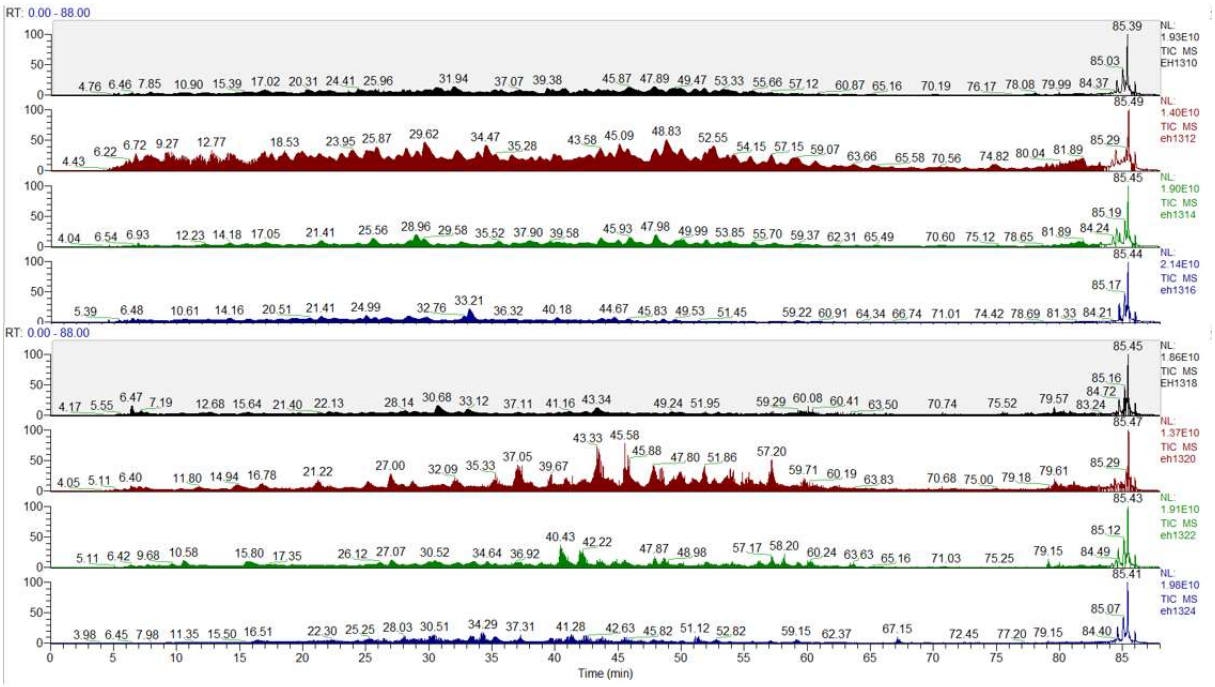

Figure A 11 TICs for each fraction of 18 µL 0.1 µg/µL HeLa fractionated with Spider Fractionation in Experiment SF04. The detection is performed with a Q-Exactive HF Orbitrap, using Evosep One with the Extended method.

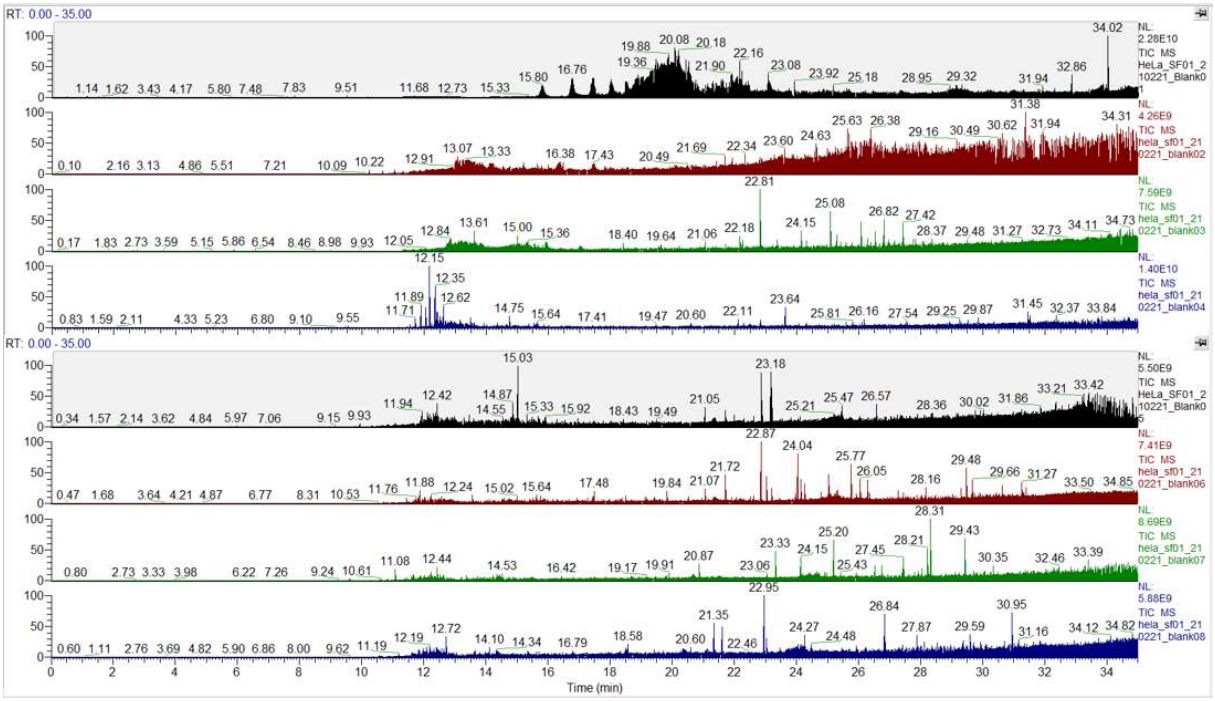

Figure A 12 TICs for the blanks performed between and after each fraction in Experiment SF01. The detection was performed with a Q-Exactive Orbitrap.

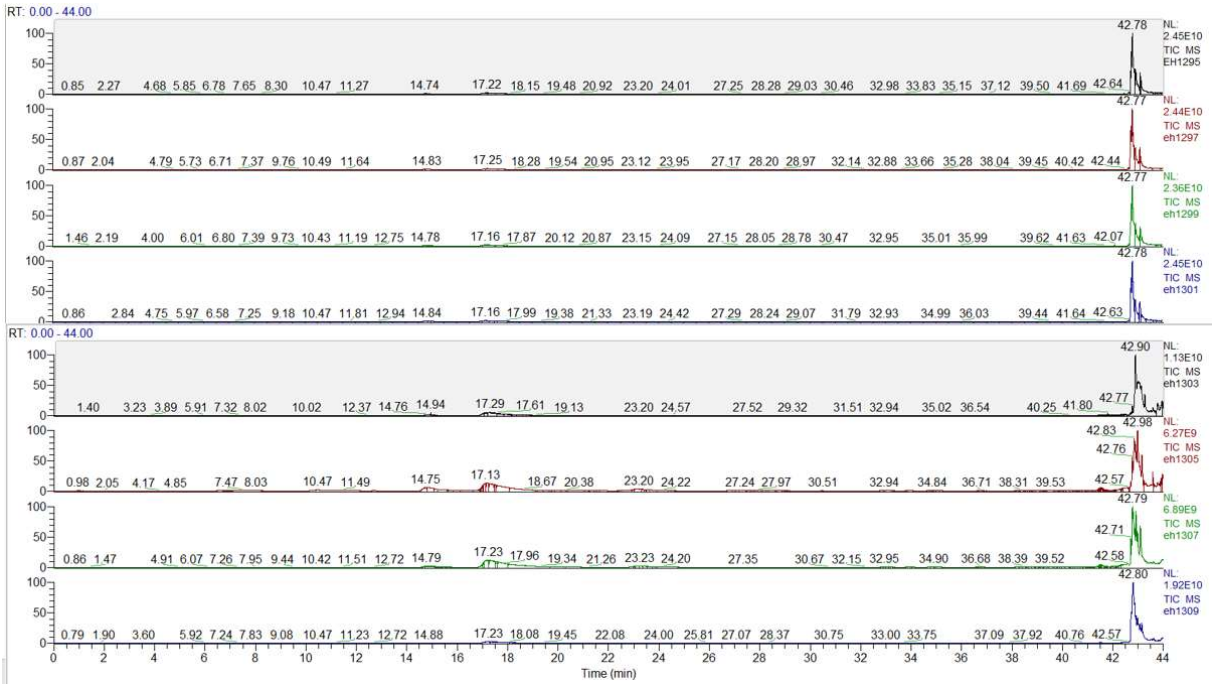

Figure A 13 TICs for the blanks performed between and after each fraction in Experiment SF03. The detection is performed with a Q-Exactive HF Orbitrap, using Evosep One with the Extended method.

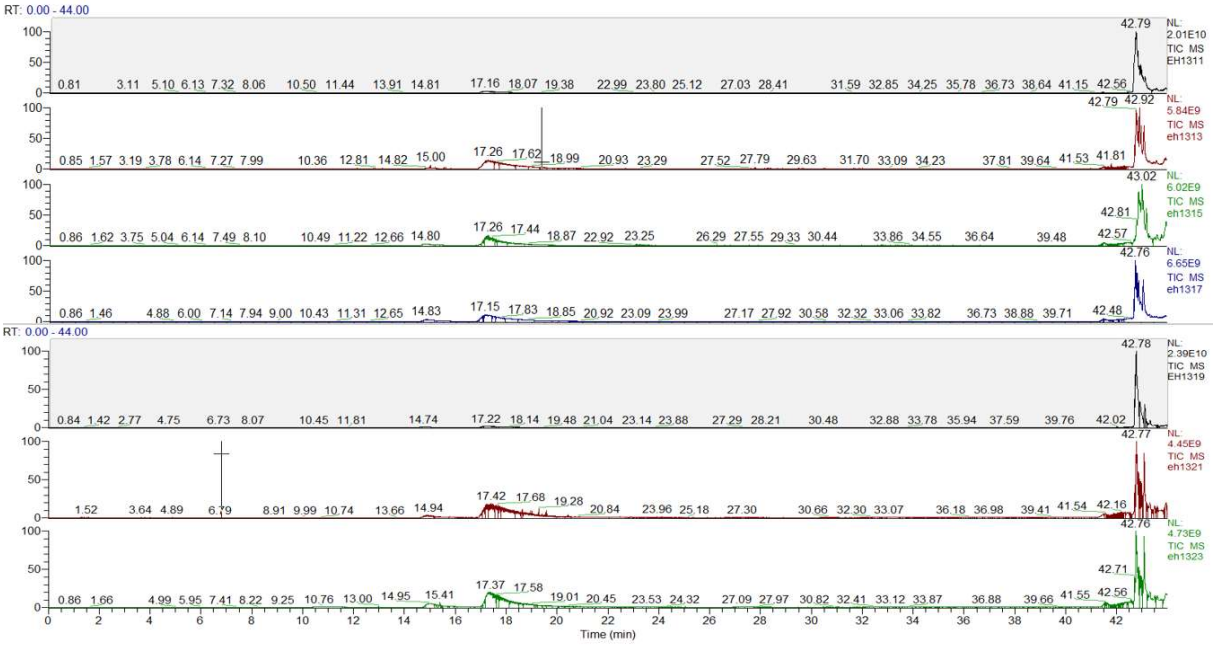

Figure A 14 TICs for the blanks performed between and after each fraction in Experiment SF04. The detection is performed with a Q-Exactive HF Orbitrap, using Evosep One with the Extended method.

6.4 Additional results and discussion for the optimized Spider Fractionation system

6.4.1 Applying UV control

The final major change to the Optimized Spider Fractionation system was the inclusion of a Dionex UV-detector, for qualifying the chromatography prior to and after each fractionation experiment. As previously mentioned, only 8 out of 10 of the ports in the spider were used for fractionation. The ninth port was used for waste when fractionation was not being performed. The tenth, remaining port was connected to a UV-detector, with the goal of detecting a peptide standard (Cyt C digest) prior to and after each fractionation experiment. This would ensure sharp, repeatable peaks for peptides eluting from the chromatographic system, and indicate that the system was working as intended. It should be noted that earlier attempts at detecting peptides with UV-detection had proved a challenge in **Section 3.3**. This turned out to be the case with this new system as well, as is described in the following parts.

In summary, UV-detection was applied to the system to qualify the chromatography prior to and after each fractionation.

6.4.2 Estimating the actual flow rate

The first step in evaluating the chromatographic capabilities of the optimized Spider Fractionation system was measuring the actual flow rate delivered by the pump. This was performed, as this pump was known to struggle somewhat when delivering nL/min flow rates (for this work 200 nL/min). Several measurements were taken, as shown below. It was observed that the flow, when set to 250 nL/min, delivered an actual flow rate of 180 ± 10 nL/min at 5% MPB, and 240 ± 10 nL/min at 50% MPB, and 95% MPB. The standard deviations at each MP composition were all approx. 10 nL/min at the flow rate of 250 nL/min, indicating stable flow. As such, the flow rate used for the troubleshooting experiments described in **Section 6.4.3** was 250 nL/min, which in actuality was somewhere between 160-260 nL/min, depending on the MP composition.

In summary, the actual flow rate of the system was measured, and found to differ from the one displayed. For all experiments 250 nL/min was set as the displayed flow rate, with an actual flow rate varying from, 170-250 nL/min, dependent on MP composition.

Raw data from measurements of actual column flow for the optimized Spider Fractionation system

The measurements of the actual flow rates delivered by the Agilent 1200 pump in the optimized Spider Fractionation system is shown in **Table A 1**-Table A 5. The average (AVG), standard deviation (SD) and relative standard deviation (RSD) are included for each experiment. The measurements were taken as described in **Section 6.4.2**, by measuring how long it took to fill 0.2 µL of a syringe attached to the end of the pump.

Table A 1 The flow rate measurements at 0.20 µL/min, 50% MPB. Shown are the measured times, and the calculated flow rates found by dividing the measured volume (0.2 µL) on the time spent. The AVG, SD, and RSD for the flow rate measurements are included.

replicate	time (mm:ss)	time (min)	flow rate (µL/min)
1	01:13	1.22	0.16
2	01:20	1.33	0.15
3	01:15	1.25	0.16
4	01:21	1.35	0.15
5	01:14	1.23	0.16
		AVG	0.16
		SD	0.01
		RSD	4.7%

Table A 2 The flow rate measurements at 0.30 µL/min, 50% MPB. Shown are the measured times, and the calculated flow rates found by dividing the measured volume (0.2 µL) on the time spent. The AVG, SD, and RSD for the flow rate measurements are included.

replicate	time (mm:ss)	time (min)	flow rate (µL/min)
1	00:46	0.77	0.26
2	00:49	0.82	0.24
3	00:56	0.93	0.21
4	00:45	0.75	0.27
		AVG	0.25
		SD	0.02
		RSD	9.5%

Table A 3 The flow rate measurements at 25 µL/min, 50% MPB. Shown are the measured times, and the calculated flow rates found by dividing the measured volume (0.2 µL) on the time spent. The AVG, SD, and RSD for the flow rate measurements are included.

replicate	time (mm:ss)	time (min)	flow rate (µL/min)
1	00:51	0.85	0.24
2	00:50	0.83	0.24
3	00:46	0.77	0.26
4	00:51	0.85	0.24
		AVG	0.24
		SD	0.01
		RSD	5.0%

Table A 4 The flow rate measurements at 25 µL/min, 95% MPB. Shown are the measured times, and the calculated flow rates found by dividing the measured volume (0.2 µL) on the time spent. The AVG, SD, and RSD for the flow rate measurements are included.

replicate	time (mm:ss)	time (min)	flow rate (µL/min)
1	01:09	1.15	0.17
2	01:08	1.13	0.18
3	01:02	1.03	0.19
4	01:14	1.23	0.16
5	01:11	1.18	0.17
		AVG	0.18
		SD	0.01
		RSD	6.7%

Table A 5 The flow rate measurements at 25 µL/min, 5% MPB. Shown are the measured times, and the calculated flow rates found by dividing the measured volume (0.2 µL) on the time spent. The AVG, SD, and RSD for the flow rate measurements are included.

replicate	time (mm:ss)	time (min)	flow rate (µL/min)
1	00:48	0.80	0.25
2	00:48	0.80	0.25
3	00:52	0.87	0.23
4	00:48	0.80	0.25
		AVG	0.25
		SD	0.01
		RSD	3.9%

6.4.3 Troubleshooting of the optimized fractionation system

As the initial tests with injections of thiourea resulted in varied chromatograms (**Figure A 15**), the autosampler was exchanged for a manual injector, which did not result in stable and repeatable chromatography (**Figure A 16**). As thiourea has minimal retention on an RP column, a single peak would be expected. The chromatograms, however, show either no peak, or several, indicating the possibility that the thiourea was stuck somewhere in the system and released to reach the detector irregularly. The column was the prime suspect, and was swapped for a commercial ACE 3 C18 column. Injections of caffeine on this new column led to the chromatograms seen in **Figure A17.**

The second chromatogram (B) shows the need for a restrictor connected after the UV-detector, as several very narrow peaks appear all over the chromatogram. After replacing the restrictor with a new one, the following five chromatograms (C-G) are much cleaner, most of them with a peak with repeatable retention time. It is evident that there is a benefit to using this column compared to the previous in-house packed Accucore column. However, the peaks vary in intensity (D-E compared to G), disappear completely (E), or contains more than one peak (C). This indicated that there was something else wrong with the system, in addition to the potentially suboptimal in-house packed column.

The column was replaced with a new in-house packed Accucore column and the manual injector was replaced with the autosampler, with the hope that the new column would yield similar chromatograms as the commercial column. The resulting chromatograms are seen in **Figure A 18-19,** and while the peaks are not as sharp as those observed with the commercial column, the rest of the chromatograms seem cleaner. Unfortunately, the repeatability is still poor. As there were some issues with couplings loosening and ferrules breaking, all tubing was replaced from 30 µm ID silica capillaries to 20 µm ID ones. Apparently, the outer diameter of the batch of 30 µm ID capillaries had caused troubles for others in the laboratory, especially with ferrules breaking when used with these capillaries. The tests following this change of tubing yielded the chromatograms shown in **Figure A 20**, which indicated that the injected standards still ended up stuck somewhere.

Having swapped out most of the system, the autosampler was again swapped out for a new manual injector. This led to the system stopping due to pressure exceeding the set system limit of 400 bar each time the pump was turned on. The pump was connected directly to the column, skipping the injector, and the system seemed stable. The manual injector was then washed

properly by dismantling it and submerging the components in MeOH in an ultrasound bath. Several ports of the injector stator were completely clogged, and had to be drilled open and cleaned properly with more MeOH. It was suspected that the material clogging the stator was remains of broken ferrule. After washing, the injector was reassembled and reattached to the system. The following injections resulted in chromatograms **Figure a 21,** with a seemingly stable signal, giving a nice peak for 240 ng/μL thiourea.

With a seemingly stable system, the injection of peptides was the next step. Cyt C was injected with the resulting chromatograms seen in **Figure A 22**.

The analysis of Cyt C in **Figure A 22** returned only two peaks, while several were to be expected when comparing with a datasheet from Waters for a different Cyt C digest standard (Waters). The low number of peaks could possibly be due to low concentrations of peptides, and as such, higher concentration solutions were prepared. It was also problematic that the detected peaks did not correspond to the injected concentrations, as would be expected. The concentration was much lower in (A) compared to (B), which was unexpected as the same concentration was injected. In addition, (B) and (C) seemed to have identical peaks, when one would expect half the peak area for (C), as its concentration is half that of (B). In hindsight, this indicated that some analytes might have ended up stuck in some part of the injection system, but this was not investigated further.

What was investigated further was whether a higher concentration of Cyt C would lead to more peptides with high enough concentrations to yield more than two peaks. Cyt C with the high concentration of 1 μg/μL was prepared and injected, with the unfortunate result of only indications of peaks, indistinguishable from the blank injected (**Figure A 23**). After this, thiourea of a similarly high concentration was injected, with the resulting chromatograms (**Figure A 24**). The injections of thiourea showed the same as before, the peak shapes, retention times and signal intensities did not produce repeatable chromatograms.

In summary, major challenges with repeatability presented themselves with this LC-UV system. To address these challenges, the column, MPs, tubing, standard solutions, the injector, and all couplings were replaced. Analytes seemed to end up stuck somewhere in the system, and kept ending up stuck, even when swapping close to all system components.

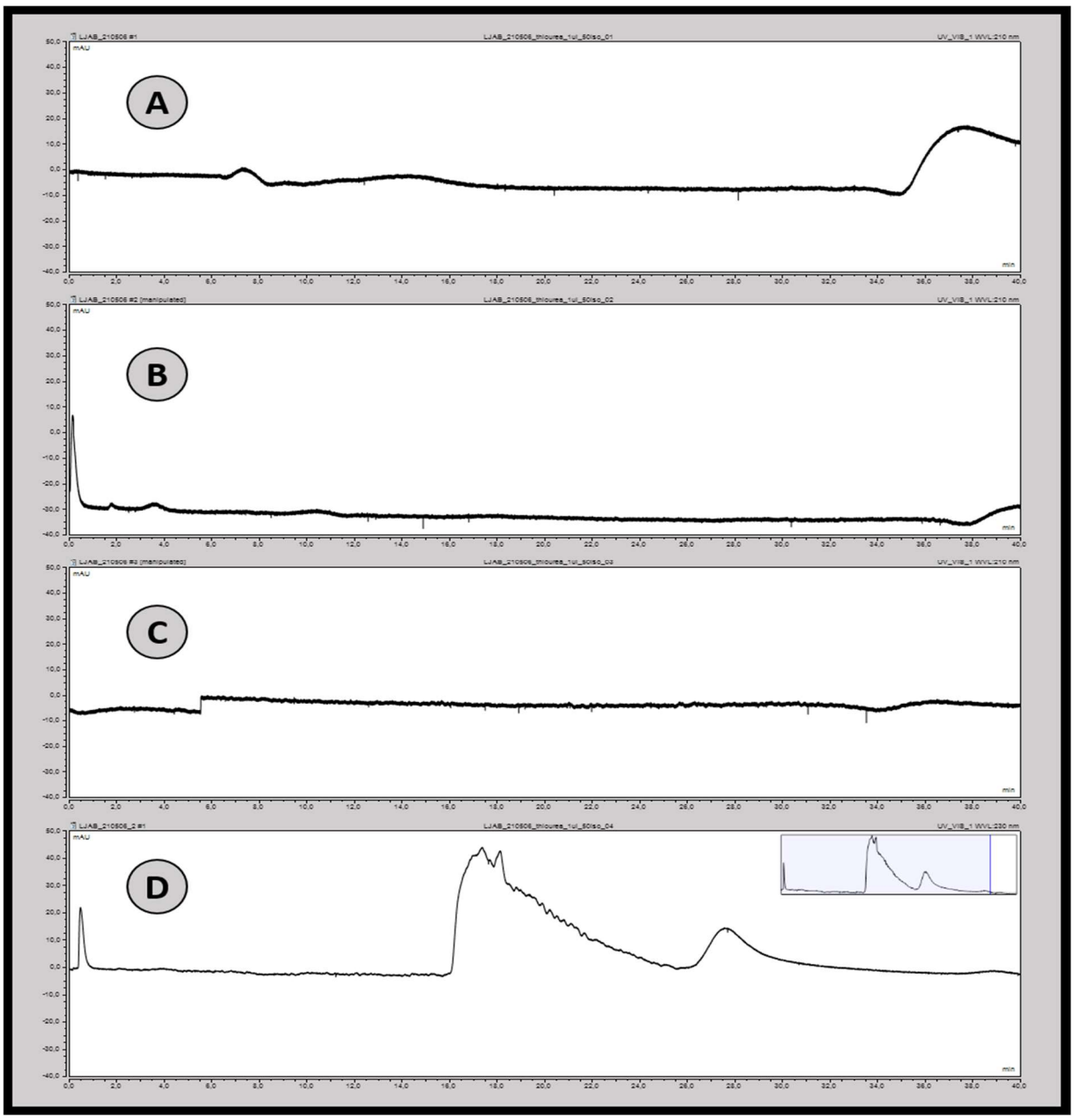

Figure A 15: UV chromatograms for the initial tests of the optimized fractionation system. Each chromatogram is the result of an injection of 1 µL of 10 ng/µL thiourea. Isocratic flow of 50% MPB was applied, with an estimated flow rate of 220 nL/min.

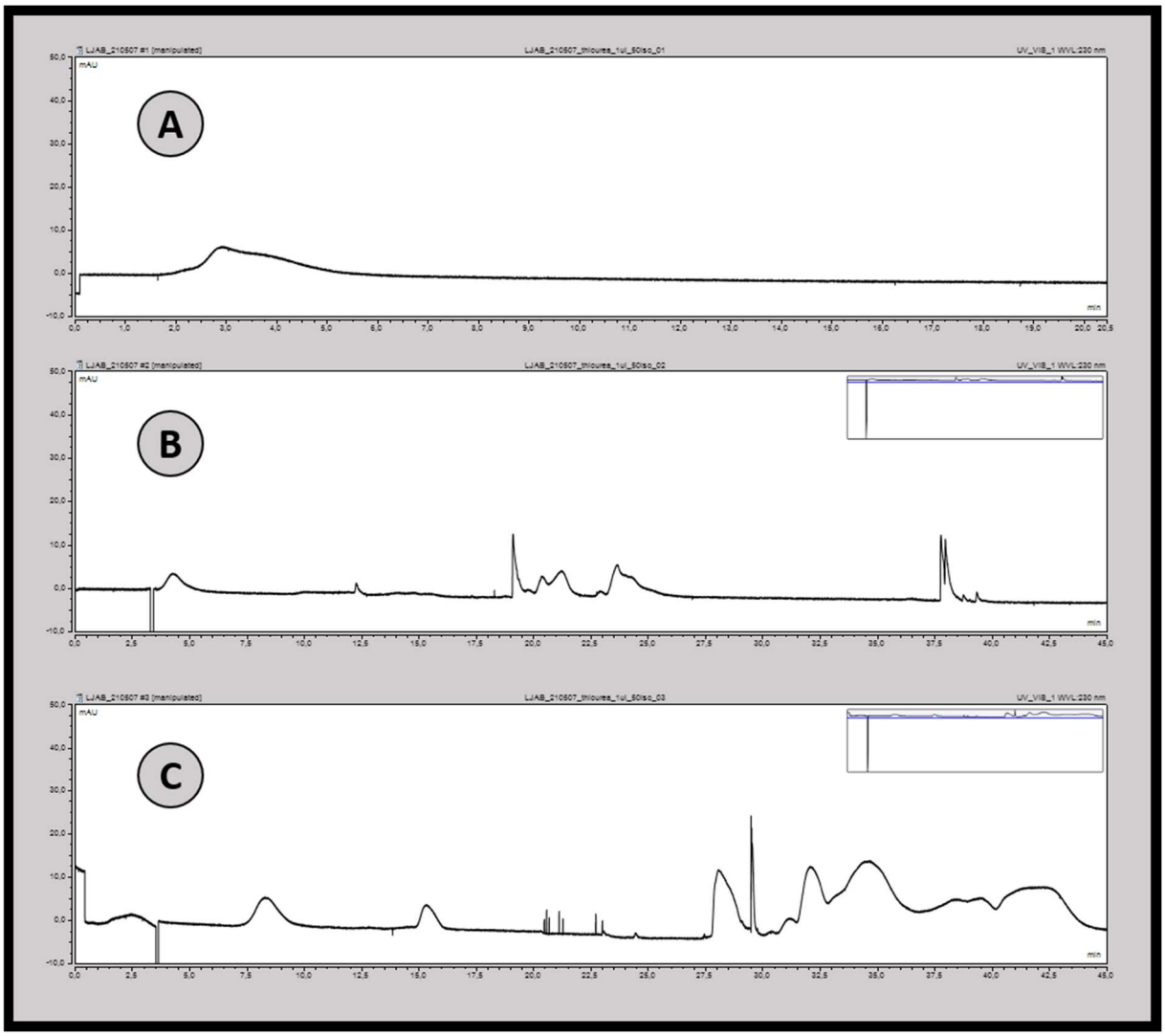

Figure A 16 UV chromatograms for the tests after switching to manual injection on the optimized fractionation system. Each chromatogram is the result of an injection of 1 µL of 10 ng/µL thiourea. Isocratic flow of 50% MPB was applied, with an estimated flow rate of 220 nL/min.

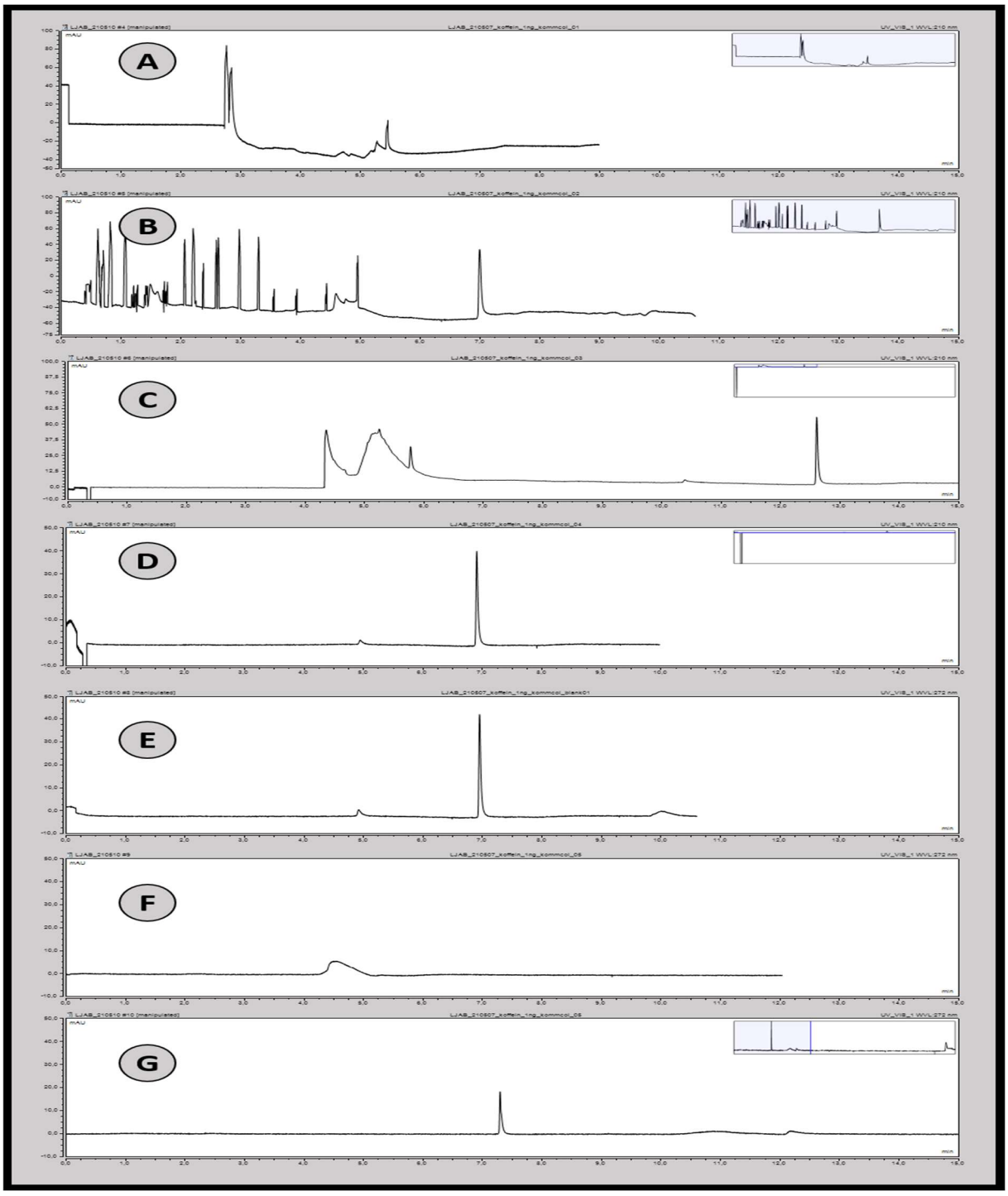

Figure A 17 UV chromatograms for the tests with an ACE 3 C18 column (100 µm ID x 15 cm, particle size 3 µm, pore size 100Å) on the optimized fractionation system. Each chromatogram is the result of an injection of 0.5 µL of 2 ng/µL caffeine. Isocratic flow of 50% MPB was applied, with an estimated flow rate of 220 nL/min.

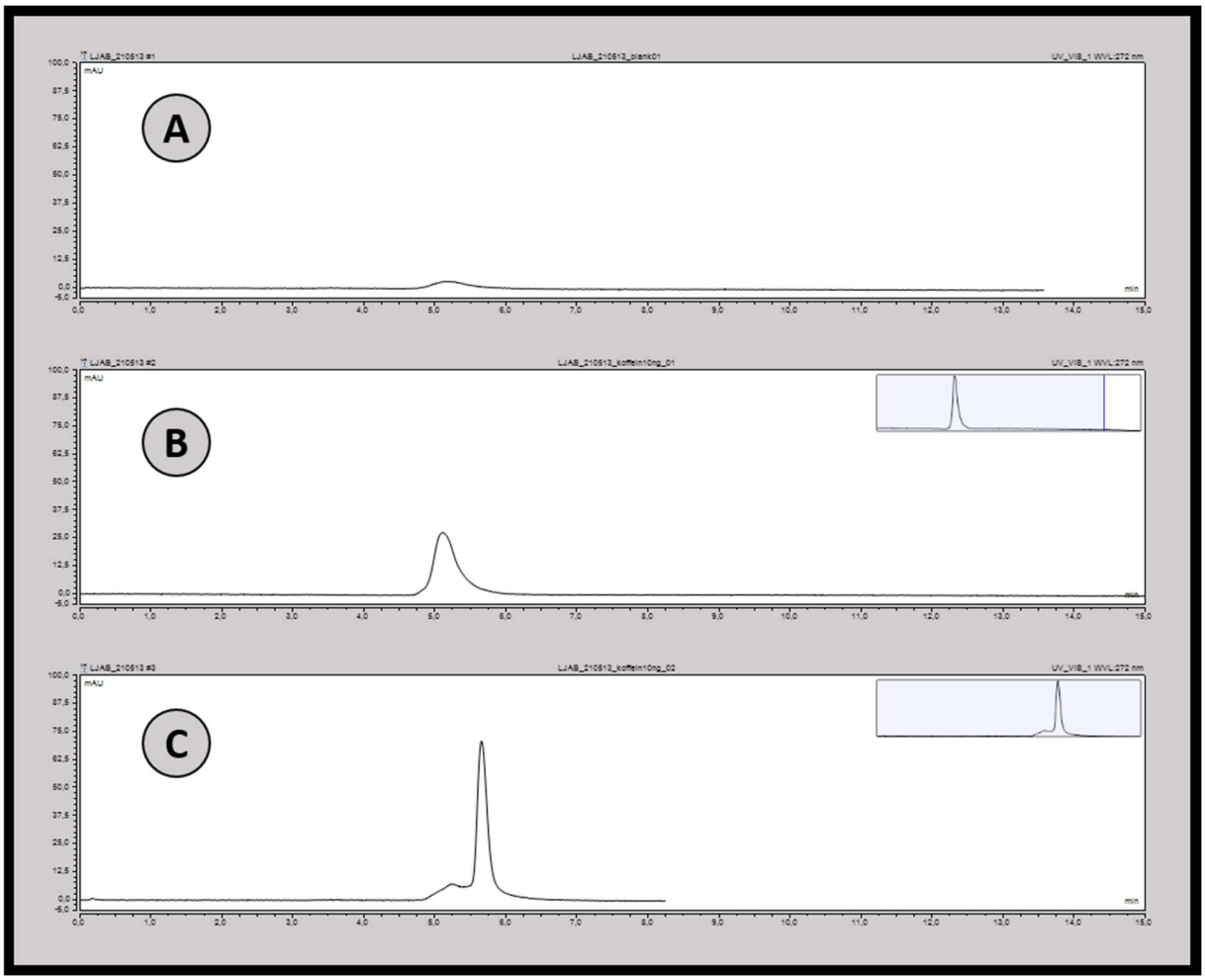

Figure A 18 UV chromatograms for the tests with a new in-house packed Accucore column and autosampler on the optimized fractionation system, part 1 of 2.. Isocratic flow of 50% MPB was applied, with an estimated flow rate of 220 nL/min. Each chromatogram is the result of an injection of 1 µL (A) MPA, (B-C) 10 ng/µL caffeine.

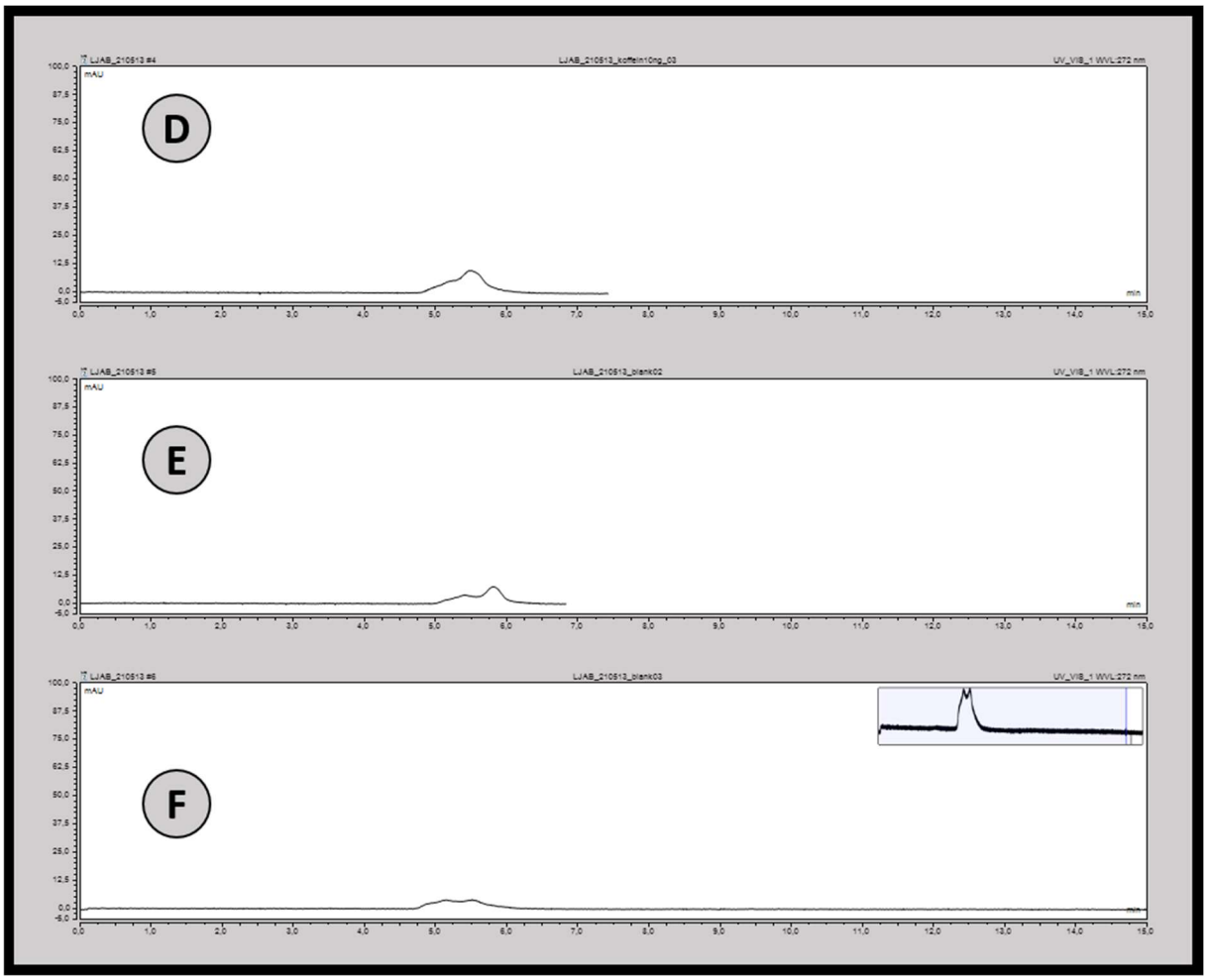

Figure A 19 UV chromatograms for the tests with a new in-house packed Accucore column and autosampler on the optimized fractionation system, part 2 of 2.. Isocratic flow of 50% MPB was applied, with an estimated flow rate of 220 nL/min. Each chromatogram is the result of an injection of 1 µL (D) 10 ng/µL caffeine, (E-F) MPA.

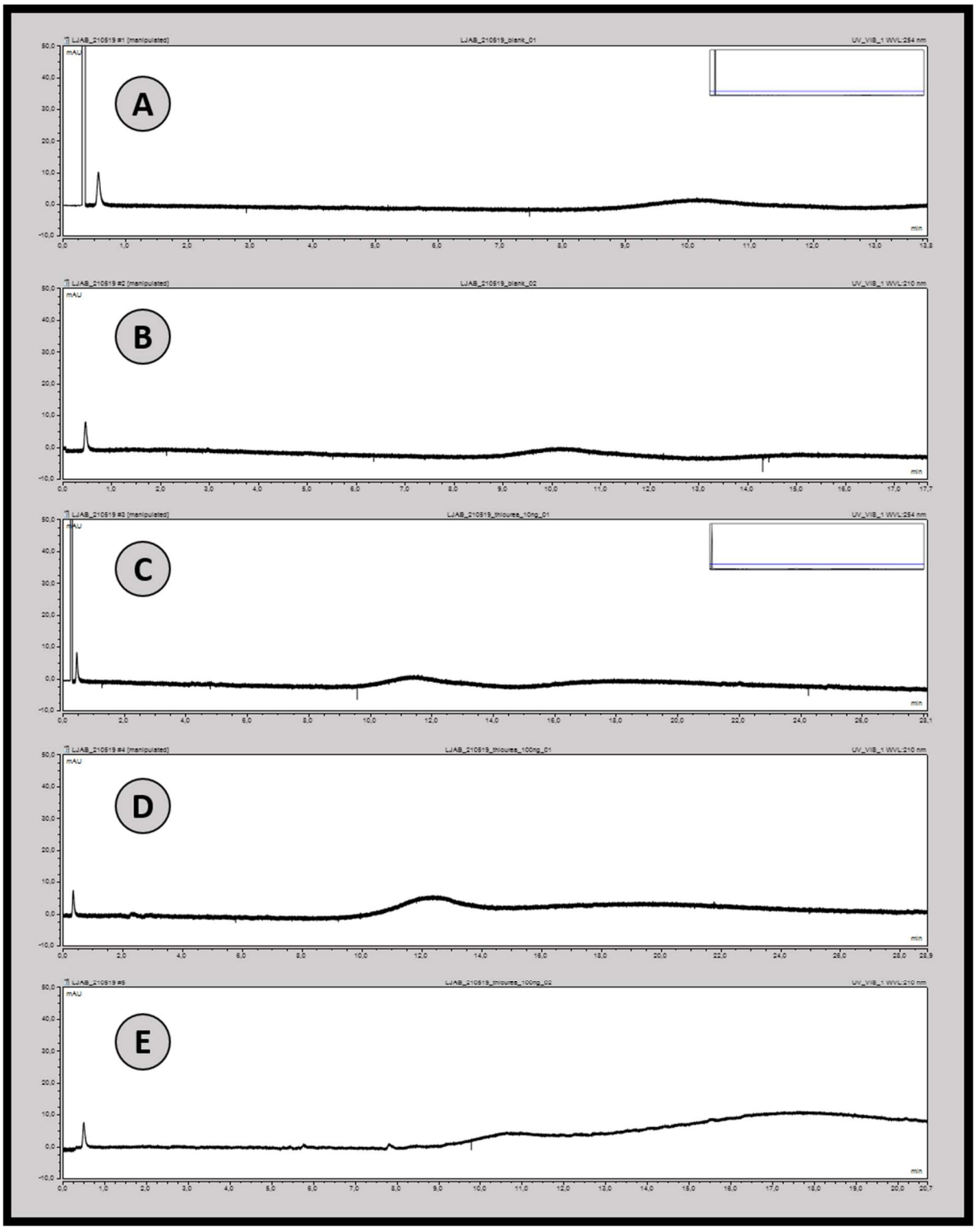

Figure A 20 UV chromatograms for the tests with new tubing with 20 µm ID (from 30 µm) on the optimized fractionation system.. Isocratic flow of 50% MPB was applied, with an estimated flow rate of 220 nL/min. Each chromatogram is the result of an injection of 1 µL (A-B) MPA, (C) 10 ng/µL thiourea, (D-E) 100 ng/µL thiourea.

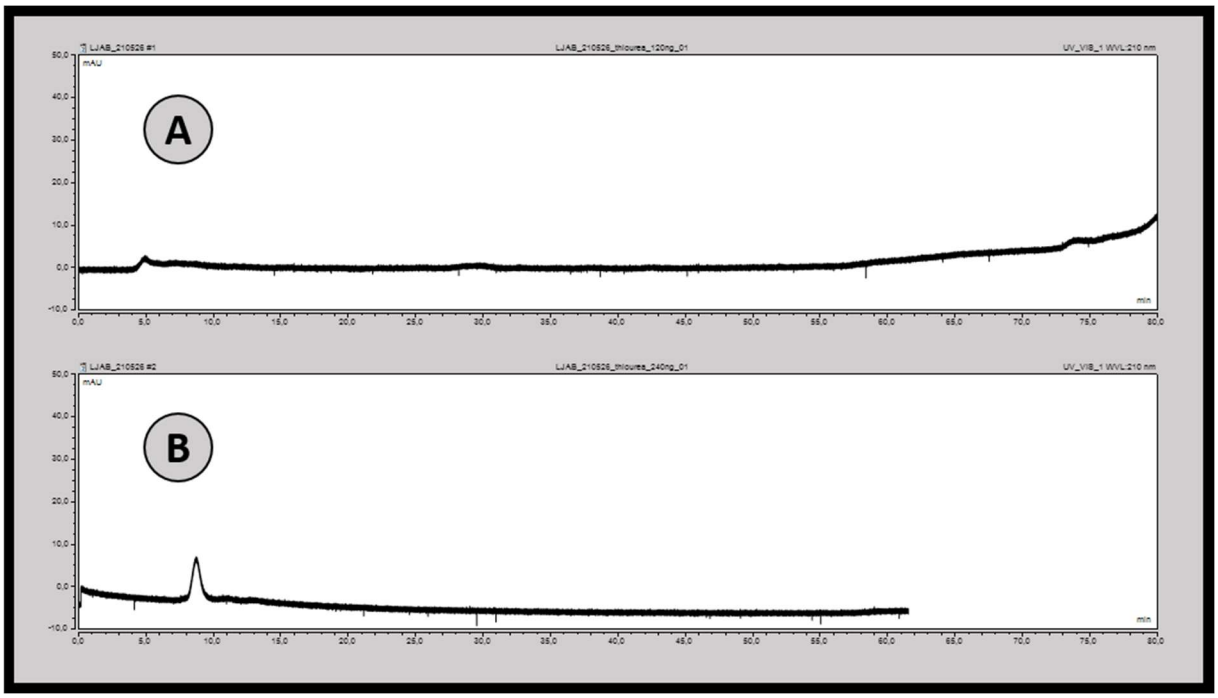

Figure A 21 UV chromatograms for the tests after dismantling and washing the manual injector on the optimized fractionation system Isocratic flow of 50% MPB was applied, with an estimated flow rate of 220 nL/min.. Each chromatogram is the result of injections of 0.5 µL. The injections were of (A) 120 ng/µL thiourea, (B) 240 ng/µL thiourea.

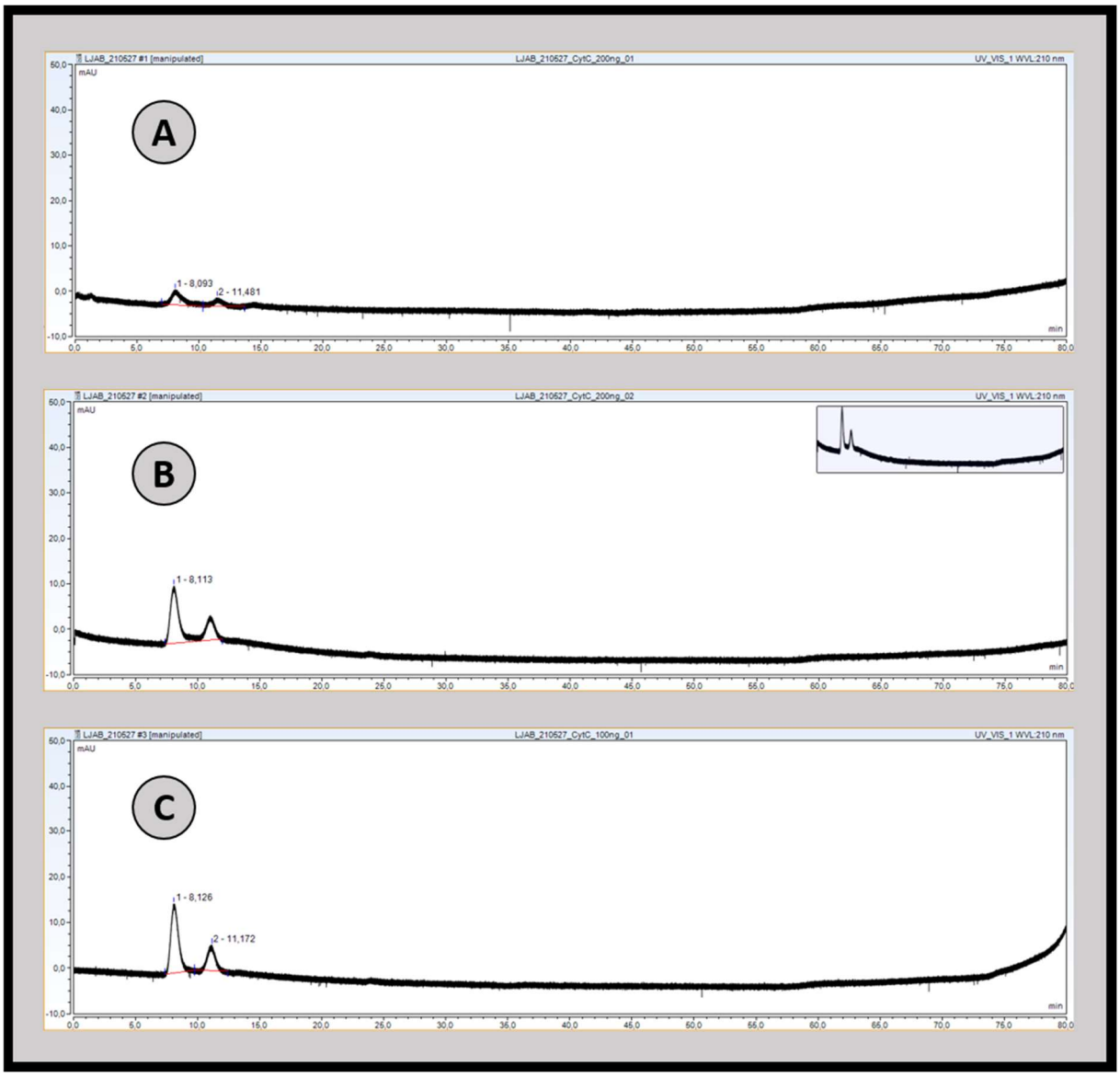

Figure A 22 UV chromatograms for the tests of Cyt C on the optimized fractionation system. Gradient flow was applied with Gradient C (Figure 17), with an estimated flow rate of 220 nL/min. Each chromatogram is the result of injections of 0.5 µL (A-B) 200 ng/µL Cyt C digest, (C) 100 ng/µL Cyt C digest.

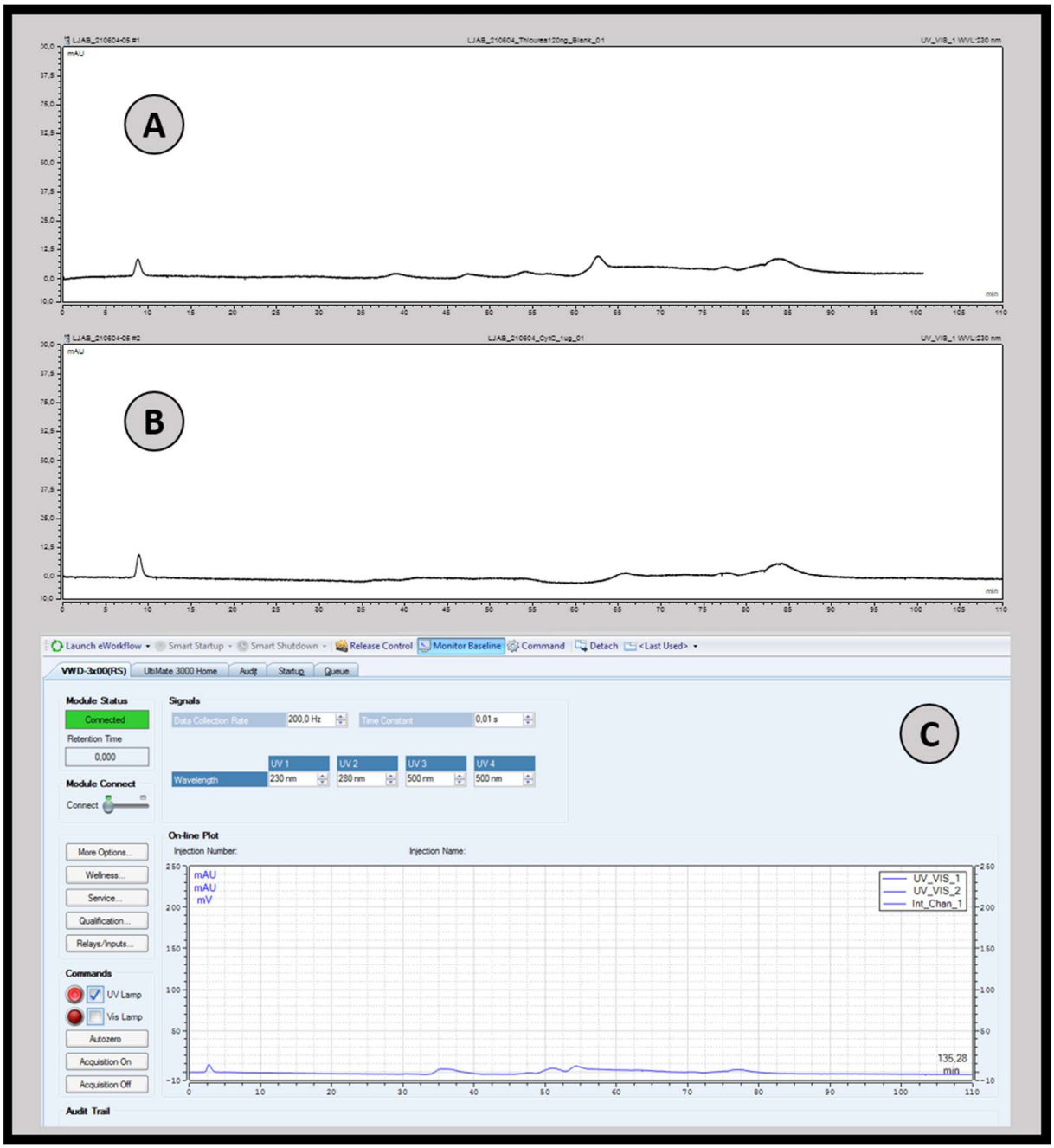

Figure A 23 UV chromatograms for the tests of high-concentration Cyt C on the optimized fractionation system. . Gradient flow was applied with Gradient C (Figure 17), with an estimated flow rate of 220 nL/min.Each chromatogram is the result of injections of 0.5 µL (A) 120 ng/µL thiourea, (B-C) 1000 ng/µL Cyt C digest. (A) functions as the injection of a blank.

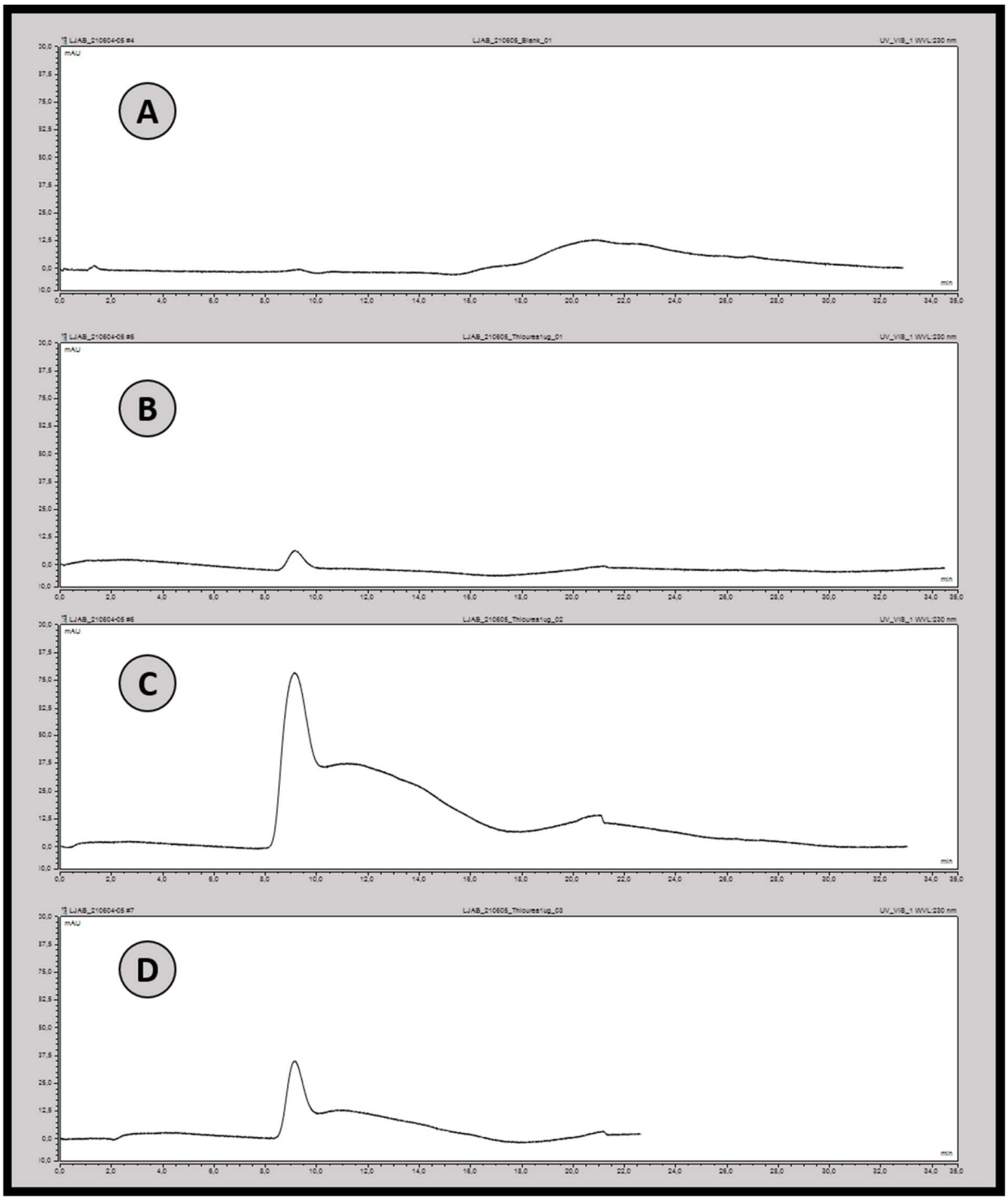

Figure A 24 UV chromatograms for the tests performed immediately after the injection of high-concentration Cyt C on the optimized fractionation system. Isocratic flow of 50% MPB was applied, with an estimated flow rate of 220 nL/min. Each chromatogram is the result of injections of 0.5 µL (A) MPA, (B-D) 1000 ng/µL thiourea.